

## A VOLUME-LIMITED PHOTOMETRIC SURVEY OF 114 $\gamma$ DORADUS CANDIDATES

Gregory W. Henry, Francis C. Fekel<sup>1</sup>

*Center of Excellence in Information Systems, Tennessee State University,  
3500 John A. Merritt Blvd., Box 9501, Nashville, TN 37209*

Stephen M. Henry

*Department of Mathematical Sciences, Clemson University,  
O-110 Martin Hall, Box 340975, Clemson, SC 29634*

gregory.w.henry@gmail.com

fekel@evans.tsuniv.edu

smhenry@clemson.edu

### ABSTRACT

We have carried out a photometric survey of a complete, volume-limited sample of  $\gamma$  Doradus candidates. The sample was extracted from the *Hipparcos* catalog and consists of 114 stars with colors and absolute magnitudes within the range of known  $\gamma$  Doradus stars and that also lie within a specified volume of 266,600 pc<sup>3</sup>. We devoted one year of observing time with our T12 0.8 m automatic photometric telescope to acquire nightly observations of the complete sample of stars. From these survey observations, we identify 37 stars with intrinsic variability of 0.002 mag or more. Of these 37 variables, eight have already been confirmed as  $\gamma$  Doradus stars in our earlier papers; we scheduled the remaining 29 variables on our T3 0.4 m automatic telescope to acquire more intensive observations over the next two years. As promising new  $\gamma$  Doradus candidates were identified from the photometry, we obtained complementary spectroscopic observations of each candidate with the Kitt Peak coudé feed telescope. Analysis of our new photometric and spectroscopic data reveals 15 new  $\gamma$  Doradus variables (and confirms two others), eight new  $\delta$  Scuti variables (and confirms one other), and three new variables with unresolved periodicity. Therefore, of the 114  $\gamma$  Doradus candidates

---

<sup>1</sup>Visiting Astronomer, Kitt Peak National Observatory, National Optical Astronomy Observatory, operated by the Association of Universities for Research in Astronomy, Inc., under cooperative agreement with the National Science Foundation.

in our volume-limited sample, we find 25 stars that are new or previously-known  $\gamma$  Doradus variables. This results in an incidence of 22% for  $\gamma$  Doradus variability among candidate field stars for this volume of the solar neighborhood. The corresponding space density of  $\gamma$  Doradus stars in this volume of space is 0.094 stars per  $10^3 pc^3$  or 94 stars per  $10^6 pc^3$ . We provide an updated list of 86 bright, confirmed,  $\gamma$  Doradus field stars.

*Subject headings:* stars: early-type — stars: fundamental parameters — stars: oscillation — stars: variable: other

## 1. INTRODUCTION

Two decades ago, Krisciunas (1993) and others began finding a small number of early-F stars that seemed to be “variables without a cause.” The first recognized examples of these low-amplitude variable stars included 9 Aurigae (Krisciunas et al. 1993),  $\gamma$  Doradus (Balona et al. 1994; Balona, Krisciunas, & Cousins 1994), HD 111828 (Mantegazza, Poretti, & Antonello 1991), HD 224638 and HD 224945 (Mantegazza & Poretti 1991; Mantegazza, Poretti, & Zerbi 1994). All five stars were found to vary with at least two photometric periods of order one day and to exhibit spectroscopic line-profile variations with the same timescale. All five were also found to lie on or near the main sequence in the Hertzsprung-Russell (H-R) diagram and to cluster around the cool edge of the  $\delta$  Scuti instability strip (Kaye & Handler 1995), despite the fact that their periods are too long to be  $p$ -mode  $\delta$  Scuti pulsations. Results from a multi-site photometric and spectroscopic observing campaign on  $\gamma$  Doradus (*MUSICOS* – 94) led Balona et al. (1996) to the conclusion that “non-radial pulsation is the only viable explanation” for their variability.

Given that  $\gamma$  Doradus is the brightest of these early-F pulsators ( $V = 4.26$ ) and was the first to be detected as a variable star (Cousins & Warren 1963), it serves as the prototype of this new, slowly-growing group of variable stars (Mantegazza, Poretti, & Zerbi 1994; Kaye & Handler 1995; Balona et al. 1996; Kaye et al. 1999a). By 1999, the group of  $\gamma$  Doradus variables had expanded to 13 stars, and Kaye et al. (1999a) described their primary observational characteristics to be (1) spectral type A7–F5, (2) luminosity class IV, IV-V, or V, (3) low-amplitude photometric variability with one or more periods in the range 0.4–3 days, and (4) spectroscopic line-profile variations accompanied by low-amplitude, radial velocity variability. Kaye et al. plotted the 13 known  $\gamma$  Doradus stars in the H-R diagram and found that their larger sample still clustered around the lower right corner of the  $\delta$  Scuti instability strip.

The most recent list of  $\gamma$  Doradus stars is given by Henry, Fekel, & Henry (2007) and contains 66 members (their Table 6). Over half of these stars were identified as  $\gamma$  Doradus candidates by Handler (1999) from his analysis of *Hipparcos* photometry and then confirmed with additional photometry and spectroscopy from our automatic telescopes at Fairborn Observatory. The  $\gamma$  Doradus stars in this larger sample usually have two or more photometric periods in the range 0.3 to 2.6 days and sinusoidal light curves with amplitudes between 0.002 and 0.10 mag (see Henry, Fekel, & Henry

2007, and references therein). Radial velocity variations of 2–4 km s<sup>-1</sup> and changing spectroscopic line profiles are also seen in many members of this larger group (e.g., Krisciunas et al. 1995; Balona et al. 1996; Hatzes 1998; Kaye et al. 1999b,c; Fekel & Henry 2003; Mathias et al. 2004; De Cat et al. 2006). Many observing campaigns on individual  $\gamma$  Doradus stars have confirmed that their photometric and spectroscopic variations arise from high-order, non-radial,  $g$ -mode pulsations (see, e.g., Balona et al. 1996; Hatzes 1998; Breger et al. 1997; Aerts & Kaye 2001; Aerts et al. 2004; Rodriguez et al. 2006b).

Significant theoretical work has been accomplished in the past decade, including determining the pulsational driving mechanisms (e.g., Guzik et al. 2000; Grigahcene et al. 2005; Dupret et al. 2005b; Guzik 2010), understanding the limits of  $\gamma$  Doradus pulsation in the H-R diagram (e.g., Warner, Kaye, & Guzik 2003; Dupret et al. 2004; Grigahcene et al. 2004), mode identification (e.g., Moya et al. 2005; Suarez et al. 2005; Dupret et al. 2005a; Miglio et al. 2008), and asteroseismic modeling (e.g., De Ridder, Arentoft, & Kjeldsen 2006; Moya et al. 2008; Pollard et al. 2008). We refer the reader to Dupret et al. (2007) and Pollard (2009) for recent reviews of the observational and theoretical status of the  $\gamma$  Doradus stars.

In this paper, we describe our photometric survey of a complete, volume-limited sample of 114 late-A to early-F dwarfs and subgiants that lie within a nearby, well-defined region of the solar neighborhood with a volume of 266,600  $pc^3$ . The stars in this sample all lie within the observed  $\gamma$  Doradus instability strip. We use our results to determine the incidence of  $\gamma$  Doradus variables within the instability strip and to compute the space density of  $\gamma$  Doradus stars at our location in the Orion Spur of the Milky Way galaxy. In the process, we have increased the number of bright  $\gamma$  Doradus stars by 23%. Finally, we provide a definitive list of 86 bright, nearby  $\gamma$  Doradus field stars that will be excellent targets for future multi-site, multi-technique, and/or space-based observing campaigns.

## 2. PHOTOMETRIC SURVEY OF 114 $\gamma$ DORADUS CANDIDATES

### 2.1. Creating the Volume-Limited Sample

Our first step was to construct a volume-limited sample of approximately 100 stars that would be well suited to the capabilities of our T12 0.8 m APT and its location at Fairborn Observatory in southern Arizona. The stars would need to be within a  $V$  magnitude range of approximately 5.5 to 8.0 to assure acceptably low coincidence-count corrections for the brighter stars and count rates that are still scintillation limited rather than photon limited for the fainter stars. The stars should lie within a Declination range of  $-10^\circ$  to  $+65^\circ$  so they can be observed at airmass values less than 1.5 from the latitude of Fairborn Observatory. Based on H-R diagrams of the small samples of  $\gamma$  Doradus stars in Aerts, Eyser, & Kestens (1998), Handler (1999), and Kaye et al. (1999a), we set  $B - V$  limits of 0.25–0.38 mag and absolute magnitude  $M_V$  limits of 1.6–3.7 for the sample.

The *Hipparcos* catalog (Perryman et al. 1997) provides an excellent source from which to draw stars for our volume-limited survey because it is complete for  $V \leq 7.5$  and “largely complete” down to  $V = 9$ . We extracted various samples from the *Hipparcos* catalog, varying the parallax limits each time, to find a spherical shell of space centered on the Sun that contained roughly the desired number of stars that satisfied our chosen limits for  $V$ ,  $B - V$ ,  $M_V$ , and declination. We converged to a final parallax range of 15 to 20 mas inclusive, which corresponds to a distance of 50.0–66.7 pc. The spherical shell, truncated at declinations of  $-10^\circ$  and  $+65^\circ$ , has a volume of 266,600 pc<sup>3</sup> and contains 126 stars that meet our search criteria. From this 126-star sample, we eliminated 11 close visual doubles and one eclipsing binary for which the *Hipparcos* magnitudes and colors represented the combined value of the components and not the individual components themselves. The final sample contains 114 stars, only one of which is slightly fainter than  $V = 7.5$  (HD 62196;  $V = 7.67$ ). Therefore, given the completeness limits of the *Hipparcos* catalog cited above, we can be certain that our sample of 114 stars constitutes a statistically-complete, volume-limited sample of  $\gamma$  Doradus candidates.

The selection criteria for the survey stars are summarized in Table 1, and the final sample of 114 stars is given in Table 2. Columns (4), (5), and (6) list the *Hipparcos*  $V$  magnitudes,  $B - V$  color indices, and parallax values for all stars; column (7) gives the absolute magnitudes computed from the  $V$  magnitudes and parallaxes (ignoring interstellar extinction). Column (8) lists the *Hipparcos* variability type; we note that only 10 of the 114 stars are flagged as possible variable stars with only three as periodic variables.

## 2.2. Photometric Observations of the 114 Star Sample

The initial photometric survey of the sample of 114 stars was carried out between 2001 April and 2002 July with our T12 0.8 m APT at Fairborn Observatory. This APT and its two-channel precision photometer are functionally identical to our T8 APT described in Henry (1999). The photometer uses two temperature-stabilized EMI 9124QB photomultiplier tubes mounted behind a dichroic beam splitter to measure photon count rates simultaneously through Strömrgren  $b$  and  $y$  filters. We programmed the telescope to make nightly observations of all target stars that were observable on a given night. Three comparison stars in the vicinity of each target star, designated A, B, and C, were measured along with the target star, D, in the following sequence, termed a group observation: DARK, A, B, C, D, A, SKY<sub>A</sub>, B, SKY<sub>B</sub>, C, SKY<sub>C</sub>, D, SKY<sub>D</sub>, A, B, C, D. We used a diaphragm 45'' in diameter and an integration time of 20 seconds for all measurements.

Each completed group observation was reduced to form three independent measures of each of the six differential magnitudes D–A, D–B, D–C, C–A, C–B, and B–A. These differential magnitudes were corrected for differential extinction with nightly extinction coefficients and transformed to the standard Strömrgren system with yearly mean transformation coefficients. The three independent measures of each differential magnitude were combined, giving one mean data point per complete group sequence for each of the six differential magnitudes. To increase the precision of

the observations, we combined the Strömgen  $b$  and  $y$  differential magnitudes into a single  $(b+y)/2$  passband. The typical precision of a group mean acquired in good conditions is 0.0015–0.0020 mag. Data taken in non-photometric conditions were eliminated by discarding all group sequences in which one or more of the mean differential magnitudes had a standard deviation of 0.01 mag or greater. For additional information on the telescope, photometer, observing procedures, data reduction techniques, and photometric precision, see Henry (1999) and Eaton, Henry, & Fekel (2003).

### 2.3. Photometric Results from the 114 Star Sample

Columns (9), (10), and (11) of Table 2 give the results of the 2001–2002 photometric survey with the T12 APT. The APT typically acquired several tens of group observations over the course of each star’s observing season, as shown in Column (9), where  $N_{obs}$  is the number of good group observations that survived the 0.01-mag “cloud filter” described above and also passed a visual inspection to eliminate any remaining outliers. A few of the stars were reobserved in 2006 for a couple of nights of monitoring observations and therefore have up to several hundred observations. Column (10) gives the Julian date range for each star over which the survey observations were acquired. Column (11) gives an estimate of each star’s intrinsic brightness variability,  $\sigma_{star}$ , in the combined  $(b+y)/2$  passband. This variability estimate is computed by subtracting the total variance of the most constant set of comparison star differential magnitudes ( $\sigma_{C-A}^2$ ,  $\sigma_{C-B}^2$ , or  $\sigma_{B-A}^2$ ) from the total variance of the program star differential magnitudes computed against the mean brightness of the two best comparison stars ( $\sigma_{D-CA}^2$ ,  $\sigma_{D-CB}^2$ , or  $\sigma_{D-BA}^2$ ). Therefore, our brightness variability estimate, given as the standard deviation  $\sigma_{star}$  in column (11) of Table 2, represents an approximation of the intrinsic stellar variability in each target star, corrected for measurement errors and possible low-level variability in the comparison stars.

In cases where the program star and the two best comparison stars are all constant or nearly so, then  $\sigma_{star}^2$ , the difference of two variances, can have either a small positive or a small negative value due to random measurement uncertainties. If  $\sigma_{star}^2$  is negative, then  $\sigma_{star}$  is imaginary so we set its value to zero in Table 2 since, in those cases, we clearly have not resolved any variability in the program star above the expected uncertainties in the measurements. Small positive values of  $\sigma_{star}$  are recorded as such in Table 2, but long experience with our APTs (e.g., Henry, Fekel, & Hall 1995; Henry 1999; Henry et al. 2000; Lockwood et al. 2007) has shown that only  $\sigma_{star}$  values of 0.002 mag or higher reliably indicate variability for stars brighter than  $V = 8.0$ . Therefore, we classify the 77 stars in Table 2 with  $\sigma_{star} < 0.002$  mag as constant stars (column (12)). The remaining 37 stars have  $\sigma_{star} \geq 0.002$  mag and so are excellent  $\gamma$  Doradus candidates.

Frequency analyses of the 114 survey stars confirmed the presence of short-period photometric variability in all 37 stars with  $\sigma_{star} \geq 0.002$  mag. All 114 stars are plotted in the H-R diagram in Figure 1, where the 37 variables are plotted as filled circles. As expected, the frequency spectra exhibit severe aliasing because the stars were generally observed only once per night. Based on these frequency spectra alone, we cannot distinguish between  $\gamma$  Doradus stars with periods in the

range 0.3–3.0 days and the more rapidly pulsating  $\delta$  Scuti stars with periods between 0.02 and 0.25 days. We designed this initial survey only to *find* all low-amplitude variables in the survey sample; we then made additional photometric and spectroscopic observations of the variable stars in the survey to improve the frequency analyses, to detect any binary stars among the variables, and to enable reliable variable star classifications and confirmation of new  $\gamma$  Doradus stars.

### 3. FOLLOW-UP PHOTOMETRY OF THE $\gamma$ DORADUS CANDIDATES

Eight of the 37  $\gamma$  Doradus candidates found in the 114-star survey are known  $\gamma$  Doradus stars from our earlier work; we kept them in the T12 survey for completeness and as a quality control measure to confirm they would be “discovered” in the survey. These eight stars include HD 69715, HD 99329, HD 124248, HD 165645, HD 167858, HD 207233, and HD 213617, confirmed as  $\gamma$  Doradus stars by Henry, Fekel, & Henry (2007), and the hybrid  $\gamma$  Doradus /  $\delta$  Scuti pulsator HD 8801 found by Henry & Fekel (2005). All eight of these known  $\gamma$  Doradus stars were detected as variable stars in our survey observations. Since detailed analyses of these eight stars have already been published, we did not make follow-up observations of them. We limited our follow-up photometry and spectroscopy to the remaining 29 variable stars.

#### 3.1. Observations

We used our T3 0.4 m APT at Fairborn Observatory to acquire the new higher-cadence Johnson *BV* photometric follow-up observations of the remaining 29 variables identified in the T12 survey. The observations were acquired between 2004 September and 2006 July; each star was observed over a single observing season. T3 is the same telescope used in most of our previous work on  $\gamma$  Doradus stars. We shortened the group observing sequence used for the survey observations by retaining only the two best comparison stars from the survey and scheduling them as the check and comparison stars in the following sequence: K, S, C, V, C, V, C, V, C, S, K, where K is a check star, C is the primary comparison star, V is the program star, and S is a sky reading.

Up to five group observations of each program star were acquired every clear night at intervals of two to three hours throughout each star’s observing season. Each star was also observed continuously for several hours on one night near its opposition. This observing strategy helps to weaken the one-day aliases in our period analyses and allows us to discriminate between  $\gamma$  Doradus variability (0.3–3.0 days) and  $\delta$  Scuti variability (0.02–0.25 days). We refer the reader to Henry, Fekel, & Henry (2007) for a more complete description of the instrument, observing techniques, and data reduction procedures.

### 3.2. Analyses

We performed period-search analyses of the new follow-up photometry on the remaining 29 variables from the survey. Our period-search technique, based on least-squares fitting of sinusoids, is described in our earlier papers (e.g., Henry et al. 2001) and is well suited for finding multiple signals in our low-amplitude light curves. Briefly, we search for periodicity in the program star minus comparison star ( $V - C$ ) differential magnitudes over the frequency range 0.01–30.0 day<sup>-1</sup>, which corresponds to the period range 0.033–100 days. We fix the first detected frequency but not its associated amplitude, phase, or mean brightness level and then introduce that frequency as a fixed parameter into a new search for additional frequencies. In an iterative process, each new search is carried out while simultaneously fitting a single new mean brightness level along with the amplitudes and phases of all frequencies introduced as fixed parameters. In the resulting least-squares frequency spectra, we plot the fractional reduction of the total variance (the reduction factor) versus the trial frequency.

We found 17 of the 29 stars to exhibit periodic variability within the period range of  $\gamma$  Doradus stars. Two of those stars (HD 65526 and HD 224945) were previously confirmed to be  $\gamma$  Doradus variables by Handler & Shobbrook (2002) and Mantegazza, Poretti, & Zerbi (1994), respectively; the other 15 stars are new variables. In addition, we found nine stars with variability on  $\delta$  Scuti timescales, only one of which was a known  $\delta$  Scuti star (Paunzen et al. 1998). Also, there were three stars among the 29 variables for which we could not determine definitive periods.

The analyses and discussion in the following sections are concerned only with the 15 new  $\gamma$  Doradus candidates plus HD 65526 and HD 224945 (mentioned above) since those two stars lack extensive APT data sets. The parameters of these 17 stars are printed in bold font in Table 2. We will refer to these 17 stars as our “ $\gamma$  Doradus candidates.” The analyses of the nine  $\delta$  Scuti variables and the three unresolved variables may appear in a future paper(s).

Table 3 lists the comparison and check stars used for each of the 17  $\gamma$  Doradus candidates as well as the standard deviations of the  $V - C$  and  $K - C$  observations. The  $\sigma_{(K-C)}$  values demonstrate that all comparison and check stars are constant to a few millimagnitudes, which is approximately the limit of precision for the T3 APT. The individual photometric observations of the 17  $\gamma$  Doradus candidates are given in electronic format in Table 4.

The results of our period analyses of the 17  $\gamma$  Doradus candidates are summarized in Table 5. The frequencies and corresponding periods in both  $B$  and  $V$  are given in columns 5 and 6; the uncertainty in each frequency measurement is estimated from the width of its peak in the frequency spectrum. The majority of the  $B$  and  $V$  frequency pairs agree within  $\pm 1 \sigma$ , the rest within  $\pm 2 \sigma$  or a bit more, indicating that our estimated uncertainties are realistic. We also note that Cuypers et al. (2009) used the 1.2 m Mercator telescope on La Palma over a period of four years to monitor a sample of 21 gamma Doradus stars, 19 of which we have confirmed as  $\gamma$  Doradus variables in our earlier papers. The vast majority of our frequencies in these 19 stars were confirmed in the Cuypers paper.

In several cases, we find very close frequencies in the same star that are separated by no more than  $0.01 \text{ day}^{-1}$  or so. A conservative criterion for frequency resolution is given by Loumos & Deeming (1978) to be  $1.5/T$  where  $T$  is the total range of the observations in days. Since most of our data sets span  $\sim 200$  days, the limit of our frequency resolution is typically around  $0.0075 \text{ day}^{-1}$ , ensuring that we can resolve such close frequencies. The peak-to-peak amplitudes reported in column (7) of Table 5 are determined for each frequency *without* prewhitening for the other frequencies. The  $B$  amplitudes range from 54 mmag down to 5 mmag and average 1.3 times larger than those in  $V$ . The individual  $B/V$  amplitude ratios and their uncertainties are listed for each frequency in column (8). Finally, times of minimum light for each frequency are given in column (9); in each case, the times of minimum in the two passbands agree within their uncertainties, so there are no detectable phase shifts in our two-color photometry.

In the same way, the  $(K - C)$  differential magnitudes were also analyzed to search for periodicities that might exist in the comparison and check stars. None of the 17  $(K - C)$  time series showed any evidence for periodicity, so we are assured that all periods reported in Table 5 are intrinsic to the program stars.

Least-squares frequency spectra and phase diagrams of the  $B$  observations for all of the 17  $\gamma$  Doradus candidates are given in §6 below. Although all analyses were done over the frequency range of  $0.01\text{--}30.0 \text{ day}^{-1}$ , the least-squares frequency spectra are plotted over more restricted ranges since none of the stars exhibited variability above  $5 \text{ day}^{-1}$ . In particular, no higher frequencies that could be attributed to  $\delta$  Scuti-type variability were found in any of the 17 stars, so we have not identified any new hybrid variables. The plots of the least-squares frequency spectra show the results of successively fixing each detected frequency until no further frequencies could be found in both passbands. For illustrative purposes only, the phase diagrams are plotted for each frequency after the data sets have been prewhitened to remove the other detected frequencies.

## 4. FOLLOW-UP SPECTROSCOPY OF THE $\gamma$ DORADUS CANDIDATES

### 4.1. Observations

We obtained our high-dispersion spectroscopic observations of the  $\gamma$  Doradus candidates at the Kitt Peak National Observatory with the coudé feed telescope, coudé spectrograph, and a CCD detector. Except for two spectrograms of HD 99267 acquired in 1995 April, our observations were collected from 2003 October to 2008 September. We have three to 13 spectra of each star. The vast majority of the spectrograms were obtained with a TI CCD, are centered at  $6430 \text{ \AA}$ , cover a wavelength range of about  $80 \text{ \AA}$ , and have a two-pixel resolution of  $0.21 \text{ \AA}$  or a resolving power of just over 30,000. The TI CCD was unavailable in 2008 September, and so a Tektronics CCD, designated T1KA, was used instead. With that CCD the spectrum was centered at  $6400 \text{ \AA}$ . Although the wavelength range covered by the T1KA increased to  $172 \text{ \AA}$ , the two-pixel resolution was  $0.34 \text{ \AA}$ , reducing the resolving power to 19,000. Typical signal-to-noise ratios of our spectra



range between 150 and 250.

## 4.2. Analyses

The reduction and analysis of the spectroscopic data are extensively described in Fekel, Warner, & Kaye (2003). Here, we provide a summary of our analysis procedures but also include additional information that is specific to some of the program stars in the current work. The basic properties of the 17  $\gamma$  Doradus candidates, determined from our spectroscopic observations, are summarized in Table 6.

The spectra of our program stars were compared with the spectra of various reference stars with well-determined spectral types. Because the lines of late A- and F-type stars in the 6430 Å region have little sensitivity to luminosity, we can only determine the spectral classes of the program stars from our spectra, which we list in column (6) of Table 6. To determine the luminosity classes given in column (7), we computed absolute magnitudes from the *Hipparcos* magnitudes and parallaxes (Perryman et al. 1997), which were then compared with canonical values of Gray (1992). Because we do not derive our luminosity classes from an examination of the spectrum itself, we do not use Roman numerals to represent those classes but instead call them dwarfs.

The strongest features in the 6430 Å region are primarily iron and calcium lines, enabling us to estimate the iron abundances of our program stars because our reference stars have spectroscopically determined [Fe/H] values in the literature. Unless otherwise noted in the discussions of the individual systems, the program stars have [Fe/H]  $\sim$ 0.0, indicating a metallicity close to the solar value. Because the 6430 Å region has both iron and calcium lines, we are able to identify the abundance peculiarities associated with Am stars.

We also have determined the projected rotational velocities of the 17  $\gamma$  Doradus candidates. For  $v \sin i$  values  $\leq 60 \text{ km s}^{-1}$ , we followed the procedure of Fekel (1997). However, several of the stars have larger values. In such cases, as well as for the stars having composite spectra, we determined the  $v \sin i$  values from spectrum addition fits (Fekel, Warner, & Kaye 2003). Fekel, Warner, & Kaye (2003) provide the estimated uncertainties of these rotational velocities, which depend on the individual  $v \sin i$  values.

A colon after a derived value in Table 6 indicates greater than usual uncertainty. For the spectral classes and projected rotational velocities, this is typically because a star has very broad and shallow lines or because the components of a binary have a large magnitude difference, making the lines of the secondary component very weak. Weak, broad lines also reduce the precision of the measured radial velocities.

Individual radial velocities, determined by cross correlation, are listed in Table 7 along with comments about the spectra. The velocities of our standard stars are adopted from Scarfe, Batten, & Fletcher (1990). The precision of our velocities depends primarily on the projected rotational velocities of

the stars. For narrow lined stars with  $v \sin i$  values that are less than  $40 \text{ km s}^{-1}$ , we estimate radial velocity uncertainties of  $0.2\text{--}0.3 \text{ km s}^{-1}$ . For faster rotating stars with  $v \sin i$  values between  $40$  and  $80 \text{ km s}^{-1}$  we estimate velocity uncertainties of  $0.5 \text{ km s}^{-1}$ . For the most rapidly rotating stars in our sample, those with  $v \sin i$  values of  $90 \text{ km s}^{-1}$  or larger, we estimate uncertainties of  $1\text{--}2 \text{ km s}^{-1}$ . Our new velocities, supplemented by older and generally lower precision velocities, enable us to establish in most cases whether a star is single or binary. However, the  $\gamma$  Doradus variables also have line-profile variations resulting from pulsation, which usually cause velocity variability of at least several  $\text{km s}^{-1}$  (e.g., Mathias et al. 2004). In the sections on the individual  $\gamma$  Doradus variables we discuss a few cases where the determination of whether a star is single or a single-lined spectroscopic binary is problematic. In column (9) of Table 6, stars for which we believe orbital motion is detected are indicated as “Binary”, while the mean radial velocities and their standard deviations are listed for the stars that we conclude are single.

For single stars and single-lined spectroscopic binaries, the determination of basic properties is relatively straightforward. However, the spectra of four of the 17 stars in our sample (HD 38309, HD 114447, HD 145005, HD 220091) show two sets of lines (see Figures 2, 3, 4, and 5), making the determination of the magnitudes and colors of the individual components more difficult than for a single star. To obtain individual magnitudes and colors for the components of a binary, a  $V$  magnitude difference is needed. The spectrum addition method described in Fekel, Warner, & Kaye (2003) produces a continuum luminosity ratio, which results in a magnitude difference that is a minimum value if the secondary has a later spectral type than the primary. If the spectral type difference is small, the continuum luminosity ratio can be adopted as the luminosity ratio from which the magnitude difference can be determined. Otherwise the continuum luminosity ratio must be adjusted for the difference in spectral types before estimating a magnitude difference. Results for the individual components of the four stars mentioned above are included in Table 6.

## 5. CRITERIA FOR CONFIRMING $\gamma$ DORADUS VARIABILITY

Throughout our series of papers on  $\gamma$  Doradus stars (see Henry, Fekel, & Henry 2007, and references therein), we have consistently used the following criteria for confirming stars as  $\gamma$  Doradus variables: (1) late-A or early-F spectral class, (2) luminosity class IV or V, and (3) periodic photometric variability in the  $\gamma$  Doradus period range that is attributable to pulsation. Our spectroscopic observations establish the spectral types of each candidate. Our photometric observations are numerous and extensive enough (typically several hundred observations over a full observing season) to minimize the effects of one cycle per day aliasing and provide the correct period identifications. This is important since the cadence of the *Hipparcos* observations, from which Handler’s candidates were identified, can result in spurious photometric periods, especially for multiperiodic stars (e.g., Eyer & Grenon 2000).

Our photometric and spectroscopic observations are also used to confirm the variability mechanism(s), especially for stars with only one photometric period. These stars could be ellipsoidal

variables in close binary systems or rapidly-rotating starspot variables rather than pulsating stars. Multiple spectroscopic observations that do not exhibit large-amplitude, short-period radial velocity variations argue strongly against the ellipticity effect. The early-F spectral types of the candidates and the high level of coherence in the light curves over hundreds of cycles both argue strongly against starspot variability. Furthermore, our observed photometric  $B/V$  amplitude ratios are indicative of pulsations in these stars. Henry et al. (2000) demonstrated that ellipsoidal variables have  $B/V$  amplitude ratios close to 1.00 while starspot variables have typical  $B/V$  ratios around 1.12–1.14. The 17 stars analyzed in this paper have a weighted mean  $B/V$  amplitude ratio of  $1.33 \pm 0.03$ , in agreement with theoretical models of  $\gamma$  Doradus stars with low spherical degree ( $\ell = 1, 2$ ) non-radial pulsations (e.g., Garrido 2000).

Our Johnson  $BV$  photometry and limited spectroscopic observations are *not* sufficient to allow us to identify uniquely the spherical degree ( $\ell$ ) or the azimuthal order ( $m$ ) of the pulsations. Stamford & Watson (1981) demonstrated for non-radial pulsations that the wavelength dependence of the photometric amplitude and the phase shift between various photometric bands is a function of  $\ell$  but not  $m$  (with an additional dependence of the amplitude on the inclination of the pulsating star’s rotation axis). In practice, the identification of the spherical degree from photometric observations has many subtle difficulties (e.g., Garrido 2000; Sterken 2002). We can only note that our observed  $B/V$  amplitude ratios and lack of detectable phase shifts between the two photometric bands (Table 5) are consistent with spherical degree  $\ell = 1$  or  $\ell = 2$  and probably inconsistent with  $\ell = 3$  (Garrido 2000). Our spectroscopic observations, obtained primarily to determine spectral class,  $v \sin i$ , and to search for evidence of duplicity, are not nearly numerous enough for line-profile variability and mode-identification studies. Such studies require much more extensive multi-site, multi-technique observing campaigns (e.g., Handler et al. 2002; Aerts et al. 2004; Mathias et al. 2004).

## 6. CONFIRMATION OF 17 NEW $\gamma$ DORADUS VARIABLES

In this section, we examine in detail our photometric and spectroscopic observations of the 17 remaining  $\gamma$  Doradus candidates that, along with previous results from the literature, allow us to determine the properties of these 17 stars and, thereby, confirm them as new  $\gamma$  Doradus variables.

### 6.1. HD 6568 = HIP 5209

We have obtained 13 red-wavelength spectrograms of HD 6568, which show only a single component with a moderate projected rotational velocity of  $55 \text{ km s}^{-1}$ . We determine that the star is an F1 dwarf. Our radial velocities from eight different epochs have a range of  $23 \text{ km s}^{-1}$ , indicating that the star is a spectroscopic binary with an, as yet, unseen lower-mass companion. The velocities that have been obtained to date suggest an orbital period of 126.5 days if the orbit

is circular or nearly circular. Observations are continuing to determine orbital elements.

The *Hipparcos* catalog does not flag HD 6568 as a variable star (Perryman et al. 1997), but our T12 survey observations (Table 2) reveal definite variability with a standard deviation of 0.0066 mag. Least-squares frequency spectra of our T3 follow-up observations in the  $B$  are plotted in Figure 6, and the results of our period analyses are given in Table 5. We find two closely spaced periods of 0.73421 and 0.74538 days with amplitudes of 18 and 15 mmag, respectively; we detect the same two periods in the  $V$  band observations. The  $B$  observations are phased with these periods and times of minimum given in Table 5 and plotted in Figure 7, which shows clear sinusoidal variations at both periods. The weighted mean of the ratio of the photometric amplitude in  $B$  to the amplitude in  $V$  is  $1.36 \pm 0.13$  for the two periods, consistent with other  $\gamma$  Doradus variables (e.g., Henry, Fekel, & Henry 2007) and inconsistent with the ellipticity effect or starspots (Henry et al. 2000, their Table 8). Given the star’s F1 dwarf classification, the two independent periods in the  $\gamma$  Doradus period range, and the  $B/V$  amplitude ratio, we confirm the primary component of HD 6568 as a new  $\gamma$  Doradus variable.

## 6.2. HD 17163 = HR 816

The only previous MK spectral classification of HD 17163 is by Abt & Morrell (1995), who called the star an A9 III. We estimate an F1: spectral class but find that it has a dwarf luminosity. The broad-lined nature of HD 17163, as discussed below, makes our classification more difficult than usual. The star may be somewhat metal rich compared to the Sun.

Danziger & Faber (1972) reported  $v \sin i = 90 \text{ km s}^{-1}$ , while Abt & Morrell (1995) found  $108 \text{ km s}^{-1}$ , which Royer et al. (2002a) rescaled to  $120 \text{ km s}^{-1}$ . Our projected rotational velocity value of  $105 \text{ km s}^{-1}$  is in reasonable agreement with the past determinations.

HD 17163 was a part of several extensive radial velocity surveys. Based on four spectra, Shajn & Albitzky (1932) reported an average velocity of  $19.9 \pm 2.5 \text{ km s}^{-1}$ . From three observations Harper (1937) gave it a mean velocity of  $16.0 \pm 4.9 \text{ km s}^{-1}$  and commented that its spectrum had numerous fuzzy lines. Wilson & Joy (1950) presented results from three additional spectrograms that have dispersions of  $36 \text{ \AA mm}^{-1}$  (Abt 1970). Those Mount Wilson observations produce an average velocity of  $22.0 \pm 7.4 \text{ km s}^{-1}$  and a range of  $25 \text{ km s}^{-1}$ . Despite noting the broad lines of the star and the reasonable agreement of their average velocity with previous means, Wilson & Joy (1950) concluded that the velocity of HD 17163 is variable. Measurement of our three KPNO spectrograms results in an average velocity of  $26.2 \pm 0.3 \text{ km s}^{-1}$ , so there is a  $10 \text{ km s}^{-1}$  range in the average velocities found at the four different observatories. Even so, given the broad, shallow lines of this star and the pulsation that we have discovered, there is no strong evidence of velocity variability resulting from orbital motion, and so we conclude that the star is single.

The *Hipparcos* satellite observed HD 17163 58 times during the course of its 3.5 year mission, resulting in its classification as a constant star (Perryman et al. 1997). Nonetheless, our T12 survey

observed it 53 times and found it to be slightly variable with a standard deviation of 0.0030 mag (Table 2).

We find a single period of 0.42351 days in the T3 APT follow-up photometry with a  $B$  amplitude of 8 mmag (Figs. 8 and 9; Table 5). The light curve approximates a sinusoid when phased with this period. The  $B/V$  amplitude ratio is  $1.16 \pm 0.20$ , consistent with pulsation but also consistent with ellipsoidal variation and the rotational modulation of starspots due to the large uncertainty of the amplitude ratio. Ellipsoidal variation in a close binary system is precluded by the fact that our spectroscopy does not reveal large radial velocity changes. Likewise, starspot activity (implying a stellar rotation period of 0.42351 days) is unlikely because of the star’s early spectral type and the coherency of the light curve over hundreds of cycles. As a result, we conclude that the photometric variability is due to pulsation and confirm this F1 dwarf as a new  $\gamma$  Doradus star.

### 6.3. HD 25906 = HIP 19408

To compile basic data for stars that were included in the *Hipparcos* mission, Duflot et al. (1995) acquired six objective-prism spectra with a dispersion of  $80 \text{ \AA mm}^{-1}$ . From those plates they measured a mean radial velocity of  $37 \text{ km s}^{-1}$  with an rms of  $4.2 \text{ km s}^{-1}$ .

From our spectrograms we have determined an F1 spectral class for HD 25906, and its *Hipparcos* parallax (Perryman et al. 1997) results in a dwarf luminosity class. The star has a moderate projected rotational velocity of  $64 \text{ km s}^{-1}$ . Our seven observations show modest night-to-night radial velocity variations, and their mean velocity is  $6.5 \pm 1.8 \text{ km s}^{-1}$ . The lines of the two spectra with the largest velocity differences have significant asymmetries, which presumably result from pulsation. However, our average velocity, with observations from five different epochs, differs by  $30 \text{ km s}^{-1}$  from the mean of Duflot et al. (1995). Those earlier velocities are from low dispersion spectra, and so high precision is not expected. Indeed, the individual velocities, which span a three yr period, range from 25 to  $53 \text{ km s}^{-1}$  and differ on consecutive nights by  $16 \text{ km s}^{-1}$  (Duflot et al. 1995). Their velocity range does not overlap ours (Table 7), and so we conclude that the star is probably a spectroscopic binary but note that additional observations will be needed to confirm its status. In Table 6 we list HD 25906 as having a variable orbital velocity, but append a question mark to indicate our uncertainty.

The *Hipparcos* mission obtained 119 photometric measurements of HD 25906, but, based on those observations, the star could not be classified as either constant or variable (Perryman et al. 1997). Our 249 T12 survey observations indicate a brightness variability of 0.0050 mag (Table 2). Analysis of the T3 follow-up observations found three independent periods of 0.79164, 0.81646, and 1.34192 days with Johnson  $B$  amplitudes of 9, 6, and 6 mmag, respectively (Figs. 10 and 11; Table 5). The light curves at all three periods are sinusoidal, and the weighted mean of the three  $B/V$  amplitude ratios from Table 7 is  $1.26 \pm 0.15$ . Therefore, based on the star’s F1 dwarf spectral type, asymmetric spectroscopic line profiles, multiple photometric periods in the  $\gamma$  Doradus period

range, and its  $B/V$  amplitude ratio, we confirm HD 25906 as a new  $\gamma$  Doradus variable.

#### 6.4. HD 31550 = HIP 23117

We obtained five spectra of HD 31550 and find it to be a F0 dwarf. The line strengths of HD 31550, compared with those of our reference stars, suggest that HD 31550 may be modestly metal poor compared to the Sun. Our mean projected rotational velocity is  $32 \text{ km s}^{-1}$ . Our five velocities have an average of  $17.6 \pm 0.5 \text{ km s}^{-1}$  and show no evidence of orbital motion. Earlier, Mason et al. (2001) obtained a lone speckle observation of HD 31550 and found no duplicity. We conclude that the star is single.

The *Hipparcos* catalog has 60 photometric observations but does not claim intrinsic variability (Perryman et al. 1997). Our T12 survey obtained 247 brightness measurements that scattered about their mean with a standard deviation of only 0.0020 mag (Table 2), equal to our defined lower limit of detectable variability. Even so, we find a variability period of 1.49566 days in the T3 photometry with a  $B$  amplitude of 7 mmag (Figs. 12 and 13; Table 5). The light curve is sinusoidal when phased with this period, although it is badly binned in phase because the period is almost exactly 1.5 days. The  $B/V$  amplitude ratio is  $1.13 \pm 0.21$ , which is consistent with both ellipsoidal and spot variation as well as pulsation. However, ellipsoidal variation in a close binary system can be ruled out by the fact that our spectroscopy, with observations taken both one and two days apart, does not reveal large radial velocity changes. Likewise, starspot activity is unlikely because of the early spectral type of the star and the coherency of the light curve over hundreds of cycles. We conclude that the photometric variability in HD 31550 is due to pulsation and confirm this F1 dwarf as a new  $\gamma$  Doradus star.

#### 6.5. HD 38309 = HR 1978 = ADS 4333A = HIP 27118

HD 38309 is component A of a visual triple system with components B and C separated from A by  $17''$ . According to the notes of The Bright Star Catalogue (Hoffleit 1982), these two additional components are optical companions of component A. Abt & Morrell (1995) classified HD 38309 as F0 IV. Danziger & Faber (1972) found a  $v \sin i$  value of  $100 \text{ km s}^{-1}$ , which Wolff & Simon (1997) revised to  $86 \text{ km s}^{-1}$ . Abt & Morrell (1995) estimated a projected rotational velocity of  $75 \text{ km s}^{-1}$ , which Royer et al. (2002a) rescaled to  $86 \text{ km s}^{-1}$ . Abt (1970) listed a single Mount Wilson Observatory radial velocity of  $9.0 \text{ km s}^{-1}$ , while Shajn & Albitzky (1932) found a similar mean velocity of  $7.0 \pm 2.1 \text{ km s}^{-1}$  from four plates.

HD 38309 is listed in Part G, the Acceleration Solution section, of the Double and Multiple Star Appendix of the *Hipparcos* catalog (Perryman et al. 1997). Unlike most of the stars observed by *Hipparcos*, the successive positions of HD 38309 during the three yr mission could not be satisfactorily modeled with just five parameters (position, parallax, and proper motion). Instead, a seven

parameter model that included two additional terms for acceleration, which is the time derivative of the proper motion, was adopted to account for a curvature in the stellar trajectory. A star with such a solution often turns out to have a companion with an orbital period that is too long to be derived from only the *Hipparcos* data.

Our eight red-wavelength spectra show a composite spectrum as does a single spectrum in the ELODIE archive (Moultaka et al. 2004). Each line of HD 38309 consists of a broad component with a weak, narrow component near its center (Figure 2). As suggested by its listing in Part G of the *Hipparcos* catalog, HD 38309 is indeed a binary. The broad-lined star, component Aa, we classify as F1, while the spectral class of the narrow-lined component, Ab, is G1:, and both stars are dwarfs. Guided by our spectrum addition fits, we adopt a magnitude difference,  $\Delta V$ , of 2.1. We also measure projected rotational velocities of 95: and 5: km s<sup>-1</sup>, for components Aa and Ab, respectively, so our  $v \sin i$  value of component Aa is similar to those previously determined.

To date, we have obtained nine radial velocity observations of HD 38309 at eight different epochs that span four yr. Radial velocities of component Ab, the narrow-lined star, show a systematic velocity decrease of nearly 5 km s<sup>-1</sup> (Table 7) during that period, indicating that it is a spectroscopic binary. The velocity of component Aa also shows variability, but because it has an early-F spectral type, its velocity changes are a combination of pulsation plus orbital motion. We assume that Aa is the binary companion of Ab.

The *Hipparcos* catalog lists 66 brightness measurements for HD 38309 but is unable to classify it as constant or variable. The 214 brightness measurements from our T12 survey (Table 2) have a standard deviation of 0.0033 mag and thereby show that HD 38309 is, indeed, a low-amplitude variable. Analysis of the follow-up observations from the T3 APT revealed three independent periods of 0.37703, 0.35993, and 0.34713 days with  $B$  amplitudes of 9, 7, and 5 mmag, respectively (Figs. 14 and 15; Table 5). The light curves at all three periods are sinusoidal, and the weighted mean of the three  $B/V$  amplitude ratios from Table 5 is  $1.07 \pm 0.14$ . This is somewhat low for a  $\gamma$  Doradus variable, but we note that our photometric measurements (made with a 55" diaphragm) were diluted by the G1 dwarf spectroscopic companion as well as by the two visual components B and C. Consequently, the  $B/V$  amplitude ratio is somewhat biased. Based on the star's F1 dwarf spectral type, asymmetric spectroscopic line profiles, and multiple photometric periods in the  $\gamma$  Doradus period range, we confirm component Aa of HD 38309 as a new  $\gamma$  Doradus variable.

## 6.6. HD 45638 = HR 2351

Cowley & Fraquelli (1974) called HD 45638 an A9 IV star, while Abt & Morrell (1995) similarly classified the star as F0 IV. Gray & Garrison (1989) designated it a mild Am star with spectral classes of A9/F0/F2 for the Ca K line, hydrogen lines, and metal lines, respectively. Our spectrum of the metal lines in the 6430 Å region is best fitted by an A9 reference star, and the Ca I lines in our spectrum are consistent with that classification. We find that the star is a dwarf, making it

less luminous than previous classifications.

Abt & Morrell (1995) found a  $v \sin i$  value of  $35 \text{ km s}^{-1}$ , which was revised by Royer et al. (2002a) to  $44 \text{ km s}^{-1}$ . Our average projected rotational velocity is  $38 \text{ km s}^{-1}$  and in reasonable agreement with both results.

The only previous velocities of HD 45638 are those of Young (1945), who included it in a radial velocity survey of 681 stars at the David Dunlap Observatory. He determined a mean velocity of  $40.6 \pm 1.3 \text{ km s}^{-1}$  from four plates. Our four velocities are in excellent agreement, having an average of  $42.4 \pm 0.4 \text{ km s}^{-1}$ ; the star appears to be single.

The results of our photometric survey with the T12 APT are given in Table 2. We derived a standard deviation of 0.0039 mag from our 160 brightness measurements, indicating that HD 45638 is a low-amplitude variable. The *Hipparcos* catalog contains only 43 brightness measurements and does not rule on the constancy or variability of the star. Analysis of our follow-up observations from T3 gives a single period of 0.86046 day with a  $B$  amplitude of 11 mmag (Figs. 16 and 17; Table 5). The sinusoidal light variations have a  $B/V$  amplitude ratio of  $1.41 \pm 0.15$  mag, which is consistent with pulsation. Ellipticity as the cause of the light variability is ruled out by the observed lack of radial velocity variations as well as by the amplitude ratio. We confirm HD 45638 as a new  $\gamma$  Doradus variable.

## 6.7. HD 62196 = HIP 37802

From its Strömgren photometric indices, Olsen (1980) concluded that HD 62196 is a metal-weak F star, and, in a major survey of F and G dwarfs in the solar neighborhood, Nordström et al. (2004) computed  $[\text{Fe}/\text{H}] = -0.64$  from those observations. Jäschek, Andriolat, & Jäschek (1989) included it in a spectroscopic survey of 350 F-type stars. Using moderate dispersion spectra, they found it to be metal weak, classifying its hydrogen lines as F3 but giving its metal lines a spectral class of A9. We determine that the star is an F2 dwarf and estimate  $[\text{Fe}/\text{H}] \sim -0.5$  from the reference star fits to our spectrum in the  $6430 \text{ \AA}$  region. Thus, we concur that the star is metal weak.

Fehrenbach et al. (1987) obtained four objective prism spectra of HD 62196 and found an average velocity of  $-3 \text{ km s}^{-1}$ . Over a timespan of 11 years Nordström et al. (2004) obtained eight radial velocities that have a mean of  $-9.0 \text{ km s}^{-1}$  but a large standard deviation of  $5.1 \text{ km s}^{-1}$ , indicating that this star is a spectroscopic binary. They also determined a  $v \sin i$  value of  $7 \text{ km s}^{-1}$  in agreement with an average  $v \sin i$  of  $6 \text{ km s}^{-1}$  determined from our spectra. Our eight radial velocities, acquired at five epochs, support the conclusion that HD 62196 is a spectroscopic binary and suggest a period of  $\sim 3.3$  yr. We are obtaining additional observations to determine an orbit.

The *Hipparcos* catalog has only 37 brightness measurements of HD 62196 and does not classify the star as either constant or variable. Our T12 survey, however, reveals brightness variability of



0.0049 mag (Table 2). Analysis of our T3 follow-up photometry reveals two closely-spaced periods of 1.00341 and 0.99236 days with  $B$  amplitudes of 14 and 13 mmag, respectively (Figs. 18 and 19; Table 5). The prewhitened light curves in Figure 19 both exhibit sinusoidal light variations of nearly identical amplitudes. Ellipticity as the cause of the light variability is ruled out by the observed lack of short-term radial velocity variations as well as by the presence of two independent periods. Brightness modulation by starspots is ruled out by the large weighted mean  $B/V$  amplitude ratio of  $1.78 \pm 0.10$  mag. We are puzzled by this large amplitude ratio, which is much larger than the typical value of  $\sim 1.3$  for  $\gamma$  Dor stars. A cooler companion (implied by the radial velocity changes) would dilute the  $V$  amplitudes more than the  $B$ , but this dilution would be very subtle since the companion’s light is not seen in our spectra. As noted above, HD 62196 is metal poor and is also the faintest variable star among the  $\gamma$  Doradus candidates in Figure 1. We confirm HD 62196 as a new  $\gamma$  Doradus variable.

### 6.8. HD 63436 = DD CMi

Mathias et al. (2004) included HD 63436 in a spectroscopic survey of  $\gamma$  Doradus candidates. They determined  $v \sin i = 66 \text{ km s}^{-1}$  and noted line-profile variations in the blue wings of the lines. Our projected rotational velocity of  $70 \text{ km s}^{-1}$  is similar to theirs. From seven observations Mathias et al. (2004) found the velocity to range from  $-15$  to  $-7 \text{ km s}^{-1}$ . Our five velocities, obtained at four different epochs, cover approximately the same velocity range and have a mean velocity of  $-13.7 \pm 1.3 \text{ km s}^{-1}$ . The velocity variations are probably due to pulsation. Using a probability neural network technique, Mahdi (2008) classified HD 63436 as A9 V. We determine a spectral class of F2 and conclude that the star is a dwarf.

The *Hipparcos* catalog lists 51 brightness measurements for HD 63436 and identifies it as an “Unsolved Variable”, recognizing that it has significant brightness variability, but the authors were unable to classify its variability type. Analyzing these observations, Handler (1999) suggested HD 63436 as a possible  $\gamma$  Doradus variable. He found several plausible periods near 0.7 days but noted that the data produced a weak signal. Martin, Bossi, & Zerbi (2003) obtained five nights of photometry of HD 63436. Their analysis of that data and also a reanalysis of the *Hipparcos* photometry led to two periods near 0.7 days, so they identified it as a  $\gamma$  Doradus variable. Based on those results, Kazarovets et al. (2006) gave it the variable star name DD CMi and assigned it to the  $\gamma$  Doradus class of variables.

The 38 brightness measurements from the T12 survey (Table 2) have a standard deviation of 0.0271 mag, the largest of all the 114 survey stars. Analysis of the follow-up observations from the T3 APT reveals four independent periods of 0.68695, 0.71327, 0.69238, and 0.54431 days with Johnson  $B$  amplitudes of 54, 35, 39, and 24 mmag, respectively (Figs. 20 and 21; Table 5). Two additional, periods of 0.72238 and 0.60310 days are suspected in the  $B$  data but could not be confirmed in the  $V$  observations; therefore, these two periods are not included in Table 5. The light curves of all four confirmed periods are sinusoidal, and the weighted mean of the four  $B/V$

amplitude ratios from Table 5 is  $1.33 \pm 0.12$ , very typical for  $\gamma$  Dor stars. Therefore, based on the star’s F1 dwarf spectral type, variable spectroscopic line profiles, multiple photometric periods in the  $\gamma$  Doradus period range, and the  $B/V$  ratio of 1.33, we confirm the earlier classification of HD 63436 as a  $\gamma$  Doradus variable.

### 6.9. HD 65526 = V769 Mon

HD 65526 was observed as part of two extensive spectroscopic surveys of candidate and confirmed  $\gamma$  Doradus stars with the goal of characterizing the line-profile variations that result from pulsations. Mathias et al. (2004) obtained a single spectrum of HD 65526 and did not detect line-profile asymmetries. However, the cross correlation functions of two spectra obtained by De Cat et al. (2006) show clear profile variations. Mathias et al. (2004) determined a  $v \sin i$  value of  $59 \text{ km s}^{-1}$ , while De Cat et al. (2006) found a mean value of  $56 \text{ km s}^{-1}$ .

We have determined that the star is an A9 dwarf that may be slightly metal poor compared to the Sun. Our three spectroscopic observations produce a constant velocity of  $-6.0 \pm 0.5 \text{ km s}^{-1}$ , and we assume that the star is single. Our projected rotational velocity of  $59 \text{ km s}^{-1}$  is in excellent agreement with the two previous determinations.

Periodic light variations were found by the *Hipparcos* team, who determined a period of 1.288 day (Perryman et al. 1997). As a result, the star was given the designation V769 Mon by Kazarovets et al. (1999), who assigned it, somewhat uncertainly, to the  $\beta$  Lyrae class of eclipsing binaries. Handler (1999) honed in on the correct variability class and photometric period when he identified HD 65526 as a prime  $\gamma$  Doradus candidate and listed two periods of 0.644 and 0.598 days, determined from the *Hipparcos* photometry. Handler & Shobbrook (2002) obtained two nights of follow-up photometry of HD 65526 that demonstrated pulsation as the cause of its multiperiodic light variations. They concluded that HD 65526 is indeed a  $\gamma$  Doradus variable. Martin, Bossi, & Zerbi (2003) obtained five nights of photometry and determined a period of 0.6427 days.

The 47 brightness measurements from our T12 survey (Table 2) have a standard deviation of 0.0233 mag, showing that HD 65526 is among the most variable stars in the survey. Analysis of the follow-up observations from the T3 APT reveals three independent periods of 0.64404, 0.59755, and 0.58476 days with Johnson  $B$  amplitudes of 52, 21, and 23 mmag, respectively (Figs. 22 and 23; Table 5). These periods are in excellent agreement with the various determinations of Handler (1999) and Martin, Bossi, & Zerbi (2003). The light curves are sinusoidal at all three periods; the weighted mean of the three  $B/V$  amplitude ratios from Table 5 is  $1.23 \pm 0.09$ . Based on the star’s A9 dwarf spectral classification, the observed line-profile variations, the photometric periods, and the  $B/V$  amplitude ratios, we confirm previous claims that HD 65526 is a  $\gamma$  Doradus star.

### 6.10. HD 69682 = HR 3258

Cowley & Cowley (1965) classified HD 69682 as F0 IV as did Abt & Morrell (1995), while Cowley & Fraquelli (1974) called it F0 V. Our result of A9 dwarf is in good agreement with those three classifications. When its spectrum is compared to that of HR 1613, an A9 V star (Abt & Morrell 1995) with solar abundances (Bikmaev et al. 2002), we conclude that HD 69682 is metal rich. Danziger & Faber (1972) found a projected rotational velocity of  $35 \text{ km s}^{-1}$ , which Wolff & Simon (1997) rescaled to  $26 \text{ km s}^{-1}$ . Abt & Morrell (1995) determined a value of  $25 \text{ km s}^{-1}$ , and Royer et al. (2002a) measured a value of  $28 \text{ km s}^{-1}$ . Our average  $v \sin i$  value of  $30 \text{ km s}^{-1}$  is in agreement with those results.

Despite its listing in The Bright Star Catalog (Hoffleit 1982), there are only two previous determinations of the mean radial velocity of HD 69682. Young (1945) reported an average velocity of  $10.0 \pm 1.0 \text{ km s}^{-1}$  from the measurement of four photographic plates. From three slit spectra with a dispersion of  $80 \text{ \AA mm}^{-1}$  Fehrenbach et al. (1987) determined a mean velocity for HD 69682, which Grenier et al. (1999a) revised to  $7.9 \pm 3.1 \text{ km s}^{-1}$ . Our three spectra have an average velocity of  $11.4 \pm 0.3 \text{ km s}^{-1}$ . The concordance of the results argues that HD 69682 has no significant velocity variability other than that expected for a  $\gamma$  Doradus variable, and so we assume that the star is single.

The *Hipparcos* catalog lists 89 brightness measurements of HD 69682 (Perryman et al. 1997) but is unable to classify the star as constant or slightly variable. Our 54 T12 survey observations (Table 2) reveal definite variability with a standard deviation of 0.0057 mag. We have over four hundred follow-up observations with the T3 APT. We find two closely-spaced periods of 0.53189 and 0.47703 days (Figs. 24 and 25; Table 5) with Johnson  $B$  amplitudes of 7 and 5 mmag, respectively; the same two periods are found in the  $V$  band. Despite the low amplitudes, clear sinusoidal variations are seen in Figure 25 at both periods. The weighted mean  $B/V$  amplitude ratio for the two periods is  $1.28 \pm 0.18$ , consistent with other  $\gamma$  Doradus variables. Given the star’s A9 dwarf classification, low-amplitude radial velocity variations, two periods in the range of other  $\gamma$  Doradus variables, and a  $B/V$  amplitude ratio of 1.28, we confirm HD 69682 as a new  $\gamma$  Doradus variable.

### 6.11. HD 99267 = HIP 55766

Young (1939) included HD 99267 in a radial velocity survey of 500 stars made at David Dunlap Observatory in the 1930s. The five observations have a mean velocity of  $-4.8 \text{ km s}^{-1}$  and show a velocity range of  $30 \text{ km s}^{-1}$ . Young concluded that the velocity was probably variable but also remarked that the spectrum was difficult to measure; he gave a spectral class of A8. Henry, Fekel, & Hall (1995) classified the star as F1 V and from two velocities obtained on the same night argued that the star was not a binary with a very short-period. From a single spectrum Fekel (1997) estimated a projected rotational velocity of  $89 \text{ km s}^{-1}$ .

For HD 99267 we have a total of five spectra, including the two mentioned by Henry, Fekel, & Hall (1995). Our velocities have an average of  $2.9 \pm 0.4 \text{ km s}^{-1}$  and a velocity range of only  $2.5 \text{ km s}^{-1}$ . Despite the conclusion of Young (1939) that the velocity is probably variable, our higher resolution observations suggest that the star is single, with its very modest velocity variations consistent with pulsation. We determine a projected rotational velocity of  $95 \text{ km s}^{-1}$  in reasonable agreement with that of Fekel (1997). A reexamination of our spectra of HD 99267 with an expanded set of reference stars and the *Hipparcos* parallax (Perryman et al. 1997) produce the same spectral classification that was found by Henry, Fekel, & Hall (1995), an F1 dwarf. Our comparison also suggests that HD 99267 is somewhat metal-rich relative to the Sun.

Light variability in HD 99267 was first noted by Henry, Fekel, & Hall (1995). They found its brightness to change by 0.03 mag with a preliminary period of  $0.575 \pm 0.001$  days but did not know the cause of variability. At that time, the  $\gamma$  Dor stars were not yet recognized as a new variability class, although a few early-F, main-sequence stars with short-period, low-amplitude variability were known to have similar properties (e.g., Krisciunas et al. 1993; Mantegazza, Poretti, & Zerbi 1994).

The *Hipparcos* satellite confirmed the low-amplitude brightness variability from its 117 observations, but the analysis team was unable to determine a period. The 53 brightness measurements from our T12 survey (Table 2) have a standard deviation of 0.0166 mag, providing another confirmation of HD 99267’s variability. Our analysis of the T3 measurements resolves a cluster of five independent periods: 0.57465, 0.56529, 0.56173, 0.58820, and 0.47553 days with Johnson *B* amplitudes of 25, 19, 20, 20, and 5 mmag, respectively (Figs. 26 and 27; Table 5). The first and highest-amplitude periodicity matches the 0.575-day period found by Henry, Fekel, & Hall (1995). The light curves are sinusoidal at all five periods; the weighted mean of the five *B/V* amplitude ratios from Table 5 is  $1.23 \pm 0.11$ . Given the star’s F1 V spectral classification, its low-amplitude velocity variations, the five photometric periods, and the *B/V* amplitude ratios, we confirm that HD 99267 is a  $\gamma$  Doradus star.

### 6.12. HD 114447 = 17 CVn = HR 4971 = ADS 8805A

The spectral classification of this moderately bright star has been determined a number of times. Appenzeller (1967) found A9 III-IV, Abt (1981) classified it as A9 IV, and Hill et al. (1976), Cowley (1976), and Abt & Morrell (1995) called it an F0 V, while Gray & Garrison (1989) similarly determined F0 IV-V. In addition to their spectral classification of HD 114447, Abt & Morrell (1995) found a  $v \sin i$  value of  $71 \text{ km s}^{-1}$ , which Royer et al. (2002a) revised to  $82 \text{ km s}^{-1}$ .

In a search for possible duplicity, HD 114447 was one of 85 stars observed interferometrically by Merrill (1922) with the 2.5 m Hooker telescope at Mount Wilson Observatory. Like the vast majority of program stars that he observed, Merrill concluded that HD 114447 was apparently single. Four radial velocities, obtained at Yerkes Observatory by Frost, Garrett, & Struve (1929) as part of a survey of 500 A stars, resulted in an average velocity of  $0.9 \text{ km s}^{-1}$  and an observed

range of  $22 \text{ km s}^{-1}$ , leading Frost, Garrett, & Struve (1929) to conclude that this star is “perhaps a spectroscopic binary.” Hill et al. (1976) included HD 114447 in their study of A and F stars in the region of the north galactic pole. They obtained 17 spectrograms, the vast majority of which had a dispersion of  $80 \text{ \AA mm}^{-1}$ . They determined a mean radial velocity of  $-20.2 \pm 2.9 \text{ km s}^{-1}$ , but also stated that the star is a possible double-lined spectroscopic binary.

We have acquired six spectra at three different epochs. The first two spectra, obtained within two days of each other, show the lines of two components that have very different radial velocities (Figure 3). However, because of the significant line broadening of both components, we estimate  $v \sin i$  values of  $50:$  and  $90:$   $\text{km s}^{-1}$  for Aa and Ab, respectively, the line pairs are partially blended with each other. In our last four spectra the lines of Aa and Ab are completely blended with each other. Thus, our observations confirm the conclusion of Hill et al. (1976) that HD 114447 is a double-lined binary. We analyzed one of the first two spectra and determined spectral classes of F0: for both stars. The *Hipparcos* parallax (Perryman et al. 1997) leads to a dwarf luminosity class for both components. Therefore, our results are in excellent agreement with most other classifications. Although the two components have very different projected rotational velocities, the magnitude difference between Aa and Ab is small. From our spectrum addition fits,  $\Delta V$  is 0.2 with an estimated uncertainty of 0.1 mag.

Percy (1978) searched for brightness variations in HD 114447 in 10.4 hours of Johnson  $V$  photometry acquired on four nights and concluded that any photometric variations were less than 0.01 mag. Similarly, no definitive variability was detected in the 114 *Hipparcos* observations (Perryman et al. 1997). We collected 81 brightness observations during our T12 APT survey and detected clear variability with a standard deviation of 0.0074 mag (Table 2). We find three distinct and independent periods in the follow-up observations with the T3 APT: 0.88621, 0.74705, and 0.68970 days. The Johnson  $B$  amplitudes are 16, 16, and 11 mmag, respectively (Figs. 28 and 29; Table 5). The light curve is sinusoidal at all three periods, and the weighted mean of the three  $B/V$  amplitude ratios from Table 5 is  $1.23 \pm 0.11$ . Therefore, we can confirm that at least one of the F0: V components, Aa and Ab of HD 114447 A, is a  $\gamma$  Doradus variable.

### 6.13. HD 138936 = HR 5791

Abt & Morrell (1995) classified HD 138936 as an A9 V star, while Gray & Garrison (1989) found A9 IV-Vs. We also determine that the star is an A9 dwarf, which is in excellent agreement with the previous results. Danziger & Faber (1972) measured a  $v \sin i$  value of  $81 \text{ km s}^{-1}$  that Wolff & Simon (1997) rescaled to  $72 \text{ km s}^{-1}$ . Abt & Morrell (1995) also determined a value of  $81 \text{ km s}^{-1}$  that was revised by Royer et al. (2002a) to  $92 \text{ km s}^{-1}$ . More recently, Jasniewicz et al. (2006) determined an even larger value of  $100 \text{ km s}^{-1}$  from a spectrum synthesis fit to their spectrum of the lithium region at  $6700 \text{ \AA}$ . Our value of  $65 \text{ km s}^{-1}$  is less than that of the two revised values and substantially less than that of Jasniewicz et al. (2006).

HD 138936 was part of a large survey of bright stars carried out at the David Dunlap Observatory (Young 1945). Young reported, based on five spectrograms, that it had an average velocity of  $-19.5 \pm 3.0 \text{ km s}^{-1}$ . Our three velocities have an average of  $-24.5 \pm 1.0 \text{ km s}^{-1}$ , in accord with the result of Young. Obtaining a single speckle observation, Mason et al. (2001) found no evidence of duplicity. Despite the range of  $v \sin i$  values, which might result from a double-lined binary with its lines seen blended at various phases, we assume that HD 138936 is a single star. Additional spectra will be needed to support this conclusion.

The *Hipparcos* satellite made 77 brightness measurements of HD 138936, and Perryman et al. (1997) classified it as a constant star. During our initial survey, the T12 APT acquired 45 measurements with a standard deviation of only 0.0029 mag, just above our 0.0020 mag cutoff for claiming variability (§2.3). T3 followed up with over 200 brightness measurements. Our analysis of the T3 data reveals three distinct periods of 0.41920, 0.41635, and 0.45790 days with  $B$  amplitudes of 8, 5, and 5 mmag, respectively (Figs. 30 and 31; Table 5). The light curve appears to be slightly asymmetric when phased with the first of the three periods. The mean  $B/V$  amplitude ratio is  $1.33 \pm 0.16$ . Given these properties, we confirm that HD 138936 is a  $\gamma$  Doradus star.

#### 6.14. HD 139478 = HR 5817

With its  $V$  magnitude of 6.70 (Perryman et al. 1997), HD 139478 is a star that is fainter than the nominal 6.5 mag limit for inclusion in The Bright Star Catalogue (Hoffleit 1982). As a result of its listing in that prominent catalog, a number of its basic properties have been previously determined. Cowley (1976) classified HD 139478 as F2 pec and stated that its metal line ratios are peculiar with strontium being enhanced. In contrast, later classifications of F4 III, F0 V, and F1 IV by Cowley & Bidelman (1979), Abt & Morrell (1995), and Gray, Napier, & Winkler (2001), respectively, indicate a normal spectrum. We conclude from our work that the star is a F1 dwarf.

HD 139478 was part of a sample of 917 mostly A-type stars observed at the Dominion Astrophysical Observatory (DAO). As a result, Harper (1937) reported a mean velocity of  $-16.9 \text{ km s}^{-1}$  from three plates and noted that “the numerous narrow lines matched against Procyon standard are reliable.” Two additional velocities, obtained by Nordström et al. (2004), have an average of  $-16.2 \text{ km s}^{-1}$  and so are in excellent agreement with the DAO mean velocity. Our five velocities, obtained at four different epochs, produce an average velocity of  $-15.7 \pm 0.1 \text{ km s}^{-1}$ , enhancing the consensus that this star is single. McAlister et al. (1987) examined the binary star frequency of 672 relatively bright stars, using speckle interferometry. They found no evidence that HD 139478 is a double star.

Abt & Morrell (1995) measured a  $v \sin i$  value of  $61 \text{ km s}^{-1}$ , which Royer et al. (2002a) rescaled to  $71 \text{ km s}^{-1}$ . The projected rotational velocity determined by Nordström et al. (2004) is substantially smaller,  $19 \text{ km s}^{-1}$ , and in excellent agreement with our result of  $20.5 \text{ km s}^{-1}$ . At our request H. Abt (2007, private communication) examined his classification dispersion spectrum of

HD 139478 and reported that the spectrum shows sharp lines that appear inconsistent with the  $v \sin i$  value given in Abt & Morrell (1995), which was based on the measurement of a different spectrum. This very substantial difference between the value of Abt & Morrell (1995) and other results, including the comments of Harper (1937), begs the question of whether HD 139478 is a double-lined binary that, except for one observation, has been observed at phases that are close to its center of mass velocity, producing a single narrow set of lines. If it is a binary, it apparently has a rather eccentric orbit, since all radial velocities and all but one  $v \sin i$  value are in excellent accord. Given the weight of the evidence, there is a possibility that the star is a double-lined spectroscopic binary, but we currently assume that HD 139478 is a single star. As with HD 138936, additional observations will be needed to confirm this conclusion.

HD 139478 has been included in several photometric surveys. Breger (1969) observed it in a search for  $\delta$  Scuti-type pulsating stars. He acquired photometry for 3.7 hours but found it constant to the precision of his measurements. The *Hipparcos* satellite acquired 107 brightness measurements over the duration of the mission, but the *Hipparcos* team (Perryman et al. 1997) left its variability undecided. Handler & Paunzen (1999) included HD 139478 in a survey for rapidly oscillating Ap stars. They monitored the star for 1.34 hours on one night and found no obvious periodicity. When Koen & Eyer (2002) reanalyzed the *Hipparcos* photometry in Perryman et al. (1997), they found a possible low-amplitude variability (9 mmag) with a period of 0.6578 days.

Our initial T12 survey easily detected photometric variability, gathering 50 measurements with a standard deviation of 0.0103 mag. T3 followed up with over 300 observations that revealed three distinct, closely-spaced periods of 0.68818, 0.71058, and 0.66419 days with  $B$  amplitudes of 24, 18, and 18 mmag, respectively (Figs. 32 and 33; Table 5). The third and shortest of the three periods, 0.66419 days, is only 0.00639 days longer than the period cited by Koen & Eyer (2002). The T3 light curve is sinusoidal when phased with each of the three periods. The mean  $B/V$  amplitude ratio is  $1.33 \pm 0.11$ . Thus, we confirm that HD 139478 is a  $\gamma$  Doradus variable.

### 6.15. HD 145005 = HIP 79122

Grenier et al. (1999b) determined a mean radial velocity of  $-10.9 \text{ km s}^{-1}$  from two spectrograms and called the velocity variable based on the  $4.6 \text{ km s}^{-1}$  difference between the two observations. They also measured a  $v \sin i$  value of  $50 \text{ km s}^{-1}$  as did Royer et al. (2002b), who analyzed the same spectra with a different technique. Makarov & Kaplan (2005) identified HD 145005 as one of 1929 stars with *Hipparcos* and Tycho proper motions that differ by more than  $3.5 \sigma$  in at least one coordinate. They designated such stars as  $\Delta\mu$  binaries. Our spectrograms show that, like HD 38309, HD 145005 is a star that has a composite spectrum with a weak, narrow line superposed near the center of each stronger, broad line (Figure 4), so we can confirm that HD 145005 is a binary. Our spectral classes for the broad-lined and narrow-lined stars, components A and B, are F0 and G4., respectively. Their positions in an H-R diagram indicate that both stars are dwarfs. Our spectrum-addition fits provide an estimated  $\Delta V = 2.8 \text{ mag}$ . We measure projected rotational

velocities of 57 and 5: for the primary and secondary, respectively. During the 2.9 years covered by our observations, we have obtained seven spectra at six different epochs. Over that time span, the velocities of the two stars have remained nearly constant,  $-9.3 \pm 0.4$  and  $-11.0 \pm 0.3$  km s<sup>-1</sup> for components A and B, respectively. The two mean velocities differ by less than 2 km s<sup>-1</sup>, and the velocities of both components are similar to the average velocity of Grenier et al. (1999b).

The 50 *Hipparcos* observations from Perryman et al. (1997) did not result in a definitive determination of whether the star was constant or variable. In contrast, our 45 T12 survey observations indicate clear variability with a standard deviation of 0.0038 mag (Table 2). We acquired approximately 150 additional observations with the T3 APT that revealed a single period of 0.46570 days with a *B* amplitude of 12 mmag (Figs. 34 and 35; Table 5). We note that the one-day alias of the 0.46570-day period at a frequency of 3.1494 day<sup>-1</sup> is nearly as strong as the 0.46570-day period. We believe we have identified the true period since both the *B* and *V* data sets converged to that period in an iterative process of removing the obvious outliers and redetermining the period. Figure 35 shows that the light curve is sinusoidal; the *B/V* amplitude ratio is 1.25. The existence of only one period allows the possibility that the light variability may be due to the ellipticity effect in a close binary or to rotational modulation of the visibility of dark starspots. The constancy of our radial velocities rules out a short-period binary, while the F0 spectral type and coherency of the low-amplitude photometric variability over hundreds of cycles rule out starspots. Therefore, the variability must be due to pulsation, and we confirm the brighter F0 component of HD 145005 as a new  $\gamma$  Doradus star.

### 6.16. HD 220091 = HIP 115288

Lanoe (1966) provided a spectral type of A9 III for HD 220091 from objective prism observations and obtained a mean radial velocity of  $-3$  km s<sup>-1</sup>. Earlier, Young (1939) had found an average radial velocity of  $-19.6$  km s<sup>-1</sup> from five plates. Based partially on the latter velocity, Montes et al. (2001) included the star as a candidate for membership in the young IC 2391 supercluster but ultimately concluded that it was not a member. In a survey of X-ray emission of A-type stars, Simon, Drake, & Kim (1995) identified HD 220091 as having a soft X-ray luminosity level well above that of the active Sun. Because only a small number of A stars have been identified as possible X-ray sources, Simon, Drake, & Kim (1995) urged that a search be made for a cooler companion, which would more likely be the X-ray emitter.

Like HD 38309, HD 220091 is listed in Part G, the Acceleration Solution section, of the Double and Multiple Star Appendix of the *Hipparcos* catalog (Perryman et al. 1997), indicating that an acceleration term was needed to account for a curvature in its stellar trajectory. A star with such a solution often turns out to have a companion with an orbital period that is too long to be derived from only the *Hipparcos* data. Mason et al. (2001) used speckle interferometry to make follow-up observations of a number of such stars and resolved HD 220091 for the first time. They determined an angular separation of 0".114: and estimated an orbital period of 7 yr. Thus, HD 220091 does



indeed have a binary companion.

Our ten spectrograms show that HD 220091 has a composite spectrum, consisting of one set of broad lines and a second set of narrow lines, components A and B, respectively (Figure 5). We find a spectral class of F1 for component A and G1: for component B. The *Hipparcos* parallax (Perryman et al. 1997) results in dwarf luminosity classes for both stars. Guided by our spectrum addition fits, we estimate  $\Delta V = 2.2$  mag. We also determine  $v \sin i$  values of 120: and 3: for A and B, respectively. Radial velocities of the components vary in opposite directions, although the broad-lined star appears to have additional velocity variations that presumably result from pulsation. Our observations currently span four yr, during which time the velocity of B has decreased by nearly  $13 \text{ km s}^{-1}$ . A period of 8.5 yr, which is in approximate agreement with the 7-yr period estimate of (Mason et al. 2001), currently provides a reasonable fit to the velocities of the narrow-lined component. However, given the modest portion of the velocity orbit covered so far, the orbital period could certainly be in the 10–25 yr range. We conclude that the spectroscopic components correspond to those of the visual binary. Our continued observation of HD 220091 should eventually allow us to obtain a well-determined orbit for at least the narrow lined component.

The *Hipparcos* team (Perryman et al. 1997) identified HD 220091 as a possible micro-variable with an amplitude less than 0.03 mag. Cutispoto et al. (2000) included the star in an optical follow-up study of EXOSAT serendipitous sources. Their photometric observations of 1990 August revealed low-amplitude variability of about 0.02 mag and a tentative period of 7.5 days. We acquired 66 observations during the T12 survey; those data demonstrate photometric variability with a standard deviation of 0.0067 mag. Our analysis of the T3 follow-up observations reveals two closely-spaced periods of 0.35364 and 0.36709 days with  $B$  amplitudes of 19 and 13 mmag, respectively (Figs. 36 and 37; Table 5). The mean  $B/V$  amplitude ratio is 1.20, and the light curve is sinusoidal when phased with either of the two periods. Given these properties, we confirm that the F1 dwarf component of the HD 220091 binary system is a  $\gamma$  Doradus star.

### 6.17. HD 224945 = BU Psc

Mathias et al. (2004) included this star in a spectroscopic survey of candidate and confirmed  $\gamma$  Doradus stars. They obtained just two spectrograms and did not comment on any line-profile variability of the star but did determine a  $v \sin i$  value of  $54 \text{ km s}^{-1}$ . Their two radial velocities were 5 and  $6.5 \text{ km s}^{-1}$ .

From our spectra of HD 224945, we find a spectral class of A9, while it has a dwarf luminosity class. Comparison with HR 1613 [A9 V, (Abt & Morrell 1995)], which has solar abundances of iron and calcium (Bikmaev et al. 2002), suggests that HD 224945 is slightly metal poor. Our  $v \sin i$  value of  $55 \text{ km s}^{-1}$  agrees with that of Mathias et al. (2004). Our four radial velocities have a mean of  $7.1 \pm 0.8 \text{ km s}^{-1}$ , which is also in accord with the results of Mathias et al. (2004). We conclude that the star is single.

Mathys, Manfroid, & Renson (1986) observed HD 224945 as a comparison star for HD 1788 and HD 224639 and had trouble characterizing the photometric variations of the two program stars. Mantegazza & Poretti (1991) obtained follow-up photometric observations of HD 224639 and discovered their comparison star, HD 224945, was also variable. Mantegazza, Poretti, & Zerbi (1994) analyzed those photometric observations of HD 224945 and found two periods of 1.494 and 1.072 days. They noted that the variability of HD 224945 was similar to that of several other early F stars. At about the same time, Balona, Krisciunas, & Cousins (1994) extensively analyzed the light variations of  $\gamma$  Dor and discussed it along with nine other similar variable stars, one of which was HD 224945. They concluded that this group constituted a new class of pulsating stars with light variations most likely generated by  $g$ -mode non-radial pulsations. Several years later, Kazarovets & Samus (1997) gave HD 224945 the variable star name BU Psc. In 1995 October, HD 224945 was the object of a multisite photometric campaign and was extensively monitored at five observatories. As a result, Poretti et al. (2002) found the star to be multiperiodic; their Table 2 listed five frequencies corresponding to periods of 0.333, 0.353, 0.413, 0.432, and 0.862 days, none of which match the periods in Mantegazza, Poretti, & Zerbi (1994) given above. In spite of having multiple sites for this observing campaign, Poretti et al. (2002) concluded that, for each detected frequency, “it is not possible to select the true value owing to the numerous aliases separated by integer values of  $\pm 1$   $\text{cd}^{-1}$ .”

Our T12 photometric survey confirmed that HD 224945 is variable. The standard deviation of the 33 observations was 0.0053 mag (Table 2). Our analysis of the 300 T3 follow-up observations revealed periods at 0.54318 and 0.77214 days with  $B$  amplitudes of 11 and 8 mmag, respectively (Figs. 38 and 39; Table 5). Our two periods do not match any of the five periods in Poretti et al. (2002) and are approximately half the two periods given by Mantegazza, Poretti, & Zerbi (1994). Figure 39 shows that our light curves are sinusoidal when phased with each of the two periods. The mean of the two  $B/V$  amplitude ratios from Table 5 is  $1.27 \pm 0.14$ . Although the identity of the true periods in HD 224945 remains uncertain, this A9 dwarf certainly has multiple photometric periods in the range of other  $\gamma$  Doradus variables. We agree with the conclusion of Mantegazza, Poretti, & Zerbi (1994) and Poretti et al. (2002) that HD 224945 is a  $\gamma$  Doradus variable.

## 7. DISCUSSION

In his review paper presented at the Sixth Vienna Workshop in Astrophysics, Breger (2000) combined the results of several unbiased variability surveys of late-A to early-F field stars searching for pulsation in the lower instability strip. Breger plotted the constant and variable stars in the H-R diagram (his Figure 4) and placed the borders of the instability strip to contain all the known  $\delta$  Scuti variables in his sample. There were 222 constant and 56 variable stars (with amplitudes greater than a few mmag) inside Breger’s instability strip, corresponding to an incidence of pulsation within the strip of 25%. Breger noted, however, that “the large number of variables with amplitudes near

the detection limit indicates that many of the so-called constant stars are also variable.”

In another study of the incidence of pulsation in the lower instability strip, Poretti et al. (2003) searched a proposed *CoRoT* mission field of view before launch to find suitable pulsating targets for *CoRoT*'s telescope. They found that 23% of their sample in the lower instability strip displayed low-amplitude, multi-periodic variability, a result in close agreement with Breger's findings from surveys of more widely-scattered field stars. Poretti et al. (2003) found a similar incidence of pulsation ( $\sim 20\%$ ) in the open cluster NGC 6633, within the same *CoRoT* field of view.

Consequently, we have good ground-based determinations of the incidence of pulsation for stars in the solar neighborhood that lie within the lower instability strip.  $\delta$  Scuti stars are the primary residents of this region of the H-R diagram, generally referred to as the  $\delta$  Scuti instability strip.

Similar determinations of the incidence of  $\gamma$  Doradus pulsations within the  $\gamma$  Doradus instability strip have yet to be done. Most known  $\gamma$  Doradus variables have been found via photometric studies of individual candidate field stars (Henry, Fekel, & Henry 2007, and references therein).  $\gamma$  Doradus candidates are also being found in galactic open star clusters such as NGC 2506 (Arentoft et al. 2007), NGC 2516 (Zerbi et al. 1998), NGC 6755 (Ciechanowska et al. 2007), NGC 6866 (Molenda-Zakowicz et al. 2009), and the Pleiades (Martin-Ruiz et al. 2008), but none of these or similar studies have defined a complete statistical sample, precluding a good estimate of  $\gamma$  Doradus incidence.

Our volume-limited sample of 114  $\gamma$  Doradus candidates in this paper *does* constitute a complete, unbiased, statistical sample of nearby field stars. Our initial photometric survey of this sample with the T12 APT found a total of 37 variable stars with intrinsic variability of 0.002 mag or more (Table 2; Figure 1). Higher-cadence observations with the T3 APT described in §3 (above) and spectroscopic observations from KPNO described in §4 (above) allowed us to classify all but three of the 37 variables and to describe their properties. The final results of the survey are listed in column (12) of Table 2. The results are also plotted in the H-R diagram of Figure 40 with separate symbols to designate the 77 constant stars, 24  $\gamma$  Doradus variables, nine  $\delta$  Scuti variables, one hybrid pulsator, and the three variables without clear periodicity. One of the 24  $\gamma$  Doradus stars is the SB2 binary HD 114447, which is composed of two F0 dwarfs (Table 6, Figs. 28 & 29, §6.12). Both components of this binary are plotted with open star symbols since we do not know which component is pulsating. Including the hybrid variable HD 8801 among the other  $\gamma$  Doradus stars gives an observed incidence of  $\frac{25}{114}$  or 22% for  $\gamma$  Doradus variables among nearby candidate field stars. This is similar to the incidence of  $\delta$  Scuti variables within the  $\delta$  Scuti instability strip found in the earlier studies referenced above. For our volume-limited sample, we can also compute the corresponding space density of  $\gamma$  Doradus stars to be 0.094 stars per  $10^3 pc^3$  or 94 per  $10^6 pc^3$ .

In addition to the results of our 114 star survey, we also provide an updated list of 86 confirmed  $\gamma$  Doradus variables in Table 8. The 15 new  $\gamma$  Doradus variables found in our survey make up the bulk of the new stars. Two more variables (HD 74504 and HD 147787) were discovered by Cuypers et al. (2009) and De Cat et al. (2009), respectively. Four new  $\gamma$  Doradus /  $\delta$  Scuti hybrids

have been found; HD 44195 and HD 49434 were discovered in ground-based preparatory observations for the *CoRoT* mission by Poretti et al. (2005) and Uytterhoeven et al. (2008), respectively. Two more hybrids (HD 114839 and BD +18 4914) were found in *MOST* spaced-based photometry by King et al. (2006) and Rowe et al. (2006), respectively. The properties of the five hybrids are listed in bold font in Table 8. We have removed the “hybrid” HD 209295 from the list because (1) its  $\gamma$  Doradus pulsations are excited by tidal effects from the presence of a neutron star or white dwarf companion (Handler et al. 2002), and (2) it lies significantly outside of the  $\gamma$  Doradus instability strip (Henry, Fekel, & Henry 2007, their Figure 25).

Table 8 does not include variables in galactic open clusters, such as the  $\gamma$  Doradus stars found in the clusters NGC 2506, NGC 2516, NGC 6755, NGC 6866, and the Pleiades mentioned above. Cluster variables, as well as future discoveries from the *MOST*, *CoRoT*, and *Kepler* missions, will generally be several magnitudes fainter than the stars in Table 8. So we restrict our list in Table 8 to bright, confirmed  $\gamma$  Doradus field stars. These bright field stars will continue to be the most useful targets for multisite spectroscopic and photometric campaigns that are required to identify pulsation modes (e.g., Handler et al. 2002; Aerts et al. 2004; Mathias et al. 2004).

Among the 86  $\gamma$  Doradus stars in Table 8 are 49 single stars, eight single-lined spectroscopic binaries, 22 double-lined binaries, and 15 visual double or multiple systems. Five of the visual double systems (HD 7169, HD 23874, HD 38309, HD 147787, and HD 220091) have one component that is a spectroscopic binary, so these five stars were counted in both the visual double and spectroscopic binary classifications. In most of the cases involving duplicity, it is clear that the primary component is the  $\gamma$  Doradus variable; in those cases, we have appended an “A” to the HD number in column (1) to designate the primary component. HD 211699, however, is a double-lined system for which Henry, Fekel, & Henry (2007) have shown that the *secondary* is probably the  $\gamma$  Doradus star; we have appended a “B” to its HD number in Table 8. Both components of the three double-lined binaries HD 86371 (Henry, Fekel, & Henry 2007), HD 113867 (Henry & Fekel 2003), and HD 114447 (this paper) have  $\gamma$  Doradus-type properties, so it is not clear which component is the  $\gamma$  Doradus variable. It is quite possible that both components of one or more of these SB2 binaries are  $\gamma$  Doradus stars. In those three cases, we have listed both the primary and secondary components in Table 8 with designations of “A:” and “B:”, indicating uncertainty in identifying the  $\gamma$  Doradus component. Therefore, Table 8 actually contains 89 entries.

For the single stars, the wide visual doubles, and the single-lined binaries in Table 8, the  $V$  magnitudes and  $B - V$  colors in columns (4) and (5) are from the *Hipparcos* catalog (Perryman et al. 1997). For all of the visual double stars and the double-lined spectroscopic binaries, the  $V$  magnitudes and  $B - V$  colors refer to the individual component designated in column (1); Henry & Fekel (2003) provide details on the determination of those values. The stellar properties listed in columns (6), (7), and (8) have all been determined from the  $V$  magnitudes,  $B - V$  colors, and parallaxes by the method outlined in Henry et al. (2001). Most of these stars have multiple photometric periods; the period given in column (9) is the one with the largest amplitude. The final column gives the literature reference that confirms each star as a  $\gamma$  Doradus variable.

We plot all 86  $\gamma$  Doradus stars from Table 8 in Figure 41. The 15 new  $\gamma$  Doradus variables discovered in our survey fall within the observed limits of the  $\gamma$  Doradus instability strip as plotted by Fekel, Warner, & Kaye (2003); those limits remain unchanged with the addition of dozens of new  $\gamma$  Doradus stars by Henry, Fekel, & Henry (2005), Henry, Fekel, & Henry (2007), and the current paper. The five known hybrid variables all lie within the overlap region between the  $\delta$  Scuti and  $\gamma$  Doradus instability strips. As mentioned in §3.3 above, none of the new  $\gamma$  Doradus stars show evidence of hybrid pulsation.

We note in Figure 40 that there are no  $\gamma$  Doradus candidates in the upper right corner of the observed instability strip redward of  $B - V = 0.38$ . In hindsight, we might have extended the  $B - V$  color index limit of our survey to about 0.42. However, when all 86 known  $\gamma$  Doradus stars are plotted in Figure 41, we see that  $\gamma$  Doradus variability is relatively rare but can occur in this corner of the instability strip. This may cause our incidence and space density values of  $\gamma$  Doradus variability to be slightly low.

Finally, we anticipate upcoming contributions from the *MOST*, *CoRoT* and *Kepler* space missions. The discovery of two new  $\gamma$  Doradus /  $\delta$  Scuti hybrid pulsators from *MOST* photometry has been mentioned above. A recent search of 131 days of *CoRoT* observations by Hareter et al. (2010) yielded 418  $\gamma$  Doradus and 274 hybrid candidates in the LRa01 field. From the first few weeks of the *Kepler* mission, Grigahcene et al. (2010) found 34 new  $\gamma$  Doradus stars and 25 hybrids with the likelihood of many more to come. They also made the surprising discovery that “there are practically no pure  $\delta$  Scuti or  $\gamma$  Doradus pulsators.” They contrast this finding with ground-based results that show a clear separation between the two types of pulsation, except for a few hybrid pulsators. Grigahcene et al. (2010) note that ground-based photometric observations are probably sensitive only to pulsations of low spherical degree ( $\ell = 1, 2$ ). When candidate pulsators are examined with the photometric precision, cadence, and time base enabled by *Kepler*, many more modes of higher degree (and lower photometric amplitude) become visible.

We thank Lou Boyd for his continuing efforts in support of our automatic telescopes at Fairborn Observatory. Astronomy at Tennessee State University is supported by NASA, NSF, Tennessee State University, and the State of Tennessee through its Centers of Excellence program. This research has made use of the SIMBAD database, operated at CDS, Strasbourg, France.

## REFERENCES

- Abt, H. A. 1961, *ApJS*, 6, 37
- Abt, H. A. 1970, *ApJS*, 19, 387
- Abt, H. A. 1981, *ApJS*, 45, 437
- Abt, H. A., & Morrell, N. 1995, *ApJS*, 99, 135
- Adelman, S. J. 2001, *A&A*, 368, 225
- Aerts, C., & Kaye, A. B. 2001, *ApJ*, 553, 814
- Aerts, C., Eyer, L., & Kestens, E. 1998, *A&A*, 337, 790
- Aerts, C., Cuypers, J., De Cat, P., Dupret, M. A., De Ridder, J., Eyer, L., Scufflaire, R., & Waelkens, C. 2004, *A&A*, 415, 1079
- Appenzeller, I. 1967 *PASP*, 79, 102
- Arentoft, T., et al. 2007, *A&A*, 465, 965
- Balona, L. A., Hearnshaw, J. B., Koen, C., Collier, A., Machi, I., Mkhosi, M., & Steenberg, C. 1994, *MNRAS*, 267, 103
- Balona, L. A., Krisciunas, K., & Cousins, A. W. J. 1994, *MNRAS*, 270, 905
- Balona, L. A., et al. 1996, *MNRAS*, 281, 1315
- Bikmaev, I. F., et al. 2002, *A&A*, 389, 537
- Breger, M. 1969, *ApJS*, 19, 79
- Breger, M. 2000, in *ASP Conf. Ser. 210, Delta Scuti & Related Stars*, ed. M. Breger & M. H. Montgomery (San Francisco: ASP), 3
- Breger, M., et al. 1997, *A&A*, 324, 566
- Ciechanowska, A., et al. 2007, *Acta Astronom.*, 57, 249
- Cousins, A. W. J., & Warren, P. R. 1963, *Mon. Notes Astron. Soc. S. Afr.*, 22, 65
- Cowley, A. P. 1976, *PASP*, 88, 95
- Cowley, A. P., & Bidelman, W. P. 1979, *PASP*, 91, 83
- Cowley, A. P., & Cowley, C. R. 1965, *PASP*, 77, 184
- Cowley, A., Cowley, C., Jaschek, M., & Jaschek, C. 1969, *AJ*, 74, 375

- Cowley, A., & Fraquelli, D. 1974, *PASP*, 86, 70
- Cutispoto, G., Pastori, L., Guerrero, A., Tagliaferri, G., Messina, S., Rodono, M., & de Medeiros, J. R. 2000, *A&A*, 364, 205
- Cuyppers, J., et al. 2009, *A&A*, 499, 967
- Danziger, I. J., & Faber, S. M. 1972, *A&A*, 18, 428
- De Cat, P., et al. 2006, *A&A*, 449, 281
- De Cat, P., et al. 2009, in *AIP Conf. Ser. 1170, Stellar Pulsation: Challenges for Theory and Observation*, eds. J. A. Guzik & P. A. Bradley (AIP: Melville, NY) p. 483
- De Ridder, J., Arentoft, T., & Kjeldsen, H. 2006, *MNRAS*, 365, 595
- Duflot, M., Fehrenbach, C., Mannone, C., Burnage, R., & Genty, V. 1995, *A&AS*, 110, 177
- Dupret, M.-A., Grigahcene, A., Garrido, R., Gabriel, M., & Scuflaire, R. 2004, *A&A*, 414, L17
- Dupret, M.-A., Grigahcene, A., Garrido, R., De Ridder, J., Scuflaire, R., & Gabriel, M. 2005a, *MNRAS*, 360, 1143
- Dupret, M.-A., Grigahcene, A., Garrido, R., Gabriel, M., & Scuflaire, R. 2005b, *A&A*, 435, 927
- Dupret, M.-A., Miglio, A., Grigahcene, A., Montalbán, J. 2007, *Comm. in Asteroseismology*, 150, 98
- Eaton, J. A., Henry, G. W., & Fekel, F. C. 2003, in *The Future of Small Telescopes in the New Millennium, Volume II - The Telescopes We Use*, ed. T. D. Oswalt (Dordrecht: Kluwer), 189
- Eyer, L., & Aerts, C. 2000, *A&A*, 361, 201
- Eyer, L., & Grenon, M. 2000, in *ASP Conf. Ser. 210, Delta Scuti & Related Stars*, ed. M. Breger & M. H. Montgomery (San Francisco: ASP), 482
- Fehrenbach, C., Burnage, R., Duflot, M., Peton, A., Rolland, L., Genty, V., & Mannone, C. 1987, *A&AS*, 71, 263
- Fehrenbach, C., Duflot, M., Burnage, R., Mannone, C., Peton, A., & Genty, V. 1987, *A&AS*, 71, 275
- Fekel, F. C. 1997, *PASP*, 109, 514
- Fekel, F. C., & Henry, G. W. 2003, *AJ*, 125, 2156
- Fekel, F. C., Warner, P. B., & Kaye, A. B. 2003, *AJ*, 125, 2196
- Frost, E. B., Garrett, S. B., & Struve, O. 1929, *Pub. Yerkes Obs.*, 7

- Garrido, R. 2000, in ASP Conf. Ser. 210, *Delta Scuti & Related Stars*, ed. M. Breger & M. H. Montgomery (San Francisco: ASP), 67
- Gray, D. F. 1992, *The Observation and Analysis of Stellar Photospheres* (Cambridge: Cambridge Univ. Press)
- Gray, R. O., & Garrison, R. F. 1989, *ApJS*, 69, 301
- Gray, R. O., Napier, M. G., & Winkler, L. I. 2001, *AJ*, 121, 2148
- Grenier, S., et al. 1999, *A&AS*, 137, 451
- Grenier, S., et al. 1999, *A&AS*, 135, 503
- Grigahcene, A., Dupret, M.-A., Garrido, R., Gabriel, M., & Scuflaire, R. 2004, *Comm. in Asteroseismology*, 145, 10
- Grigahcene, A., Dupret, M.-A., Gabriel, M., Garrido, R., & Scuflaire, R. 2005, *A&A*, 434, 1055
- Grigahcene, A., Moya, A., Suarez, J.-C., & Martin-Ruiz, S. 2010, [arXiv:1004.1976](https://arxiv.org/abs/1004.1976)
- Grenier, S., et al. 2010, *ApJ*, 713, L192
- Guzik, J. A. 2010, [arXiv:1005.5406](https://arxiv.org/abs/1005.5406)
- Guzik, J. A., Kaye, A. B., Bradley, P. A., Cox, A. N., & Neuforge, C. 2000, *ApJ*, 542, L57
- Handler, G. 1999, *MNRAS*, 309, L19
- Handler, G., & Paunzen, E. 1999, *A&AS*, 135, 57
- Handler, G., & Shobbrook, R. R. 2002, *MNRAS*, 333, 251
- Handler, G., et al. 2002, *MNRAS*, 333, 262
- Hareter, M., et al. 2010, [arXiv:1007.3176](https://arxiv.org/abs/1007.3176)
- Harper, W. E. 1937, *Pub. Dom. Astroph. Obs.*, 7, 1
- Hatzes, A. P. 1998, *MNRAS*, 299, 403
- Henry, G. W. 1999, *PASP*, 111, 845
- Henry, G. W., & Fekel, F. C. 2002, *PASP*, 114, 988
- Henry, G. W., & Fekel, F. C. 2003, *AJ*, 126, 3058
- Henry, G. W., & Fekel, F. C. 2005, *AJ*, 129, 2026
- Henry, G. W., Fekel, F. C., & Hall, D. S. 1995, *AJ*, 110, 2926



- Henry, G. W., Fekel, F. C., & Henry, S. M. 2005, *AJ*, 129, 2815
- Henry, G. W., Fekel, F. C., & Henry, S. M. 2007, *AJ*, 133, 1421
- Henry, G. W., Fekel, F. C., Henry, S. M., & Hall, D. S. 2000, *ApJS*, 130, 201
- Henry, G. W., Fekel, F. C., Kaye, A. B., & Kaul, A. 2001, *AJ*, 122, 3383
- Hoffleit, D. 1982, *The Bright Star Catalogue*, 4th edition (New Haven: Yale Univ. Obs.)
- Hill, G., Allison, A., Fisher, W. A., Odgers, G. J., Pfannenschmidt, E. L., Younger, P. F., & Hilditch, R. W. 1976, *MmRAS*, 82, 69
- Jasniewicz, G., Recio-Blanco, A., de Laverny, P., Parthasarathy, M., & de Medeiros, J. R. 2006, *A&A*, 453, 717
- Jaschek, M., Andrillat, Y., & Jaschek, C. 1989, *A&A*, 218, 180
- Kaye, A. B., Gray, R. O., & Griffin, R. F. 2004, *PASP*, 116, 558
- Kaye, A. B., & Handler, G. 1995, *Inf. Bull. Variable Stars*, No. 4195
- Kaye, A. B., Handler, G., Krisciunas, K., Poretti, E., & Zerbi, F. M. 1999a, *PASP*, 111, 840
- Kaye, A. B., Henry, G. W., Fekel, F. C., Gray, R. O., Rodríguez, E., Martín, S., Gies, D. R., Bagnuolo, W. G., & Hall, D. S. 1999b, *AJ*, 118, 2997
- Kaye, A. B., Henry, G. W., Fekel, F. C., & Hall, D. S. 1999c, *MNRAS*, 308, 1081
- Kazarovets, A. V., & Samus, N. N. 1997, *Inf. Bull. Variable Stars*, No. 4471
- Kazarovets, A. V., Samus, N. N., Durlevich, O. V., Kireeva, N. N., Pastukhova, E. N. 2006, *Inf. Bull. Variable Stars*, No. 5721
- Kazarovets, A. V., Samus, N. N., Durlevich, O. V., Frolov, M. S., Antipin, S. V., Kireeva, N. N., & Pastukhova, E. N. 1999, *Inf. Bull. Variable Stars*, No. 4659
- King, H., et al. 2006, *Comm. in Asteroseismology*, 148, 28
- Koen, C., & Eyer, L. 2002, *MNRAS*, 331, 45
- Krisciunas, K. 1993, *DSSN*, 6, 23
- Krisciunas, K., Griffin, R. F., Guinan, E. F., Luedeke, K. D., & McCook, G. P. 1995, *MNRAS*, 273, 662
- Krisciunas, K., et al. 1993, *MNRAS*, 263, 781
- Kurtz, D. W., Breger, M., Evans, S. W., & Sandmann, W. H. 1976, *ApJ*, 207, 181

- Lanoe, C. 1966, *J. Obs.*, 49, 205
- Lockwood, G. W., Skiff, B. A., Henry, G. W., Henry, S. M., Radick, R. R., Baliunas, S. L., Donahue, R. A., & Soon, W. 2007, *ApJS*, 171, 260
- Loumos, G. L., & Deeming, T. J. 1978, *Ap&SS*, 56, 285
- Mahdi, B. 2008, *Bull. Astr. Soc. India*, 36, 1
- Makarov, V. V., & Kaplan, G. H. 2005, 129, 2420
- Mantegazza, L., & Poretti, E. 1991, *Inf. Bull. Variable Stars*, No. 3690
- Mantegazza, L., Poretti, E. & Antonello, E. 1991, *Inf. Bull. Variable Stars*, No. 3612
- Mantegazza, L., Poretti, E., & Zerbi, F. M. 1994, *MNRAS*, 270, 439
- Martin, S., Bossi, M., & Zerbi, F. M. 2003, *A&A*, 401, 1077
- Martin-Ruiz, S., et al. 2008, *J. Phys. Conf. Ser.* 118, 012049
- Mason, B. D., Hartkopf, W. I., Holdenried, E. R., & Rafferty, T. J. 2001, *AJ*, 121, 3224
- Mathias, P., et al. 2004, *A&A*, 417, 189
- Mathys, G., Manfroid, J., & Renson, P. 1986, *A&AS*, 63, 403
- McAlister, H. A., Hartkopf, W. I., Hutter, D. J., Shara, M. M., & Franz, O. G. 1987, *AJ*, 93, 183
- Merrill, P. W. 1922, *ApJ*, 56, 40
- Miglio, A., Montalbán, J., Noels, A., & Eggenberger, P. 2008, *MNRAS*, 386, 1487
- Molenda-Zakowicz, J., Kopacki, G., Steslicki, M., & Narwid, A. 2009, *Acta Astronom.*, 59, 193
- Montes, D., Lopez-Santiago, J., Galvez, M. C., Fernandez-Figueroa, M. J., de Castro, E., & Cornide, M. 2001, *MNRAS*, 328, 45
- Moultaka, J., Ilovaisky, S. A., Prugniel, P., & Soubiran, C. 2004, *PASP*, 116, 693
- Moya, A., Suarez, J. C., Amado, P. J., Martin-Ruiz, S., & Garrido, R. 2005, *A&A*, 432, 189
- Moya, A., Suarez, J. C., Martin-Ruiz, S., Amado, P. J., Rodriguez-Lopez, C., Grigahcene, A., Dupret, M. A., Rodriguez, E., & Garrido, R. 2008, *Astronomische Nachrichten*, 329, 541
- Nordström, B., Stefanik, R. P., Latham, D. W., & Andersen, J. 1997, *A&AS*, 126, 21
- Nordström, B., et al. 2004, *A&A*, 418, 989
- Olsen, E. H. 1980, *A&AS*, 39, 205

- Paunzen, E., et al. 1998, *A&A*, 335, 533
- Percy, J. R. 1978, *PASP*, 90, 703
- Perryman, M. A. C., et al. 1997, *The Hipparcos & Tycho Catalogues* (ESA-SP 1200; Noordwijk: ESA)
- Pollard, K. R. 2009, in *AIP Conf. Ser. 1170, Stellar Pulsation: Challenges for Theory and Observation*, eds. J. A. Guzik & P. A. Bradley (AIP: Melville, NY) p. 455
- Pollard, K. R., Wright, D. J., Zima, W., Cottrell, P. L., & De Cat, P. 2008, *Comm. in Asteroseismology*, 157, 118
- Poretti, E., et al. 2002, *A&A*, 384, 513
- Poretti, E., et al. 2003, *A&A*, 406, 203
- Poretti, E., et al. 2005, *AJ*, 129, 2461
- Rodriguez, E., et al. 2006, *A&A*, 450, 715
- Rodriguez, E., et al. 2006, *A&A*, 456, 261
- Royer, F., Gerbaldi, M., Faraggiana, R., & Gomez, A. E. 2002, *A&A*, 381, 105
- Royer, F., Grenier, S., Baylac, M.-O., Gomez, A. E., & Zorec, J. 2002, *A&A*, 393, 897
- Rowe, J. F., et al. 2006, *Comm. in Asteroseismology*, 148, 34
- Scarfe, C. D., Batten, A. H., & Fletcher, J. M. 1990, *Publ. Dominion Astrophys. Obs. Victoria*, 18, 21
- Shajn, G., & Albitzky, V. 1932, *MNRAS*, 92, 771
- Simon, T., Drake, S. A., Kim, P. D. 1995, *PASP*, 107, 1034
- Stamford, P. A., & Watson, R. D., *Ap&SS*, 77, 131
- Sterken, C. 2002, in *ASP Conf. Ser. 256, Observational Aspects of Pulsating B and A Stars*, ed. C. Sterken & D. W. Kurtz (San Francisco: ASP), 91
- Suarez, J. C., Moya, A., Martin-Ruiz, S., Amado, P. J., Grigahcene, A., & Garrido, R. 2005, *A&A*, 443, 271
- Uytterhoeven, K., et al. 2008, *A&A*, 489, 1213
- Vaniček, P. 1971, *Ap&SS*, 12, 10
- Warner, P. B., Kaye, A. B., & Guzik, J. A. 2003, *ApJ*, 593, 1049

- Wilson, R. E., & Joy, A. 1950, *ApJ*, 111, 221
- Wolff, S. C., & Simon, T. 1997, *PASP*, 109, 759
- Young, R. K. 1939, *Pub. David Dunlap Obs.*, 1, 69
- Young, R. K. 1945, *Pub. David Dunlap Obs.*, 1, 311
- Zerbi, F. M., et al. 1997a, *MNRAS*, 290, 401
- Zerbi, F. M., et al. 1997b, *MNRAS*, 292, 43
- Zerbi, F. M., et al. 1998, *PASP*, 110, 804
- Zerbi, F. M., et al. 1999, *MNRAS*, 303, 275

Table 1. SELECTION CRITERIA FOR THE VOLUME-LIMITED SAMPLE

Parameter	Range or Value
<i>Hipparcos</i> Catalog Number	1 – 118,218
$V$ (mag)	5.5 – 8.0
$B - V$ (mag)	0.25 – 0.38
Parallax (mas)	15.0 – 20.0
Distance (pc)	50.0 – 66.7
Declination (deg)	–10 – +65
$M_V$ (mag)	1.6 – 3.7
<i>Hipparcos</i> Multiplicity Status	Single

Table 2. VOLUME-LIMITED SAMPLE OF 114  $\gamma$  DORADUS CANDIDATES

HD (1)	HIP (2)	Other Names (3)	$V^a$ (mag) (4)	$B - V^a$ (mag) (5)	$\pi^a$ (mas) (6)	$M_V$ (mag) (7)	<i>Hipparcos</i> Variable Type <sup>b</sup> (8)	$N_{obs}$ (9)	Date Range (HJD - 2,400,000) (10)	$\sigma_{star}$ (mag) (11)	Final Status (12)
1917	1892	...	6.57	0.380	18.64±0.69	2.92		39	52,172.86–52,287.63	0.0000	Constant
4818	3965	V526 Cas, HR 238	6.38	0.307	15.00±0.72	2.26	C	43	52,168.82–52,312.62	0.0018	Constant
6288	4979	26 Cet, HR 301, ADS 875A	6.06	0.271	17.66±0.72	2.30	M	30	52,161.88–52,288.62	0.0000	Constant
<b>6568</b>	<b>5209</b>	...	<b>6.93</b>	<b>0.301</b>	<b>15.31±0.93</b>	<b>2.86</b>		<b>271</b>	<b>52,162.83–52,991.75</b>	<b>0.0066</b>	$\gamma$ Dor
8801	6794	HR 418, ADS 1151A	6.42	0.311	17.91±0.75	2.68	U	532	52,161.89–52,980.83	0.0054	$\gamma$ Dor + $\delta$ Sct
9780	7447	HR 457	5.95	0.259	16.75±0.82	2.07		45	52,161.83–52,313.63	0.0023	Variable
12354	9452	...	6.61	0.339	15.39±0.77	2.55	C	55	52,162.86–52,317.64	0.0000	Constant
13683	10356	...	6.51	0.356	15.02±1.10	2.39	C	51	52,162.85–52,314.63	0.0000	Constant
15559	11796	...	6.76	0.363	18.69±0.79	3.12		57	52,162.87–52,327.63	0.0000	Constant
15745	11847	...	7.47	0.360	15.70±0.99	3.45	C	60	52,163.93–52,330.64	0.0000	Constant
<b>17163</b>	<b>12862</b>	<b>HR 816</b>	<b>6.04</b>	<b>0.312</b>	<b>19.50±0.90</b>	<b>2.49</b>	<b>C</b>	<b>53</b>	<b>52,163.85–52,317.65</b>	<b>0.0030</b>	$\gamma$ Dor
20193	15191	HR 975, ADS 2431A	6.30	0.366	16.13±0.90	2.34	C	57	52,163.86–52,331.66	0.0000	Constant
22090	16719	...	7.01	0.337	16.58±0.96	3.11		70	52,163.88–52,339.67	0.0006	Constant
23245	17470	ADS 2735A	6.75	0.370	15.67±0.93	2.72	C	57	52,164.85–52,338.65	0.0000	Constant
23384	17675	...	6.90	0.373	18.05±0.85	3.18	C	68	52,161.85–52,338.66	0.0003	Constant
<b>25906</b>	<b>19408</b>	...	<b>7.08</b>	<b>0.345</b>	<b>15.19±0.80</b>	<b>2.99</b>		<b>249</b>	<b>52,163.88–53,011.78</b>	<b>0.0050</b>	$\gamma$ Dor
27176	20087	51 Tau, HR 1331	5.64	0.277	18.25±0.82	1.95	C	45	52,168.90–52,342.68	0.0009	Constant
28294	20873	76 Tau, HR 1408	5.90	0.325	18.42±1.93	2.23	C	34	52,169.88–52,317.70	0.0006	Constant
28704	21242	57 Per, HR 1434, ADS 2239A	6.09	0.370	15.48±0.90	2.04		48	52,169.89–52,348.67	0.0008	Constant
28734	21369	...	6.65	0.314	15.77±1.27	2.64	C	35	52,169.87–52,326.66	0.0008	Constant
29499	21670	HR 1480	5.38	0.257	19.44±0.86	1.82	C	38	52,170.93–52,344.66	0.0000	Constant
30144	22300	HR 1515	6.32	0.320	19.60±0.82	2.78	C	35	52,169.87–52,326.66	0.0004	Constant
<b>31550</b>	<b>23117</b>	...	<b>6.74</b>	<b>0.335</b>	<b>17.13±0.97</b>	<b>2.91</b>	<b>D</b>	<b>247</b>	<b>52,169.89–53,032.77</b>	<b>0.0020</b>	$\gamma$ Dor
37788	26762	HR 1955	5.93	0.311	19.46±1.04	2.38	C	63	52,169.95–52,348.67	0.0000	Constant
38189	27192	HR 1974	6.57	0.256	16.29±0.83	2.63		58	52,161.93–52,348.69	0.0020	$\delta$ Sct
<b>38309</b>	<b>27118</b>	<b>HR 1978, ADS 4333A</b>	<b>6.09</b>	<b>0.320</b>	<b>19.79±1.01</b>	<b>2.57</b>		<b>214</b>	<b>52,169.96–53,047.76</b>	<b>0.0033</b>	$\gamma$ Dor
41074	28823	39 Aur, HR 2132	5.90	0.358	19.38±0.80	2.34		75	52,173.93–52,348.71	0.0000	Constant
42278	29210	HR 2179	6.16	0.352	16.39±0.87	2.23	C	79	52,169.98–52,348.68	0.0000	Constant
43749	30278	3 Lyn	7.20	0.380	16.21±0.86	3.25		45	52,193.92–52,328.73	0.0000	Constant
44071	30188	...	7.02	0.375	17.81±1.22	3.27	C	46	52,161.96–52,348.73	0.0000	Constant
44497	30318	HR 2287	6.00	0.319	15.87±1.00	2.00	C	160	52,169.96–53,074.74	0.0000	Constant
44536	30605	...	6.87	0.371	16.87±0.80	3.01	C	44	52,171.97–52,348.74	0.0008	Constant
<b>45638</b>	<b>30886</b>	<b>HR 2351</b>	<b>6.59</b>	<b>0.293</b>	<b>16.45±1.02</b>	<b>2.67</b>		<b>160</b>	<b>52,169.96–53,074.74</b>	<b>0.0039</b>	$\gamma$ Dor
47882	32125	...	7.04	0.359	16.25±0.92	3.09	C	71	52,168.95–52,348.75	0.0000	Constant
48412	32350	...	6.93	0.351	18.38±0.86	3.25	C	71	52,168.95–52,348.75	0.0000	Constant
50277	33024	HR 2551	5.75	0.270	15.98±0.75	1.77		53	52,168.99–52,348.71	0.0000	Constant
54944	34897	...	6.75	0.296	15.07±0.77	2.64		57	52,169.97–52,345.78	0.0000	Constant
57927	35941	59 Gem, HR 2816	5.77	0.368	15.57±1.37	1.73		47	52,168.98–52,348.78	0.0035	$\delta$ Sct
60915	37107	...	6.85	0.339	16.90±0.90	2.99	C	56	52,170.00–52,348.78	0.0025	Variable
<b>62196</b>	<b>37802</b>	...	<b>7.67</b>	<b>0.313</b>	<b>15.29±1.20</b>	<b>3.59</b>		<b>61</b>	<b>52,173.99–52,348.79</b>	<b>0.0049</b>	$\gamma$ Dor
<b>63436</b>	<b>38138</b>	<b>DD CMi</b>	<b>7.46</b>	<b>0.356</b>	<b>16.26±1.02</b>	<b>3.52</b>	<b>U</b>	<b>38</b>	<b>52,188.00–52,345.75</b>	<b>0.0271</b>	$\gamma$ Dor
64491	38723	DD Lyn, HR 3083	6.23	0.277	16.55±0.92	2.32		54	52,175.98–52,348.79	0.0031	$\delta$ Sct
<b>65526</b>	<b>39017</b>	<b>V769 Mon</b>	<b>6.98</b>	<b>0.297</b>	<b>16.20±1.00</b>	<b>3.03</b>	<b>P</b>	<b>47</b>	<b>52,188.02–52,348.75</b>	<b>0.0233</b>	$\gamma$ Dor
<b>69682</b>	<b>40878</b>	<b>HR 3258</b>	<b>6.50</b>	<b>0.300</b>	<b>15.94±0.75</b>	<b>2.51</b>		<b>54</b>	<b>52,178.01–52,345.82</b>	<b>0.0057</b>	$\gamma$ Dor
69715	40791	BDS 4550A	7.18	0.360	15.19±0.89	3.09	U	57	52,176.01–52,342.83	0.0107	$\gamma$ Dor
72617	42049	HR 3380	6.04	0.332	17.22±0.89	2.22	C	39	52,203.98–52,345.80	0.0009	Constant
79066	45150	HR 3649	6.34	0.328	19.65±0.80	2.81	C	61	52,197.01–52,348.80	0.0000	Constant
79392	45389	...	6.75	0.367	19.79±0.97	3.23	C	50	52,189.00–52,346.86	0.0000	Constant
87974	49694	...	6.68	0.366	17.27±0.96	2.87	C	52	52,217.02–52,348.82	0.0000	Constant

Table 2—Continued

HD (1)	HIP (2)	Other Names (3)	$V^a$ (mag) (4)	$B - V^a$ (mag) (5)	$\pi^a$ (mas) (6)	$M_V$ (mag) (7)	<i>Hipparcos</i> Variable Type <sup>b</sup> (8)	$N_{obs}$ (9)	Date Range (HJD - 2,400,000) (10)	$\sigma_{star}$ (mag) (11)	Final Status (12)
88270	49882	...	6.64	0.364	18.92±0.85	3.03	C	55	52,206.02–52,348.84	0.0000	Constant
89565	50584	HR 4060	6.31	0.338	18.77±1.05	2.68		46	52,230.01–52,348.82	0.0011	Constant
93901	53005	...	6.59	0.333	15.82±0.90	2.59		51	52,212.01–52,448.66	0.0034	$\delta$ Sct
95771	54027	HR 4303	6.12	0.269	18.31±0.81	2.43	C	37	52,234.01–52,348.84	0.0000	Constant
95804	54063	...	6.97	0.265	16.17±0.87	3.01	C	51	52,212.01–52,448.66	0.0000	Constant
<b>99267</b>	<b>55766</b>	...	<b>6.88</b>	<b>0.322</b>	<b>15.77±0.80</b>	<b>2.87</b>	<b>U</b>	<b>53</b>	<b>52,216.02–52,449.67</b>	<b>0.0166</b>	$\gamma$ Dor
99329	55791	80 Leo, HR 4410	6.35	0.345	16.28±0.85	2.41		39	52,234.02–52,348.85	0.0044	$\gamma$ Dor
101688	57082	HR 4505	6.65	0.364	16.30±0.89	2.71	C	29	52,234.03–52,348.86	0.0006	Constant
102660	57646	HR 4535	6.05	0.278	15.96±0.81	2.07	C	45	52,241.00–52,448.67	0.0005	Constant
102910	57779	HR 4543	6.37	0.294	18.08±0.74	2.66		45	52,241.00–52,448.67	0.0027	$\delta$ Sct
102942	57805	HR 4545	6.25	0.345	15.87±0.70	2.25	C	53	52,230.00–52,440.68	0.0000	Constant
105584	59258	...	7.51	0.348	17.32±0.83	3.70	C	76	52,044.65–52,462.67	0.0000	Constant
107054	60018	HR 4680	6.23	0.310	18.06±0.82	2.51		69	52,038.77–52,460.69	0.0000	Constant
107326	60168	HR 4694	6.16	0.306	16.50±0.72	2.25		66	52,038.75–52,348.89	0.0000	Constant
112097	62933	41 Vir, HR 4900	6.25	0.282	16.40±0.78	2.32		72	52,029.83–52,460.69	0.0058	$\delta$ Sct
<b>114447</b>	<b>64246</b>	<b>17 CVn, HR 4971, ADS 8805A</b>	<b>5.91</b>	<b>0.294</b>	<b>16.12±0.81</b>	<b>1.95</b>	<b>D</b>	<b>81</b>	<b>52,030.86–52,461.71</b>	<b>0.0074</b>	$\gamma$ Dor
115810	64979	HR 5025, ADS 8861D	6.01	0.277	15.34±0.74	1.94	C	79	52,029.84–52,461.72	0.0000	Constant
117436	65892	72 Vir, HR 5088, ADS 8924A	6.10	0.341	18.47±0.73	2.43	C	47	52,029.82–52,461.66	0.0000	Constant
120317	67379	...	6.81	0.340	16.69±0.85	2.92		45	52,030.90–52,461.71	0.0008	Constant
120600	67483	HR 5204	6.43	0.256	15.41±0.80	2.37	C	89	52,030.92–52,460.72	0.0000	Constant
123255	68940	95 Vir, HR 5290	5.46	0.347	18.22±1.07	1.76	C	36	52,032.74–52,443.67	0.0012	Constant
123691	69040	...	6.80	0.372	19.65±0.68	3.27		70	52,030.87–52,461.73	0.0010	Constant
124248	69403	$\mu$ Vir, 97 Vir	7.15	0.333	15.27±0.96	3.07	P	58	52,031.72–52,461.70	0.0195	$\gamma$ Dor
124915	69727	HR 5341	6.44	0.275	19.19±1.75	2.86		50	52,030.85–52,460.71	0.0036	$\delta$ Sct
130044	72066	...	6.73	0.292	15.60±0.57	2.70	C	75	52,030.93–52,448.79	0.0000	Constant
132772	73369	40 Boo, HR 5588	5.64	0.336	19.83±0.57	2.13		64	52,030.88–52,462.81	0.0000	Constant
136751	75093	HR 5716	6.14	0.369	18.60±0.61	2.49	C	66	52,030.94–52,461.79	0.0000	Constant
137006	75342	8 Ser, HR 5721	6.11	0.264	18.20±0.78	2.41	C	39	52,031.81–52,443.73	0.0018	Constant
138100	75752	...	6.69	0.370	17.18±0.65	2.87	C	70	52,031.71–52,449.81	0.0009	Constant
138290	75971	HR 5758	6.57	0.380	19.73±0.92	3.05	C	57	52,031.72–52,443.74	0.0007	Constant
138803	76198	HR 5783	6.49	0.341	15.92±0.86	2.50		67	52,031.84–52,446.75	0.0025	Variable
<b>138936</b>	<b>76291</b>	<b>HR 5791</b>	<b>6.55</b>	<b>0.281</b>	<b>16.95±0.76</b>	<b>2.70</b>	<b>C</b>	<b>45</b>	<b>52,031.75–52,444.74</b>	<b>0.0029</b>	$\gamma$ Dor
<b>139478</b>	<b>76384</b>	<b>HR 5817</b>	<b>6.70</b>	<b>0.329</b>	<b>16.77±0.59</b>	<b>2.82</b>		<b>50</b>	<b>52,031.86–52,461.79</b>	<b>0.0103</b>	$\gamma$ Dor
<b>145005</b>	<b>79122</b>	...	<b>7.25</b>	<b>0.349</b>	<b>15.22±0.92</b>	<b>3.16</b>		<b>45</b>	<b>52,031.80–52,445.75</b>	<b>0.0038</b>	$\gamma$ Dor
150557	81734	14 Oph, HR 6205	5.74	0.336	19.70±0.86	2.21	C	24	52,035.96–52,445.79	0.0019	Constant
151087	81911	HR 6222	6.02	0.321	18.19±0.57	2.32	C	63	52,032.89–52,448.83	0.0000	Constant
151372	82142	...	6.72	0.356	16.48±1.08	2.81	C	33	52,032.79–52,444.79	0.0005	Constant
157224	84785	...	6.66	0.332	15.04±0.57	2.55		78	52,032.77–52,461.85	0.0027	$\delta$ Sct
162898	87211	...	6.70	0.373	19.34±0.55	3.13		...	...	...	Constant <sup>c</sup>
163929	87744	HR 6699	6.09	0.316	17.75±0.51	2.34		44	52,034.79–52,450.87	0.0000	Constant
163968	87882	...	7.32	0.355	15.43±0.63	3.26	C	63	52,034.80–52,461.86	0.0013	Constant
165373	88528	V831 Her, HR 6754	6.34	0.306	16.12±0.68	2.38	C	71	52,034.90–52,449.87	0.0000	Constant
165645	88565	HR 6767, ADS 11054A	6.38	0.287	17.44±0.56	2.59		42	52,034.83–52,447.84	0.0020	$\gamma$ Dor
167858	89601	V2502 Oph, HR 6844	6.62	0.312	15.98±0.80	2.64	P	53	52,033.90–52,461.82	0.0241	$\gamma$ Dor
169268	90174	HR 6890	6.36	0.351	15.10±0.79	2.26		62	52,034.88–52,447.82	0.0013	Constant
173417	91883	HR 7044	5.68	0.360	19.27±0.60	2.10	C	56	52,034.83–52,461.88	0.0000	Constant
174504	92291	...	6.97	0.347	16.20±0.55	3.02	C	52	52,034.93–52,461.88	0.0000	Constant
175592	92879	...	6.62	0.353	19.37±0.88	3.06	C	65	52,034.85–52,461.87	0.0013	Constant
184761	96313	...	6.74	0.290	15.49±0.75	2.69	C	70	52,034.86–52,450.90	0.0000	Constant

Table 2—Continued

HD (1)	HIP (2)	Other Names (3)	$V^a$ (mag) (4)	$B - V^a$ (mag) (5)	$\pi^a$ (mas) (6)	$M_V$ (mag) (7)	<i>Hipparcos</i> Variable Type <sup>b</sup> (8)	$N_{obs}$ (9)	Date Range (HJD - 2,400,000) (10)	$\sigma_{star}$ (mag) (11)	Final Status (12)
186998	97319	HR 7533	6.66	0.295	16.37±0.74	2.73		45	52,038.92–52,450.91	0.0000	Constant
190172	98809	HR 7661	6.68	0.347	15.39±1.12	2.62	C	64	52,036.94–52,461.88	0.0050	$\delta$ Sct
198638	102801	...	6.65	0.372	15.70±0.58	2.63	C	53	52,036.91–52,461.92	0.0000	Constant
199611	103359	HR 8025, ADS 14460A	5.83	0.337	18.75±0.53	2.19	C	45	52,036.91–52,449.94	0.0000	Constant
203015	105254	...	6.70	0.366	19.11±0.80	3.11	D	48	52,043.91–52,450.92	0.0000	Constant
203803	105652	HR 8190	5.70	0.314	18.05±0.65	1.98		73	52,037.92–52,461.94	0.0000	Constant
205924	106856	4 Peg, HR 8270, ADS 15157A	5.66	0.265	18.74±0.75	2.02	C	55	52,038.97–52,461.91	0.0000	Constant
207223	107558	HR 8330	6.18	0.350	19.90±0.80	2.67		74	52,037.96–52,450.95	0.0099	$\gamma$ Dor
208703	108453	HR 8376	6.33	0.378	17.98±0.81	2.60	C	49	52,061.97–52,461.90	0.0000	Constant
209193	108660	...	7.26	0.347	15.14±0.79	3.16		79	52,038.96–52,450.96	0.0000	Constant
210074	109209	HR 8435	5.74	0.331	16.39±0.62	1.81	C	68	52,038.97–52,461.96	0.0000	Constant
213617	111278	39 Peg, HR 8586	6.43	0.350	18.90±0.83	2.81	U	73	52,038.98–52,461.97	0.0151	$\gamma$ Dor
215664	112417	HR 8666	5.84	0.358	18.79±0.64	2.21	C	54	52,045.95–52,443.96	0.0000	Constant
<b>220091</b>	<b>115288</b>	...	<b>6.67</b>	<b>0.329</b>	<b>15.11±0.90</b>	<b>2.57</b>	<b>M</b>	<b>66</b>	<b>52,054.96–52,436.97</b>	<b>0.0067</b>	$\gamma$ Dor
223277	117394	...	6.66	0.324	17.54±0.81	2.88		47	52,161.80–52,286.59	0.0000	Constant
<b>224945</b>	<b>159</b>	<b>BU Psc</b>	<b>6.93</b>	<b>0.292</b>	<b>16.92±0.81</b>	<b>3.07</b>	<b>C</b>	<b>33</b>	<b>52,161.87–52,276.62</b>	<b>0.0053</b>	$\gamma$ Dor

<sup>a</sup>From the *Hipparcos* catalog.

<sup>b</sup>A “blank” in this column indicates the star could not be classified as variable or constant, C = no variability detected (“constant”), D = duplicity induced variability, M = possible micro-variable (amplitude <0.03 mag), P = periodic variable, U = unresolved variable.

<sup>c</sup>T12 APT survey observations failed because of a bright, nearby companion. HD 162898 was added to the T3 follow-up list and found to be constant.



Table 3. COMPARISON & CHECK STARS FOR NEW  $\gamma$  DORADUS STARS

$\gamma$ Doradus Star	Comparison Star	Check Star	$\sigma_{(V-C)}^a$ (mag)	$\sigma_{(K-C)}^a$ (mag)
HD 6568	HD 6120	HD 7446	0.0092	0.0046
HD 17163	HD 16647	HD 18258	0.0055	0.0051
HD 25906	HD 25877	HD 26755	0.0058	0.0047
HD 31550	HD 30617	HD 30708	0.0043	0.0033
HD 38309	HD 40259	HD 38145	0.0050	0.0049
HD 45638	HD 45089	HD 44853	0.0059	0.0042
HD 62196	HD 64106	HD 60063	0.0066	0.0046
HD 63436	HD 62724	HD 60490	0.0277	0.0058
HD 65526	HD 66351	HD 68145	0.0234	0.0050
HD 69682	HD 67991	HD 71952	0.0061	0.0044
HD 99267	HD 99207	HD 101091	0.0167	0.0039
HD 114447	HD 114905	HD 117261	0.0099	0.0047
HD 138936	HD 139044	HD 138562	0.0053	0.0060
HD 139478	HD 139778	HD 139357	0.0135	0.0048
HD 145005	HD 146173	HD 145894	0.0067	0.0071
HD 220091	HD 218079	HD 220044	0.0085	0.0045
HD 224945	HD 6	HD 406	0.0065	0.0061

<sup>a</sup>In the Johnson  $B$  photometric band.

Table 4. PHOTOMETRIC OBSERVATIONS OF NEW  $\gamma$  DORADUS STARS

HD	Date (HJD – 2,400,000)	Var $B$ (mag)	Var $V$ (mag)	Chk $B$ (mag)	Chk $V$ (mag)
6568	53,255.7637	–0.088	–0.133	–0.225	–1.033
6568	53,255.8545	–0.095	–0.135	–0.236	–1.037
6568	53,258.7573	–0.099	–0.141	–0.228	–1.033
6568	53,258.8455	–0.093	–0.136	–0.232	–1.035
6568	53,258.9367	–0.092	–0.136	–0.232	–1.040
6568	53,259.7536	–0.098	–0.142	99.999	99.999

Note. — Table 4 is presented in its entirety in the electronic edition of the *Astronomical Journal*. A portion is shown here for guidance regarding the form and content.

Table 5. PHOTOMETRIC RESULTS FOR NEW  $\gamma$  DORADUS STARS

HD (1)	Photometric Band (2)	Date Range (HJD - 2,400,000) (3)	$N_{obs}$ (4)	Frequency ( $\text{day}^{-1}$ ) (5)	Period (days) (6)	Peak-to-Peak Amplitude (mmag) (7)	$B/V$ Amplitude Ratio (8)	$T_{min}$ (HJD - 2,400,000) (9)
6568	$B$	53,255.76–53,405.59	223	$1.3620 \pm 0.0004$	$0.73421 \pm 0.00022$	$17.6 \pm 1.3$	$1.45 \pm 0.17$	$53,300.612 \pm 0.009$
				$1.3416 \pm 0.0004$	$0.74538 \pm 0.00022$	$15.2 \pm 1.5$	$1.23 \pm 0.20$	$53,300.055 \pm 0.011$
	$V$	53,255.76–53,405.59	211	$1.3629 \pm 0.0004$	$0.73373 \pm 0.00019$	$12.1 \pm 1.2$		$53,300.630 \pm 0.012$
				$1.3425 \pm 0.0005$	$0.74488 \pm 0.00028$	$12.4 \pm 1.2$		$53,300.036 \pm 0.012$
17163	$B$	53,630.92–53,793.60	296	$2.3612 \pm 0.0003$	$0.42351 \pm 0.00005$	$8.1 \pm 0.8$	$1.16 \pm 0.20$	$53,700.059 \pm 0.007$
				$2.3609 \pm 0.0003$	$0.42357 \pm 0.00005$	$7.0 \pm 0.7$		$53,700.047 \pm 0.007$
25906	$B$	53,255.86–53,460.62	295	$1.2632 \pm 0.0003$	$0.79164 \pm 0.00019$	$8.6 \pm 0.9$	$1.28 \pm 0.21$	$53,350.785 \pm 0.012$
				$1.2248 \pm 0.0002$	$0.81646 \pm 0.00013$	$5.5 \pm 0.9$	$0.91 \pm 0.28$	$53,350.593 \pm 0.022$
	$V$	53,255.86–53,460.62	304	$0.7452 \pm 0.0003$	$1.34192 \pm 0.00054$	$6.3 \pm 0.9$	$1.86 \pm 0.38$	$53,350.165 \pm 0.031$
				$1.2636 \pm 0.0003$	$0.79139 \pm 0.00019$	$6.8 \pm 0.7$		$53,350.760 \pm 0.013$
				$1.2246 \pm 0.0002$	$0.81659 \pm 0.00017$	$6.1 \pm 0.7$		$53,350.594 \pm 0.016$
				$0.7456 \pm 0.0003$	$1.34120 \pm 0.00054$	$3.4 \pm 0.8$		$53,350.207 \pm 0.051$
31550	$B$	53,630.95–53,838.62	284	$0.6686 \pm 0.0003$	$1.49566 \pm 0.00067$	$7.3 \pm 0.7$	$1.13 \pm 0.21$	$53,701.169 \pm 0.020$
				$0.6683 \pm 0.0002$	$1.49633 \pm 0.00045$	$6.5 \pm 0.8$		$53,701.178 \pm 0.025$
38309	$B$	53,258.96–53,472.62	230	$2.6523 \pm 0.0003$	$0.37703 \pm 0.00004$	$8.9 \pm 0.8$	$1.31 \pm 0.22$	$53,350.363 \pm 0.005$
				$2.7783 \pm 0.0003$	$0.35993 \pm 0.00003$	$7.3 \pm 0.8$	$0.91 \pm 0.22$	$53,350.093 \pm 0.006$
				$2.8808 \pm 0.0003$	$0.34713 \pm 0.00004$	$5.1 \pm 0.8$	$0.91 \pm 0.32$	$53,350.161 \pm 0.010$
				$2.6507 \pm 0.0003$	$0.37726 \pm 0.00004$	$6.8 \pm 0.9$		$53,350.346 \pm 0.008$
				$2.7779 \pm 0.0003$	$0.35998 \pm 0.00003$	$8.0 \pm 0.9$		$53,350.087 \pm 0.006$
				$2.8796 \pm 0.0002$	$0.34727 \pm 0.00002$	$5.6 \pm 0.9$		$53,350.162 \pm 0.009$
45638	$B$	53,641.01–53,849.63	329	$1.1622 \pm 0.0002$	$0.86046 \pm 0.00015$	$10.8 \pm 0.8$	$1.41 \pm 0.15$	$53,750.700 \pm 0.009$
				$1.1615 \pm 0.0003$	$0.86096 \pm 0.00019$	$7.7 \pm 0.6$		$53,750.715 \pm 0.012$
62196	$B$	53,258.99–53,510.64	296	$0.9966 \pm 0.0002$	$1.00341 \pm 0.00020$	$14.2 \pm 0.7$	$1.89 \pm 0.13$	$53,400.541 \pm 0.008$
				$1.0077 \pm 0.0002$	$0.99236 \pm 0.00020$	$12.8 \pm 0.8$	$1.65 \pm 0.14$	$53,400.038 \pm 0.010$
	$V$	53,258.99–53,506.63	275	$0.9972 \pm 0.0002$	$1.00281 \pm 0.00020$	$7.5 \pm 0.6$		$53,400.548 \pm 0.013$
				$1.0070 \pm 0.0003$	$0.99305 \pm 0.00025$	$7.8 \pm 0.6$		$53,400.031 \pm 0.012$
63436	$B$	53,635.01–53,860.63	211	$1.4557 \pm 0.0003$	$0.68695 \pm 0.00012$	$53.7 \pm 4.0$	$1.28 \pm 0.15$	$53,750.112 \pm 0.008$
				$1.4020 \pm 0.0003$	$0.71327 \pm 0.00015$	$34.6 \pm 5.2$	$1.18 \pm 0.28$	$53,750.037 \pm 0.016$

Table 5—Continued

HD (1)	Photometric Band (2)	Date Range (HJD - 2,400,000) (3)	$N_{obs}$ (4)	Frequency ( $\text{day}^{-1}$ ) (5)	Period (days) (6)	Peak-to-Peak Amplitude (mmag) (7)	$B/V$ Amplitude Ratio (8)	$T_{min}$ (HJD - 2,400,000) (9)
				$1.4443 \pm 0.0003$	$0.69238 \pm 0.00012$	$38.8 \pm 5.0$	$1.69 \pm 0.31$	$53,750.646 \pm 0.013$
				$1.8372 \pm 0.0003$	$0.54431 \pm 0.00009$	$24.2 \pm 5.2$	$1.34 \pm 0.44$	$53,750.511 \pm 0.019$
	<i>V</i>	53,635.01–53,860.63	217	$1.4559 \pm 0.0003$	$0.68686 \pm 0.00014$	$41.8 \pm 3.1$		$53,750.108 \pm 0.008$
				$1.4018 \pm 0.0003$	$0.71337 \pm 0.00013$	$29.4 \pm 3.9$		$53,750.052 \pm 0.014$
				$1.4443 \pm 0.0003$	$0.69238 \pm 0.00014$	$22.9 \pm 4.1$		$53,750.643 \pm 0.018$
				$1.8369 \pm 0.0003$	$0.54440 \pm 0.00007$	$18.0 \pm 4.0$		$53,750.530 \pm 0.020$
65526	<i>B</i>	53,644.01–53,861.63	223	$1.5527 \pm 0.0003$	$0.64404 \pm 0.00012$	$51.9 \pm 2.8$	$1.21 \pm 0.10$	$53,750.245 \pm 0.005$
				$1.6735 \pm 0.0003$	$0.59755 \pm 0.00009$	$21.2 \pm 4.4$	$1.29 \pm 0.42$	$53,750.018 \pm 0.019$
				$1.7101 \pm 0.0003$	$0.58476 \pm 0.00009$	$23.0 \pm 4.1$	$1.39 \pm 0.38$	$53,750.425 \pm 0.017$
	<i>V</i>	53,644.01–53,861.63	232	$1.5528 \pm 0.0003$	$0.64400 \pm 0.00010$	$43.0 \pm 2.1$		$53,750.239 \pm 0.005$
				$1.6734 \pm 0.0002$	$0.59759 \pm 0.00009$	$16.5 \pm 3.5$		$53,750.037 \pm 0.020$
				$1.7101 \pm 0.0003$	$0.58476 \pm 0.00010$	$16.6 \pm 3.3$		$53,750.426 \pm 0.020$
69682	<i>B</i>	53,637.98–53,884.64	425	$1.8801 \pm 0.0002$	$0.53189 \pm 0.00006$	$7.2 \pm 0.8$	$1.53 \pm 0.25$	$53,750.113 \pm 0.009$
				$2.0963 \pm 0.0002$	$0.47703 \pm 0.00005$	$5.4 \pm 0.8$	$0.99 \pm 0.27$	$53,750.161 \pm 0.011$
	<i>V</i>	53,637.98–53,884.64	429	$1.8798 \pm 0.0002$	$0.53197 \pm 0.00006$	$4.7 \pm 0.7$		$53,750.115 \pm 0.013$
				$2.0965 \pm 0.0002$	$0.47699 \pm 0.00005$	$5.5 \pm 0.7$		$53,750.178 \pm 0.009$
99267	<i>B</i>	53,309.02–53,562.65	352	$1.7402 \pm 0.0002$	$0.57465 \pm 0.00005$	$24.7 \pm 2.2$	$1.12 \pm 0.17$	$53,400.107 \pm 0.008$
				$1.7690 \pm 0.0002$	$0.56529 \pm 0.00006$	$18.7 \pm 2.4$	$1.51 \pm 0.29$	$53,400.440 \pm 0.011$
				$1.7802 \pm 0.0002$	$0.56173 \pm 0.00006$	$19.9 \pm 2.3$	$1.35 \pm 0.25$	$53,400.489 \pm 0.010$
				$1.7001 \pm 0.0002$	$0.58820 \pm 0.00007$	$19.7 \pm 2.3$	$1.18 \pm 0.23$	$53,400.514 \pm 0.011$
				$2.1029 \pm 0.0002$	$0.47553 \pm 0.00005$	$5.2 \pm 2.5$	$1.15 \pm 0.94$	$53,400.352 \pm 0.037$
	<i>V</i>	53,309.02–53,561.65	336	$1.7402 \pm 0.0002$	$0.57465 \pm 0.00007$	$22.1 \pm 1.7$		$53,400.094 \pm 0.007$
				$1.7690 \pm 0.0003$	$0.56529 \pm 0.00010$	$12.4 \pm 2.0$		$53,400.441 \pm 0.014$
				$1.7804 \pm 0.0002$	$0.56167 \pm 0.00006$	$14.7 \pm 1.9$		$53,400.506 \pm 0.012$
				$1.6999 \pm 0.0002$	$0.58827 \pm 0.00007$	$16.7 \pm 1.9$		$53,400.499 \pm 0.011$
				$2.1031 \pm 0.0003$	$0.47549 \pm 0.00006$	$4.6 \pm 2.1$		$53,400.357 \pm 0.036$
114447	<i>B</i>	53,330.03–53,563.66	328	$1.1284 \pm 0.0003$	$0.88621 \pm 0.00024$	$16.5 \pm 1.2$	$1.39 \pm 0.15$	$53,450.503 \pm 0.011$
				$1.3386 \pm 0.0002$	$0.74705 \pm 0.00011$	$16.2 \pm 1.3$	$1.60 \pm 0.18$	$53,450.201 \pm 0.009$

Table 5—Continued

HD (1)	Photometric Band (2)	Date Range (HJD - 2,400,000) (3)	$N_{obs}$ (4)	Frequency ( $\text{day}^{-1}$ ) (5)	Period (days) (6)	Peak-to-Peak Amplitude (mmag) (7)	$B/V$ Amplitude Ratio (8)	$T_{min}$ (HJD - 2,400,000) (9)
138936	V	53,330.03–53,563.66	326	$1.4499 \pm 0.0002$	$0.68970 \pm 0.00012$	$10.6 \pm 1.4$	$1.31 \pm 0.27$	$53,450.067 \pm 0.015$
				$1.1278 \pm 0.0002$	$0.88668 \pm 0.00020$	$11.8 \pm 0.9$		$53,450.493 \pm 0.011$
				$1.3388 \pm 0.0002$	$0.74694 \pm 0.00014$	$10.1 \pm 1.0$		$53,450.208 \pm 0.012$
				$1.4492 \pm 0.0003$	$0.69004 \pm 0.00014$	$8.1 \pm 1.1$		$53,450.084 \pm 0.014$
138936	B	53,371.05–53,566.75	217	$2.3855 \pm 0.0003$	$0.41920 \pm 0.00005$	$8.5 \pm 0.8$	$1.45 \pm 0.22$	$53,500.076 \pm 0.007$
				$2.4018 \pm 0.0004$	$0.41635 \pm 0.00007$	$5.5 \pm 0.9$	$1.70 \pm 0.41$	$53,500.307 \pm 0.012$
				$2.1839 \pm 0.0003$	$0.45790 \pm 0.00006$	$5.5 \pm 1.0$	$0.92 \pm 0.30$	$53,500.409 \pm 0.013$
138936	V	53,372.05–53,566.75	220	$2.3869 \pm 0.0003$	$0.41895 \pm 0.00005$	$5.8 \pm 0.7$		$53,500.066 \pm 0.009$
				$2.4006 \pm 0.0003$	$0.41656 \pm 0.00005$	$3.2 \pm 0.8$		$53,500.321 \pm 0.017$
				$2.1834 \pm 0.0003$	$0.45800 \pm 0.00006$	$5.9 \pm 0.8$		$53,500.409 \pm 0.009$
				$1.4531 \pm 0.0002$	$0.68818 \pm 0.00009$	$24.1 \pm 1.7$	$1.40 \pm 0.16$	$53,400.128 \pm 0.008$
139478	B	53,255.63–53,566.75	309	$1.4073 \pm 0.0002$	$0.71058 \pm 0.00010$	$18.5 \pm 2.0$	$1.19 \pm 0.21$	$53,400.565 \pm 0.012$
				$1.5056 \pm 0.0002$	$0.66419 \pm 0.00007$	$17.8 \pm 1.9$	$1.35 \pm 0.23$	$53,400.345 \pm 0.012$
				$1.4530 \pm 0.0002$	$0.68823 \pm 0.00009$	$17.3 \pm 1.6$		$53,400.134 \pm 0.010$
139478	V	53,255.63–53,567.67	330	$1.4071 \pm 0.0002$	$0.71068 \pm 0.00010$	$15.5 \pm 1.7$		$53,400.566 \pm 0.012$
				$1.5056 \pm 0.0002$	$0.66419 \pm 0.00009$	$13.2 \pm 1.7$		$53,400.355 \pm 0.014$
				$2.1473 \pm 0.0004^b$	$0.46570 \pm 0.00009^b$	$11.9 \pm 1.2$	$1.25 \pm 0.24$	$53,850.406 \pm 0.008$
145005	B	53,758.06–53,907.78	154	$2.1481 \pm 0.0004$	$0.46553 \pm 0.00008$	$9.5 \pm 1.3$		$53,850.426 \pm 0.020$
220091	B	53,255.67–53,567.92	253	$2.8277 \pm 0.0002$	$0.35364 \pm 0.00003$	$19.3 \pm 1.0$	$1.21 \pm 0.11$	$53,400.347 \pm 0.003$
				$2.7241 \pm 0.0002$	$0.36709 \pm 0.00003$	$13.0 \pm 1.3$	$1.15 \pm 0.20$	$53,400.051 \pm 0.006$
220091	V	53,255.67–53,567.92	244	$2.8276 \pm 0.0002$	$0.35366 \pm 0.00003$	$16.0 \pm 0.9$		$53,400.342 \pm 0.003$
				$2.7242 \pm 0.0002$	$0.36708 \pm 0.00003$	$11.2 \pm 1.1$		$53,400.046 \pm 0.006$
				$1.8410 \pm 0.0006$	$0.54318 \pm 0.00018$	$11.4 \pm 0.9$	$1.37 \pm 0.17$	$53,700.190 \pm 0.007$
224945	B	53,636.69–53,763.58	302	$1.2951 \pm 0.0005$	$0.77214 \pm 0.00030$	$7.7 \pm 1.0$	$1.06 \pm 0.24$	$53,700.043 \pm 0.016$
				$1.8407 \pm 0.0004$	$0.54327 \pm 0.00013$	$8.3 \pm 0.8$		$53,700.172 \pm 0.008$
				$1.2953 \pm 0.0004$	$0.77202 \pm 0.00021$	$7.3 \pm 0.8$		$53,700.088 \pm 0.014$

Note. — The individual photometric observations are given in Table 4.

<sup>a</sup>First frequency has slightly asymmetrical light curve.

<sup>b</sup>Frequency identification uncertain due to aliasing.

Table 6. BASIC PROPERTIES OF NEW  $\gamma$  DORADUS STARS

HD (1)	Other Names (2)	Component (3)	$V^a$ (mag) (4)	$B-V^a$ (mag) (5)	Spectral Class <sup>b</sup> (6)	Luminosity Class <sup>b</sup> (7)	$v \sin i^b$ (km s <sup>-1</sup> ) (8)	Velocity <sup>b,c</sup> (km s <sup>-1</sup> ) (9)
6568	...	...	6.93	0.301	F1	Dwarf	55	Binary
17163	HR 816	...	6.04	0.312	F1:	Dwarf	105	26.2 $\pm$ 0.3
25906	...	...	7.08	0.345	F1	Dwarf	64	Binary?
31550	...	...	6.74	0.335	F0	Dwarf	32	17.6 $\pm$ 1.8
38309	HR 1978	A	6.09	0.320				
		Aa	6.24	0.32	F1	Dwarf	95:	Binary
		Ab	8.34	0.61	G1:	Dwarf	5:	Binary
45638	HR 2351	...	6.59	0.293	A9	Dwarf	38	42.4 $\pm$ 0.4
62196	...	...	7.67	0.313	F2	Dwarf	6	Binary
63436	DD CMi	...	7.46	0.356	F2	Dwarf	70	13.7 $\pm$ 1.3
65526	V769 Mon	...	6.98	0.297	A9	Dwarf	59	-6.0 $\pm$ 0.5
69682	HR 3258	...	6.50	0.300	A9	Dwarf	30	11.4 $\pm$ 0.3
99267	...	...	6.88	0.322	F1	Dwarf	95	2.9 $\pm$ 0.4
114447	17 CVn, HR 4971	A	5.91	0.294				
		Aa	6.57	0.29	F0:	Dwarf	50:	Binary
		Ab	6.77	0.29	F0:	Dwarf	90:	Binary
138936	HR 5791	...	6.55	0.281	A9	Dwarf	65	-24.5 $\pm$ 1.0
139478	HR 5817	...	6.70	0.329	F1	Dwarf	20	-15.7 $\pm$ 0.1
145005	...	A,B	7.25	0.349				
		A	7.33	0.30	F0	Dwarf	57	-9.3
		B	10.13	0.66	G4:	Dwarf	5:	-11.0
220091	...	A,B	6.67	0.329				
		A	6.80	0.33	F1	Dwarf	120:	Binary
		B	9.00	0.61	G1:	Dwarf	3:	Binary
224945	BU Psc	...	6.93	0.292	A9	Dwarf	55	7.1 $\pm$ 0.8

<sup>a</sup>Single star values and combined values of binary components are from the *Hipparcos* catalog. For the individual binary components see the text.

<sup>b</sup>Values from this paper. A colon indicates greater uncertainty than usual.

<sup>c</sup>Velocity noted as “Binary” indicates velocity variability produced by orbital motion.

Table 7. INDIVIDUAL RADIAL VELOCITIES OF NEW  $\gamma$  DORADUS STARS

HD (1)	Date (HJD – 2,400,000) (2)	Radial Velocity (km s <sup>-1</sup> ) (3)	Comments (4)
6568	52,940.820	–13.8	
	52,942.777	–13.8	
	53,273.902	–4.1	
	53,534.978	–6.4	
	53,634.837	8.4	Asymmetric lines
	53,635.907	4.2	Asymmetric lines
	53,637.870	6.3	Very asymmetric lines
	54,001.866	9.5	

Note. — Table 7 is published in its entirety in the electronic edition of the *Astronomical Journal*. A portion is shown here for guidance regarding its form and content.

Table 8. PROPERTIES OF  $\gamma$  DORADUS FIELD STARS

HD <sup>a,b</sup> (1)	Other Names (2)	Duplicity <sup>c</sup> (3)	V (mag) (4)	(B-V) (mag) (5)	M <sub>V</sub> (mag) (6)	L (L <sub>⊙</sub> ) (7)	R (R <sub>⊙</sub> ) (8)	Period (days) (9)	Reference (10)
277	...	single	8.37	0.379	3.31	3.7	1.4	0.9005	Henry et al. (2001)
2842	...	single	7.99	0.325	2.83	5.7	1.6	0.65070	Henry, Fekel, & Henry (2005)
6568A	...	SB1	6.93	0.301	2.86	5.6	1.5	0.7342	This paper
7169A	HDS 160	VB,SB2	7.42	0.329	2.98	5.0	1.5	0.5486	Henry & Fekel (2003)
<b>8801A</b>	<b>HR 418, ADS 1151A</b>	<b>VB</b>	<b>6.42</b>	<b>0.311</b>	<b>2.68</b>	<b>6.5</b>	<b>1.7</b>	<b>0.40331</b>	<b>Henry &amp; Fekel (2005)</b>
9365A	...	VB	8.17	0.361	2.76	6.1	1.7	0.62582	Henry, Fekel, & Henry (2007)
12901	...	single	6.74	0.311	2.35	8.9	1.9	0.82270	Eyer & Aerts (2000)
17163	HR 816	single	6.04	0.312	2.49	7.8	1.8	0.42351	This paper
17310A	...	SB1	7.76	0.378	2.56	7.3	1.9	2.13584	Henry, Fekel, & Henry (2005)
18995	...	single	6.72	0.342	2.32	9.1	2.1	1.0833	Henry & Fekel (2002)
19684A	...	SB1	6.96	0.301	1.86	13.8	2.4	0.34722	Henry & Fekel (2002)
23874A	ADS 2785 A	VB,SB2	8.45	0.329	2.67	6.6	1.7	0.4432	Henry & Fekel (2003)
25906A	...	SB1?	7.08	0.345	2.99	4.9	1.5	0.7916	This paper
27290	$\gamma$ Dor, HR 1338	single	4.26	0.312	2.72	6.3	1.6	0.7570	Balona, Krisciunas, & Cousins (1994)
31550	...	single	6.74	0.335	2.91	5.3	1.6	1.4957	This paper
32348A	...	SB2	7.40	0.31	2.57	7.2	1.7	0.79422	Henry, Fekel, & Henry (2007)
32537A	V398 Aur, 9 Aur, HR 1637, ADS 3675 A	VB	4.98	0.343	2.89	5.4	1.6	1.2582	Zerbi et al. (1997a)
38309Aa	HR 1978, ADS 4333 A	VB,SB2	6.24	0.32	2.72	6.3	1.7	0.37703	This paper
40745	HR 2118, AC Lep	single	6.21	0.358	2.32	9.1	2.1	0.82427	Henry, Fekel, & Henry (2007)
41448	...	single	7.60	0.299	2.76	6.1	1.6	0.41992	Henry, Fekel, & Henry (2007)
41547A	HR 2150	SB2	6.41	0.35	2.56	7.3	1.9	0.81123	Henry, Fekel, & Henry (2007)
<b>44195</b>	...	<b>single</b>	<b>7.56</b>	<b>0.315</b>	<b>2.72</b>	<b>6.3</b>	<b>1.6</b>	<b>~ 0.34</b>	<b>Poretti et al. (2005)</b>
45638	HR 2351	single	6.59	0.293	2.67	6.6	1.6	0.8605	This paper
48271	...	single	7.49	0.315	2.62	6.9	1.7	1.0959	Henry & Fekel (2003)
48501A	HR 2481, ADS 5377 A	VB	6.26	0.321	2.81	5.8	1.6	0.7750 <sup>d</sup>	Eyer & Aerts (2000)
49015A	...	VB	7.04	0.375	2.83	5.7	1.7	0.52718	Henry & Fekel (2002)
<b>49434</b>	<b>HR 2514</b>	<b>single</b>	<b>5.75</b>	<b>0.292</b>	<b>2.74</b>	<b>6.2</b>	<b>1.6</b>	<b>0.57644</b>	<b>Uytterhoeven et al. (2008)</b>
55892	QW Pup, HR 2740	single	4.49	0.324	2.86	5.5	1.6	0.9584	Perryman et al. (1997)
62196A	...	SB1	7.67	0.313	3.59	2.8	1.1	1.0034	This paper
62454A	DO Lyn	SB2	7.43	0.329	2.67	6.6	1.7	0.62447	Kaye et al. (1999b)
63436	DD CMi	single	7.46	0.356	3.52	3.0	1.2	0.6870	This paper
64729	...	single	7.57	0.321	2.55	7.4	1.8	0.7248	Henry & Fekel (2003)
65526	V769 Mon	single	6.98	0.297	3.03	4.7	1.4	0.6440	Handler & Shobbrook (2002), This paper
68192	KO UMa	single	7.15	0.363	2.29	9.4	2.1	0.7691	Kaye et al. (1999b)
69682	HR 3258	single	6.50	0.300	2.51	7.6	1.8	0.53189	This paper
69715A	BDS 4550 A	VB	7.18	0.360	3.09	4.5	1.5	0.40707	Henry, Fekel, & Henry (2005)
70645A	...	SB1	8.12	0.344	2.51	7.7	1.9	1.10314	Mathias et al. (2004), Henry, Fekel, & Henry (2005)
74504	...	single	8.86	0.333	1.92	13.2	2.4	0.52474	Cuyppers et al. (2009)
80731A	...	SB1	8.46	0.345	2.61	7.0	1.8	1.11595	Mathias et al. (2004), Henry, Fekel, & Henry (2005)
86358A	HR 3936	SB2	6.87	0.300	2.75	6.1	1.6	0.7753	Henry & Fekel (2003)
86371A:	...	SB2	7.37	0.314	2.91	5.3	1.5	1.6784	Handler & Shobbrook (2002), Henry, Fekel, & Henry (2007)
86371B:	...	SB2	7.37	0.314	2.91	5.3	1.5	1.6784	Handler & Shobbrook (2002), Henry, Fekel, & Henry (2007)
89781	...	single	7.48	0.355	1.95	12.8	2.5	0.38060	Henry, Fekel, & Henry (2007)
99267	...	single	6.88	0.322	2.87	5.5	1.5	0.57465	This paper
99329	80 Leo, HR 4410	single	6.35	0.345	2.41	8.4	2.0	0.45286	Henry & Fekel (2002)
100215A	...	SB2	8.08	0.265	2.91	5.3	1.4	0.7564	Henry & Fekel (2003)
103751	...	single	7.97	0.397	2.47	8.0	2.1	1.01143	Henry, Fekel, & Henry (2007)
105085A	...	SB2	7.59	0.300	2.82	5.7	1.5	0.6879	Henry & Fekel (2003)
105458	...	single	7.77	0.299	2.84	5.6	1.5	0.7571	Henry et al. (2001)



Table 8—Continued

HD <sup>a,b</sup> (1)	Other Names (2)	Duplicity <sup>c</sup> (3)	<i>V</i> (mag) (4)	( <i>B</i> − <i>V</i> ) (mag) (5)	<i>M<sub>V</sub></i> (mag) (6)	<i>L</i> ( <i>L</i> <sub>⊙</sub> ) (7)	<i>R</i> ( <i>R</i> <sub>⊙</sub> ) (8)	Period (days) (9)	Reference (10)
108100A	DD CVn	SB2	7.27	0.329	2.68	6.5	1.7	0.7541	Breger et al. (1997), Henry & Fekel (2002)
112429	IR Dra, 8 Dra, HR 4916	single	5.23	0.303	2.93	5.2	1.5	0.42450	Henry, Fekel, & Henry (2005)
113867A:	...	SB2	7.40	0.265	2.53	7.5	1.7	1.1252	Henry & Fekel (2003)
113867B:	...	SB2	7.80	0.329	2.93	5.2	1.5	1.1252	Henry & Fekel (2003)
114447Aa:	HR 4971, 17 CVn, ADS 8805A	SB2	6.57	0.29	2.61	7.0	1.7	0.8862	This paper
114447Ab:	HR 4971, 17 CVn, ADS 8805A	SB2	6.77	0.29	2.81	5.8	1.5	0.8862	This paper
<b>114839</b>	...	<b>single</b>	<b>8.46</b>	<b>0.310</b>	<b>1.97</b>	<b>12.5</b>	<b>2.3</b>	<b>0.42779</b>	<b>King et al. (2006)</b>
115466	LP Vir, 58 Vir	single	6.89	0.338	2.39	8.5	2.0	0.83022	Henry, Fekel, & Henry (2005)
124248	MU Vir, 97 Vir	single	7.15	0.333	3.07	4.6	1.4	0.76144	Henry, Fekel, & Henry (2005)
138936	HR 5791	single	6.55	0.281	2.70	6.4	1.6	0.41920	This paper
139095	CF UMa, HR 4550	single	7.91	0.366	2.62	7.0	1.9	0.634	Handler & Shobbrook (2002)
139478	HR 5817	single	6.70	0.329	2.82	5.8	1.6	0.68818	This paper
144451A	...	VB	7.84	0.358	3.06	4.6	1.5	0.62617	Henry, Fekel, & Henry (2007)
145005A	...	SB2	7.33	0.30	3.24	3.9	1.3	0.46570	This paper
147787A	ι TrA, HR 6109	VB,SB2	6.03	0.36	3.00	4.9	1.5	1.4556	Aerts, Eyser, & Kestens (1998), De Cat et al. (2009)
152896	V645 Her	single	7.55	0.314	2.85	5.6	1.5	0.7472	Henry & Fekel (2003)
155154	HR 6379	single	6.17	0.306	2.91	5.3	1.5	0.34510	Henry et al. (2001)
160295A	V2381 Oph	SB2	7.87	0.354	2.38	8.6	2.0	0.7553	Henry & Fekel (2003)
160314A	...	VB	7.74	0.405	2.54	7.5	2.0	0.82763	Henry et al. (2001)
164615	V2118 Oph	single	7.03	0.354	2.82	5.8	1.7	0.8117	Zerbi et al. (1997b), Hatzes (1998)
165645A	HR 6767, ADS 11054 A	VB	6.38	0.287	2.59	7.1	1.7	0.4210	Henry & Fekel (2003)
166233A	73 Oph, HR 6795, ADS 11111 A	VB	6.03	0.320	2.49	7.8	1.8	0.61439	Fekel & Henry (2003)
167858A	V2502 Oph, HR 6844	SB1	6.62	0.312	2.64	6.8	1.7	1.307	Handler & Shobbrook (2002), Fekel & Henry (2003)
171244	...	single	7.75	0.397	2.06	11.7	2.5	1.0040	Henry & Fekel (2003)
175337	...	single	7.39	0.364	2.76	6.1	1.7	0.78691	Mathias et al. (2004), Henry, Fekel, & Henry (2005)
181998	...	single	7.67	0.328	2.81	5.8	1.6	1.334	Handler & Shobbrook (2002)
187615	...	single	7.95	0.300	2.84	5.6	1.5	0.49806	Henry, Fekel, & Henry (2007)
195068/9	V2121 Cyg, 43 Cyg, HR 7828	single	5.73	0.339	2.85	5.6	1.6	0.79955	Mathias et al. (2004), Henry, Fekel, & Henry (2005)
206043	NZ Peg, HR 8276	single	5.77	0.314	2.81	5.8	1.6	0.41113	Henry et al. (2001)
207223	V372 Peg, HR 8330	single	6.18	0.350	2.67	6.6	1.8	2.59381	Kaye et al. (1999c)
211699B	PR Peg	SB2	10.51	0.36	3.56	2.9	1.2	1.07204	Henry, Fekel, & Henry (2007)
213617	39 Peg, HR 8586	single	6.43	0.350	2.81	5.8	1.7	0.75574	Henry, Fekel, & Henry (2005)
218396	V342 Peg, HR 8799	single	5.97	0.259	2.96	5.0	1.4	0.5053	Zerbi et al. (1999)
218427	...	single	8.17	0.29	2.70	6.6	1.8	0.7504	Rodriguez et al. (2006a)
220091A	...	VB,SB2	6.80	0.33	2.70	6.4	1.7	0.35364	This paper
221866B	...	SB2	8.62	0.380	3.25	3.9	1.4	1.1416	Henry & Fekel (2002), Kaye, Gray, & Griffin (2004)
224638	BT Psc	single	7.49	0.342	2.98	4.9	1.5	1.2323	Mantegazza, Poretti, & Zerbi (1994)
224945	BU Psc	single	6.93	0.292	3.07	4.5	1.4	0.5432	Mantegazza, Poretti, & Zerbi (1994), This paper
239276	...	single	9.09	0.27	2.83	5.8	1.6	0.4747	Rodriguez et al. (2006b)
...	<b>BD+18 4914</b>	<b>single</b>	<b>10.6</b>	<b>0.29</b>	<b>2.43</b>	<b>8.2</b>	<b>1.8</b>	<b>0.56088</b>	<b>Rowe et al. (2006)</b>

<sup>a</sup>Colon indicates component A and/or B could be the  $\gamma$  Doradus star.<sup>b</sup>Bold indicates  $\gamma$  Doradus /  $\delta$  Scuti hybrid<sup>c</sup>VB = visual binary or double star. SB = spectroscopic binary.<sup>d</sup>Also has period of 10.959 days with a slightly larger amplitude.

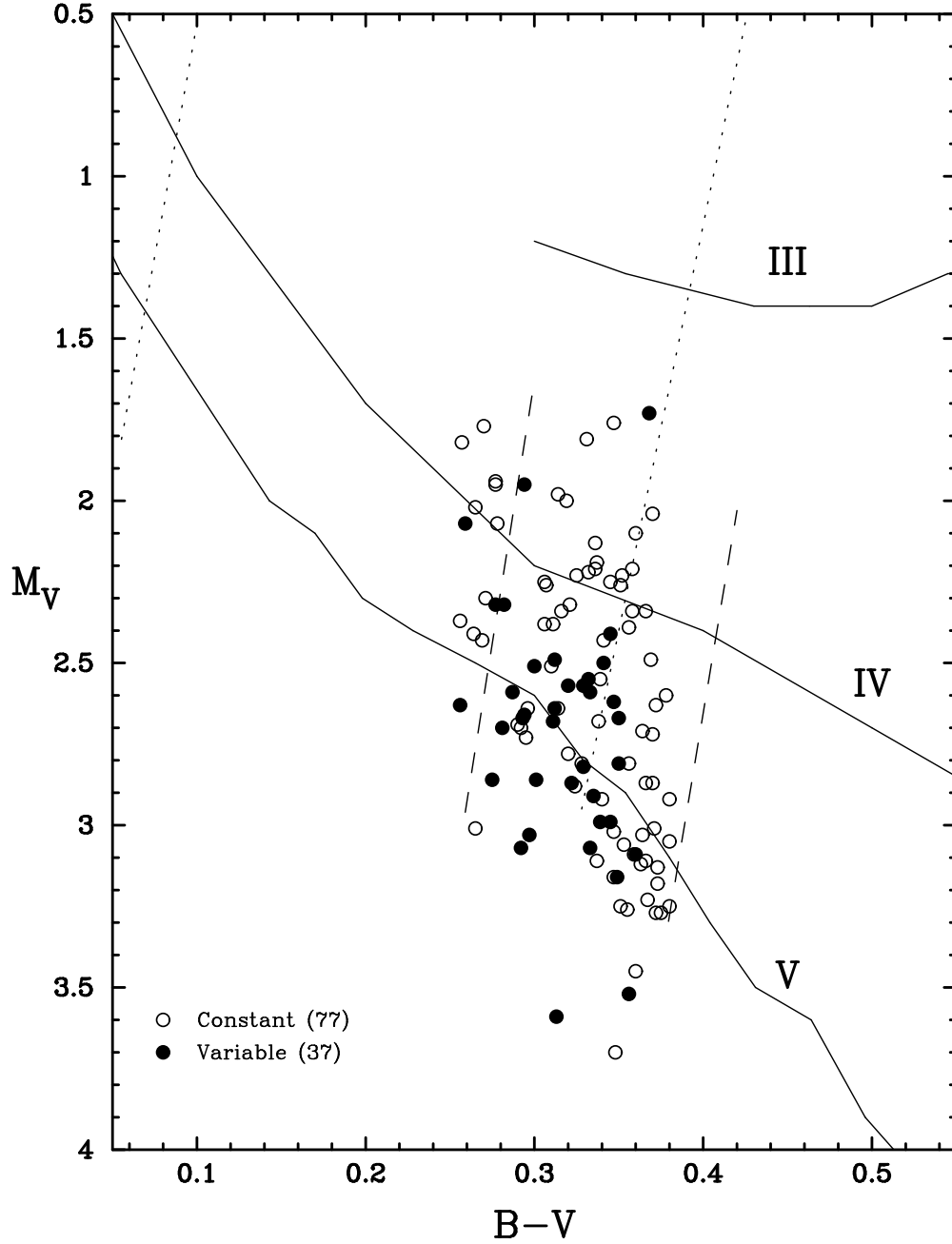


Fig. 1.— H-R diagram of the complete volume-limited sample of 114  $\gamma$  Doradus candidates listed in Table 2. Solid lines indicate observed average locations of normal main-sequence (V), sub-giant (IV), and giant (III) stars. The dotted lines indicate the boundaries of the  $\delta$  Scuti instability strip, converted from those of Breger (2000). The dashed lines show the observed domain of the  $\gamma$  Doradus pulsators, adopted from Fekel, Warner, & Kaye (2003). The one-year photometric survey with the T12 0.8 m APT found 37 variable stars with  $\sigma_{star} \geq 0.002$  mag (filled circles) and 77 constant stars with  $\sigma_{star} < 0.002$  mag (open circles).

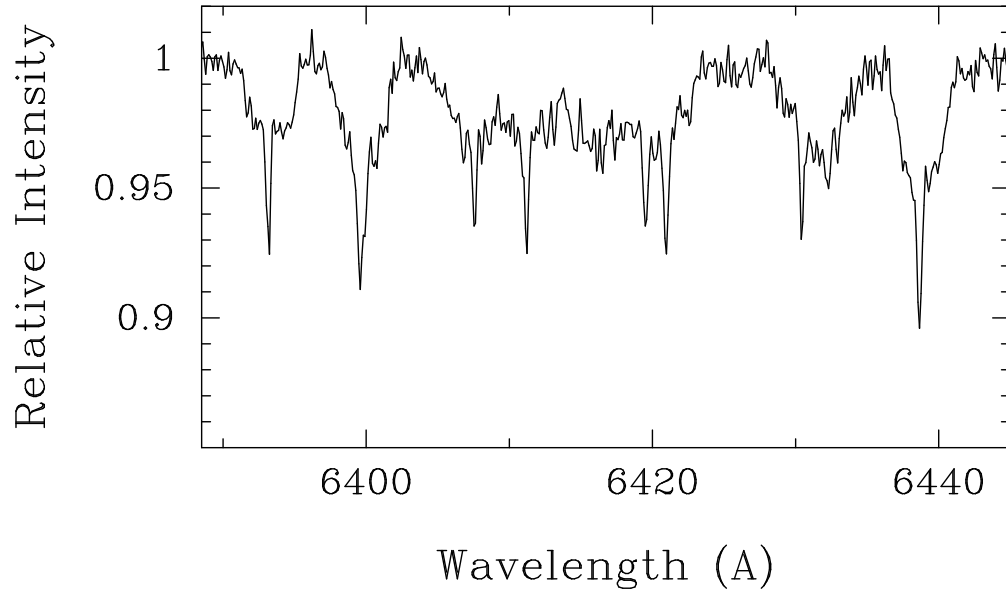


Fig. 2.— Spectrum of HD 38309 in the 6430 Å region, which shows the composite profiles of the lines. Component A is the broad-lined star, and component B is the narrow-lined star.

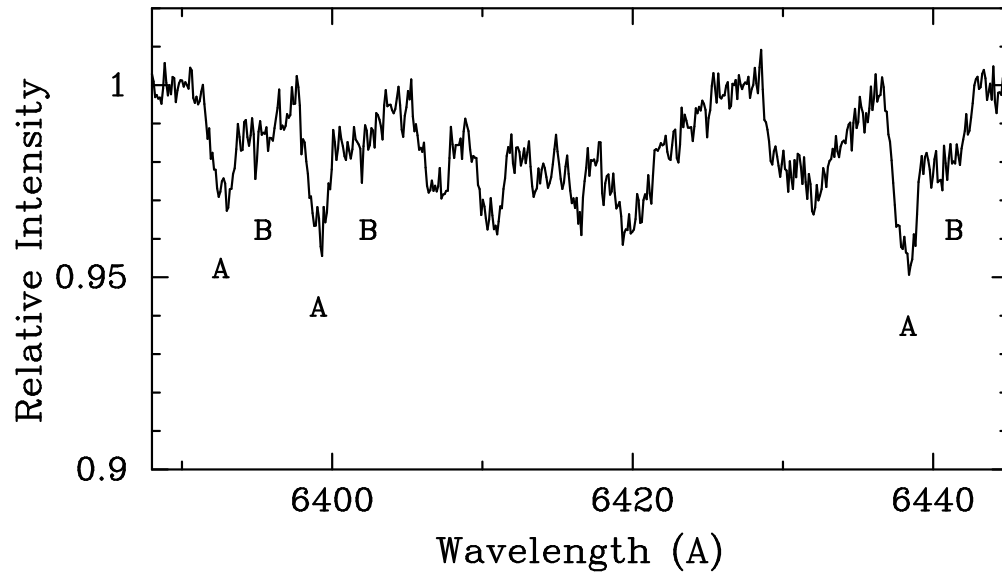


Fig. 3.— Spectrum of HD 114447 in the 6430 Å region, which shows the blended lines of the two components. Component A has the deeper blue shifted lines, while component B has the shallower red shifted lines.

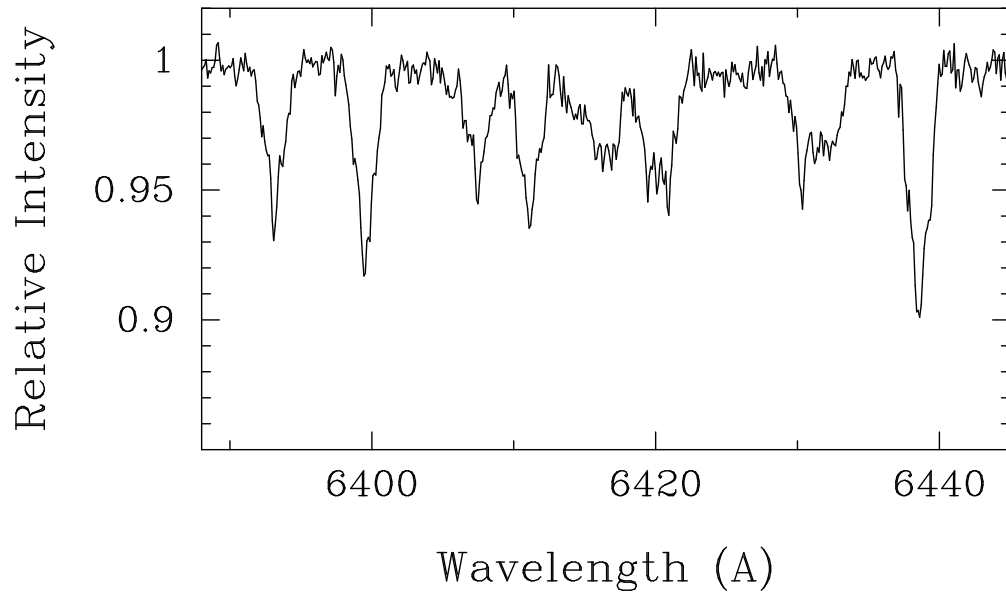


Fig. 4.— Spectrum of HD 145005 in the 6430 Å region, which shows the composite profiles of the lines. Component A is the broad-lined star, and component B is the narrow-lined star.

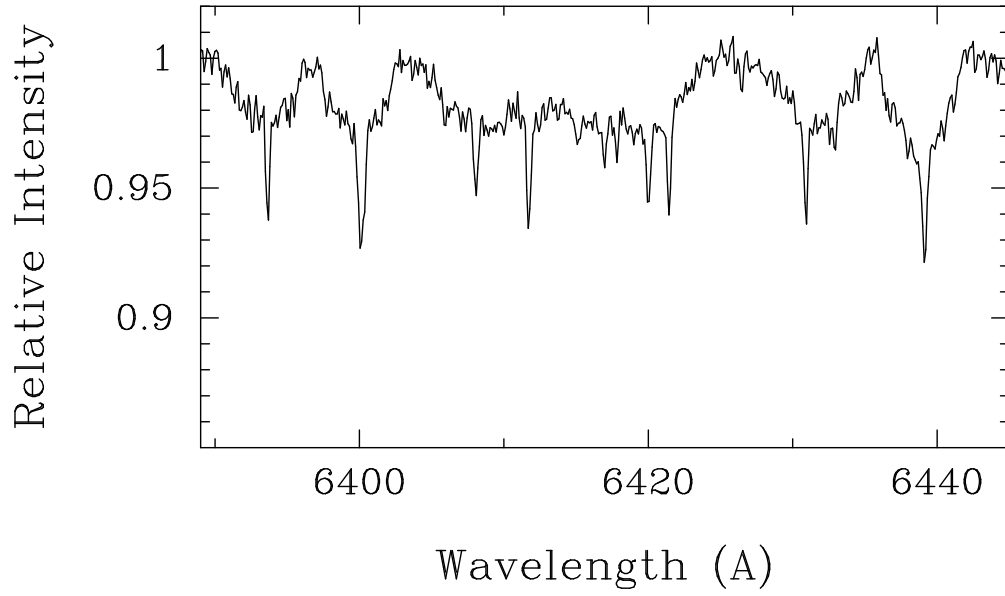


Fig. 5.— Spectrum of HD 22091 in the 6430 Å region, which shows the composite profiles of the lines. Component A is the broad-lined star, and component B is the narrow-lined star.

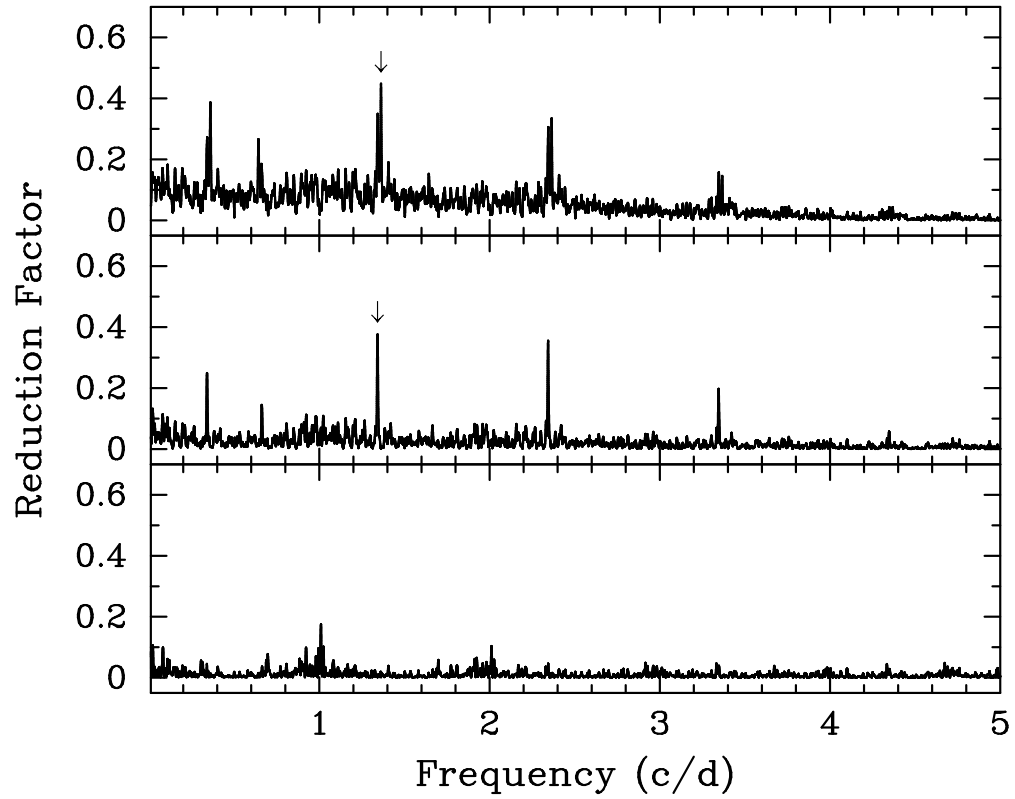


Fig. 6.— Least-squares frequency spectra of the HD 6568 Johnson *B* data set, showing the results of progressively fixing the two detected frequencies. The arrows indicate the two frequencies at  $1.3620 \text{ day}^{-1}$  (*top*) and  $1.3416 \text{ day}^{-1}$  (*middle*). The bottom panel shows the frequency spectrum with these two frequencies fixed. Both frequencies were confirmed in the Johnson *V* data set.

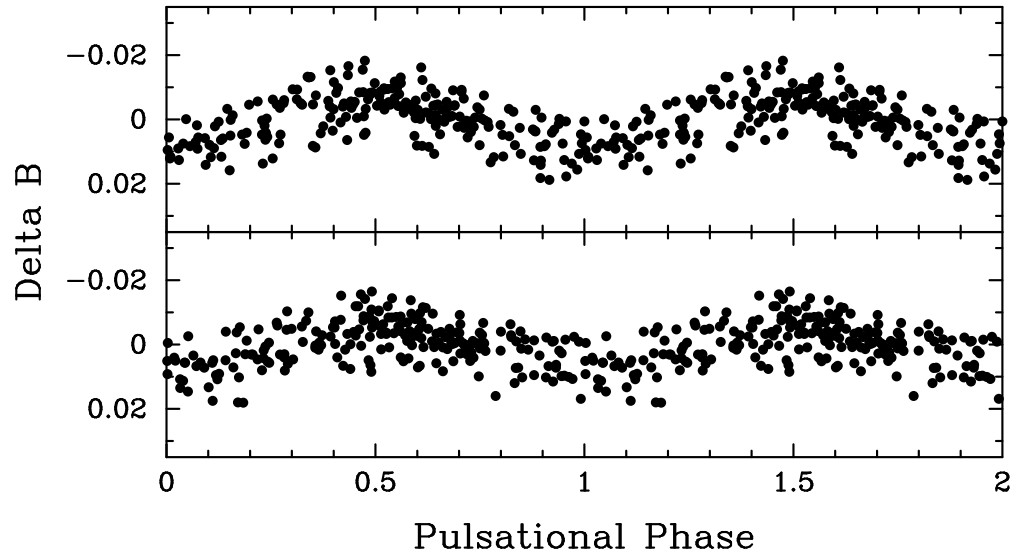


Fig. 7.— The Johnson  $B$  photometric data for HD 6568, phased with the two frequencies and times of minimum from Table 5. The two frequencies are  $1.3620 \text{ day}^{-1}$  (*top*) and  $1.3416 \text{ day}^{-1}$  (*bottom*). For each panel, the data set has been prewhitened to remove the other known frequency.



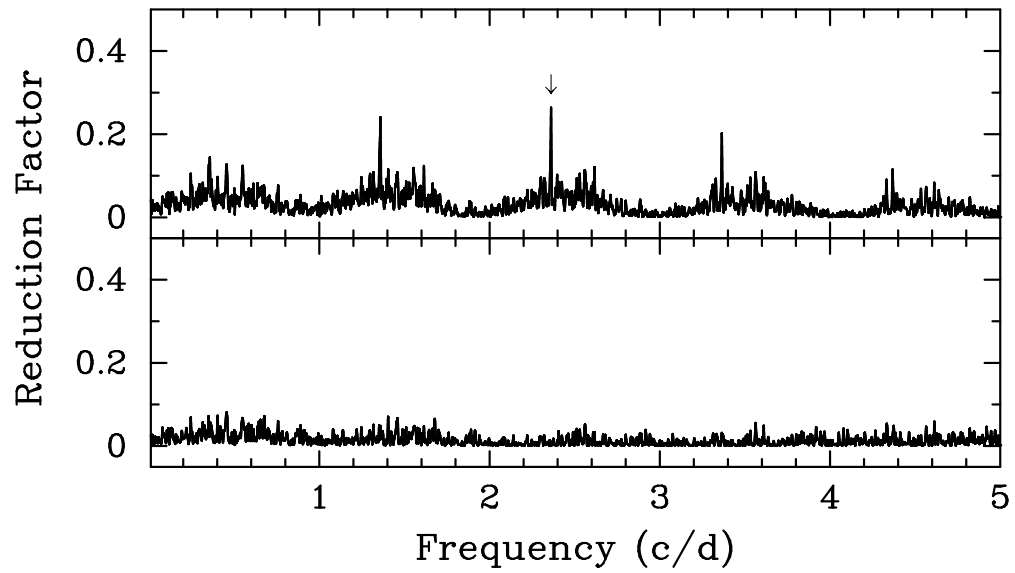


Fig. 8.— Least-squares frequency spectra of the HD 17163 Johnson *B* data set. The arrow in the top panel indicates the single detected frequency at  $2.3612 \text{ day}^{-1}$ . The bottom panel shows the frequency spectrum with the  $2.3612 \text{ day}^{-1}$  frequency fixed. The same frequency was confirmed in the Johnson *V* data set.

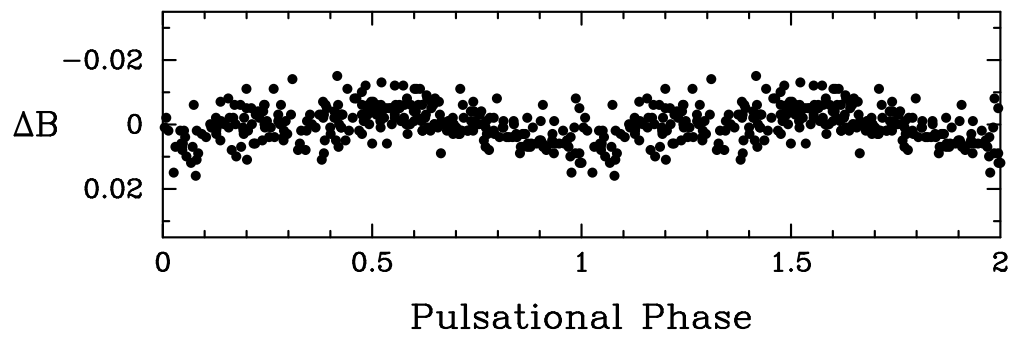


Fig. 9.— The Johnson *B* photometric data for HD 17163 phased with the single frequency of  $2.3612 \text{ day}^{-1}$  and the time of minimum from Table 5.

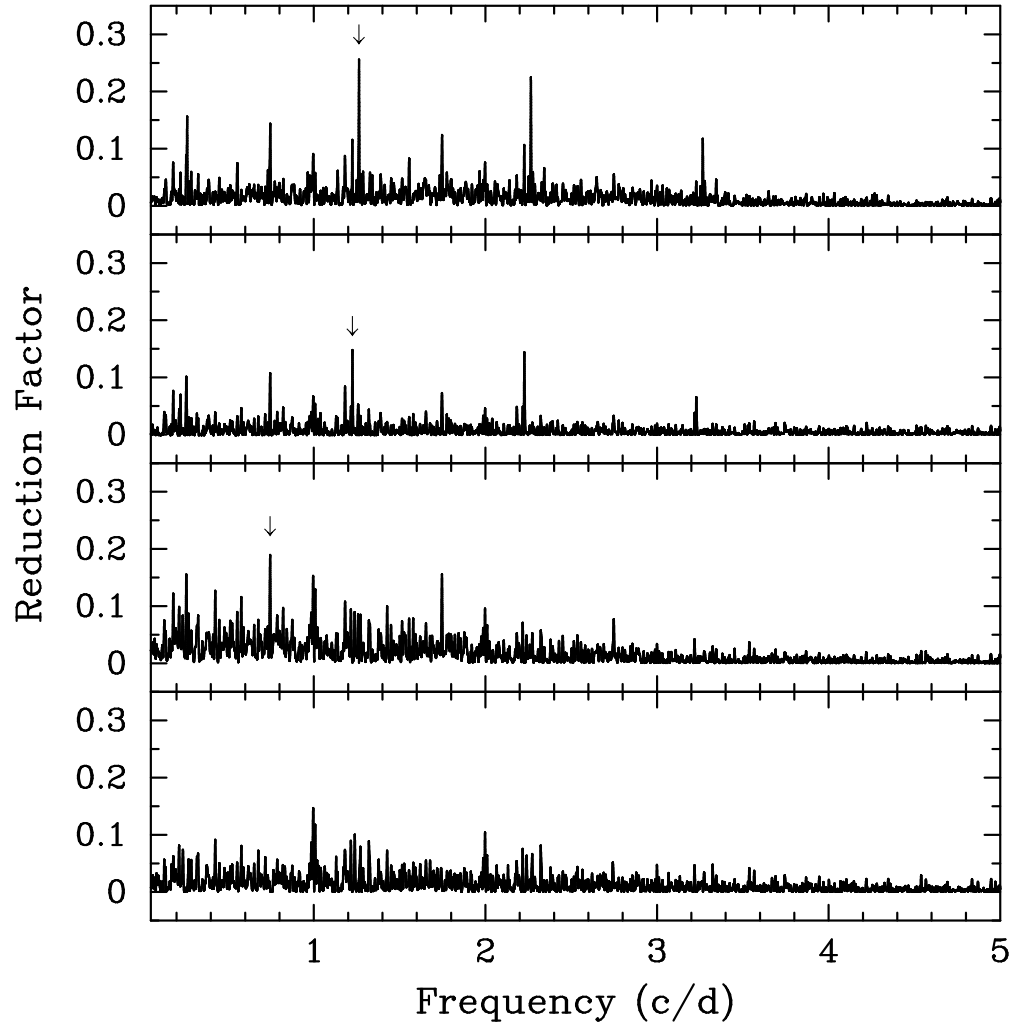


Fig. 10.— Least-squares frequency spectra of the HD 25906 Johnson *B* data set, showing the results of progressively fixing the three detected frequencies. The arrows indicate the three frequencies (*top to bottom*) 1.2632, 1.2248, and 0.7452  $\text{day}^{-1}$ . All three frequencies were confirmed in the Johnson *V* data set.

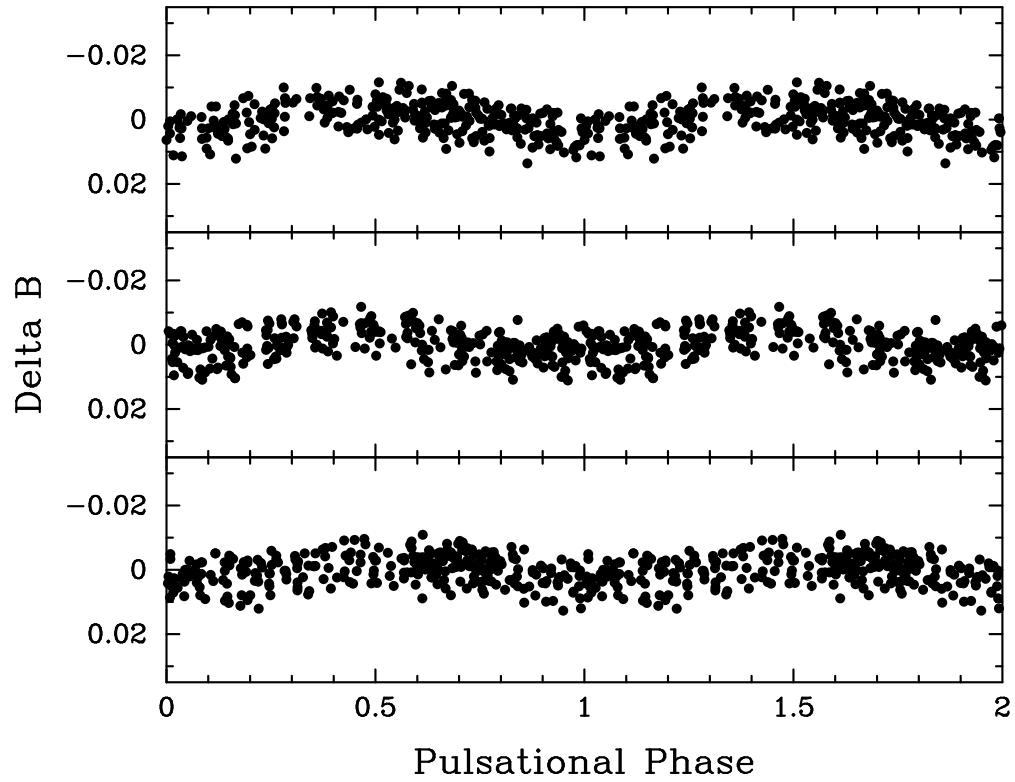


Fig. 11.— The Johnson  $B$  photometric data for HD 25906, phased with the three frequencies and times of minimum from Table 5. The three frequencies are (*top to bottom*) 1.2632, 1.2248, and  $0.7452 \text{ day}^{-1}$ . For each panel, the data set has been prewhitened to remove the other two known frequencies.

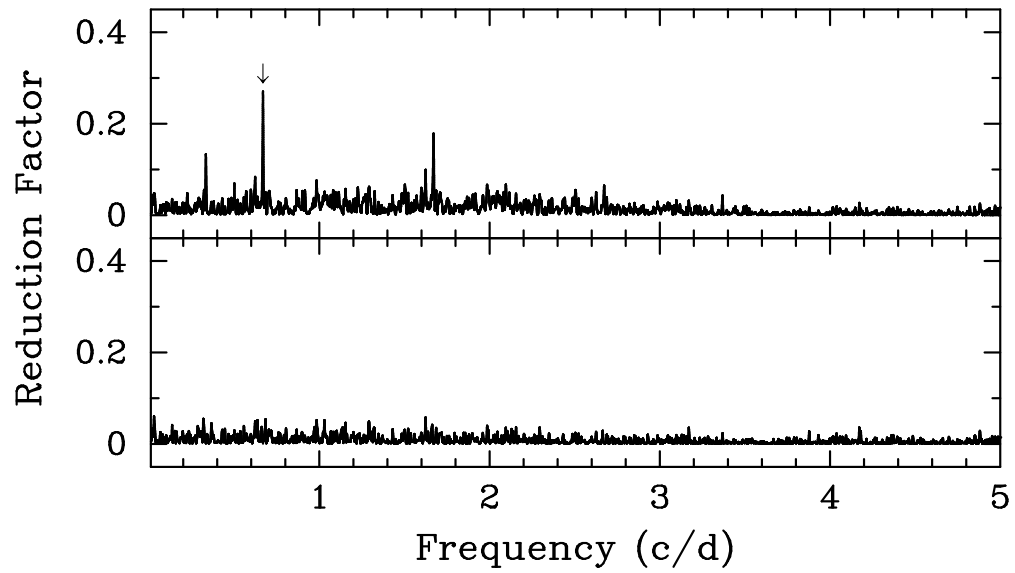


Fig. 12.— Least-squares frequency spectra of the HD 31550 Johnson *B* data set. The arrow in the top panel indicates the single detected frequency of  $0.6686 \text{ day}^{-1}$ . The bottom panel is the frequency spectrum resulting when the  $0.6686 \text{ day}^{-1}$  frequency is fixed. The same frequency was found in the Johnson *V* data set.

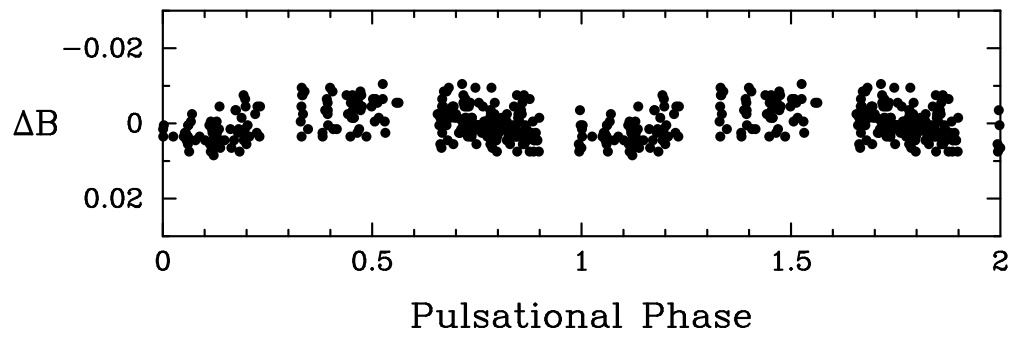


Fig. 13.— The Johnson  $B$  photometric data for HD 31550, phased with the  $0.6686 \text{ day}^{-1}$  frequency and time of minimum from Table 5.

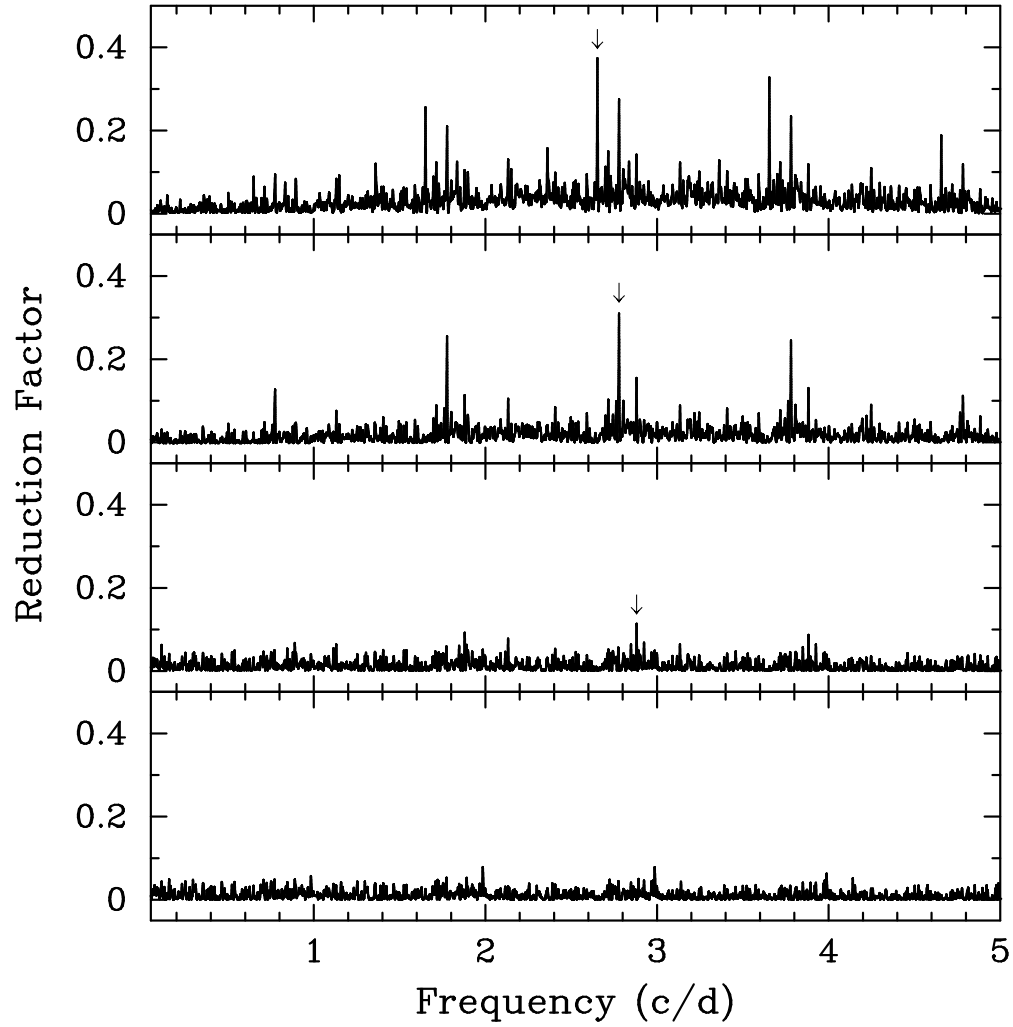


Fig. 14.— Least-squares frequency spectra of the HD 38309 Johnson  $B$  data set, showing the results of progressively fixing the three detected frequencies. The arrows indicate the three frequencies (*top to bottom*) 2.6523, 2.7783, and 2.8808  $\text{day}^{-1}$ . All three frequencies were confirmed in the Johnson  $V$  data set.

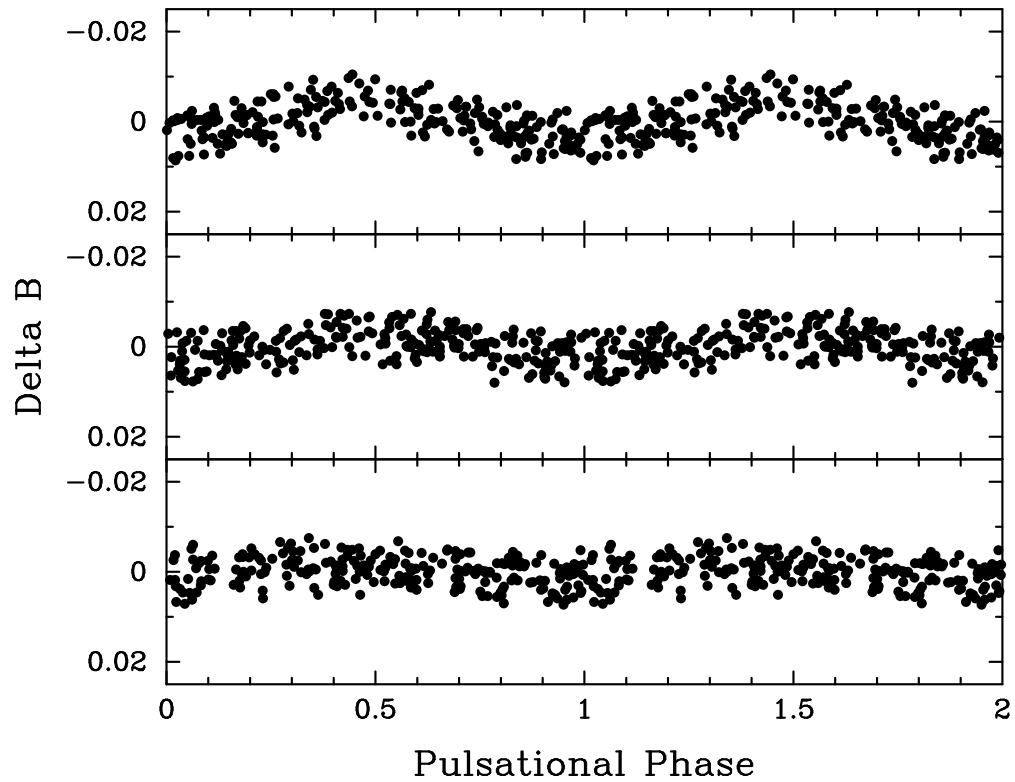


Fig. 15.— The Johnson  $B$  photometric data for HD 38309, phased with the three frequencies and times of minimum from Table 5. The three frequencies are (*top to bottom*) 2.6523, 2.7783, and 2.8808  $\text{day}^{-1}$ . For each panel, the data set has been prewhitened to remove the other known frequencies.



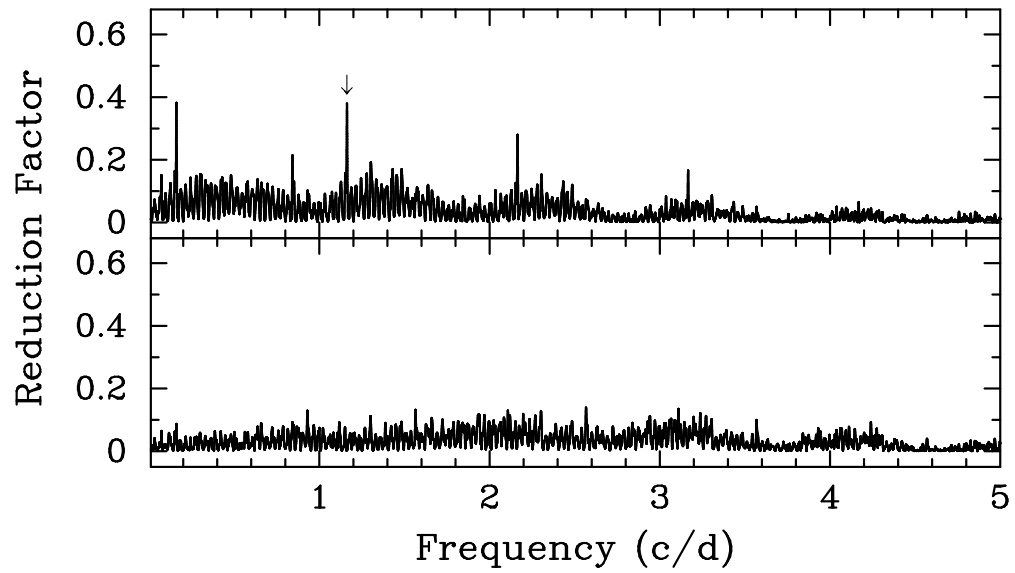


Fig. 16.— Least-squares frequency spectra of the HD 45638 Johnson *B* data set. The arrow in the top panel indicates the single detected frequency at  $1.1622 \text{ day}^{-1}$ . The bottom panel shows the frequency spectrum with the  $1.1622 \text{ day}^{-1}$  frequency fixed. The same frequency was confirmed in the Johnson *V* data set.

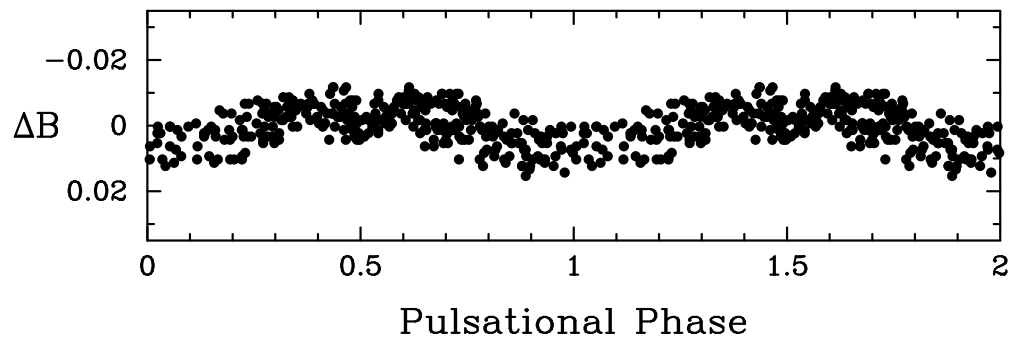


Fig. 17.— The Johnson  $B$  photometric data for HD 45638 phased with the single frequency of  $1.1622 \text{ day}^{-1}$  and the time of minimum from Table 5.

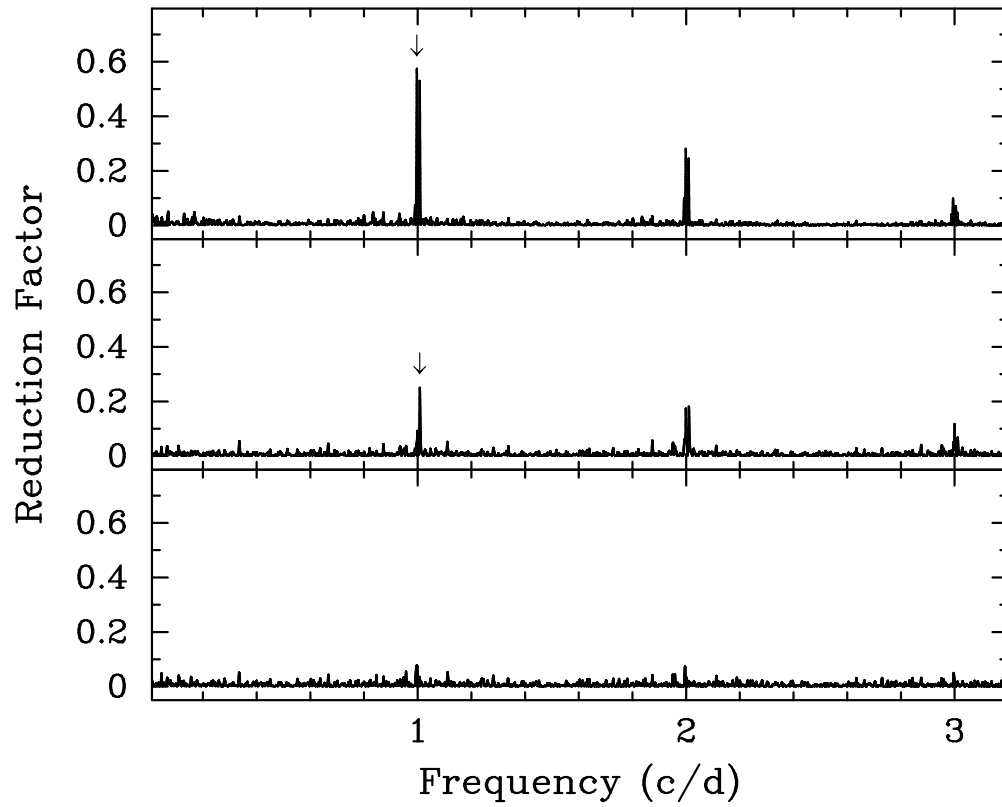


Fig. 18.— Least-squares frequency spectra of the HD 62196 Johnson  $B$  data set, showing the results of progressively fixing the two detected frequencies. The arrows indicate the two frequencies at  $0.9966 \text{ day}^{-1}$  (*top*) and  $1.0077 \text{ day}^{-1}$  (*middle*). Both frequencies were confirmed in the Johnson  $V$  data set.

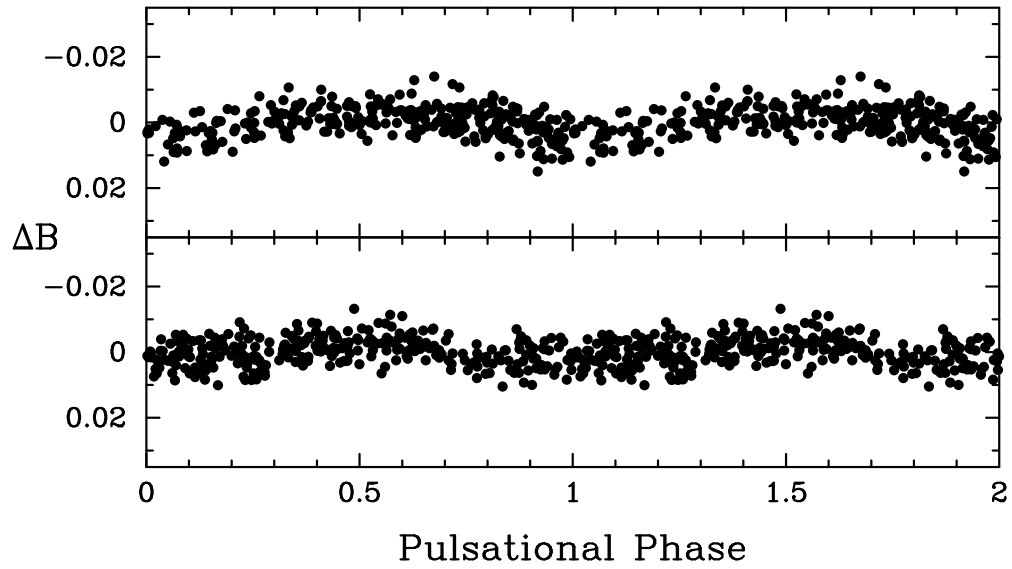


Fig. 19.— The Johnson  $B$  photometric data for HD 62196, phased with the two frequencies and times of minimum from Table 5. The two frequencies are  $0.9966 \text{ day}^{-1}$  (*top*) and  $1.0077 \text{ day}^{-1}$  (*bottom*). For each panel, the data set has been prewhitened to remove the other known frequency.

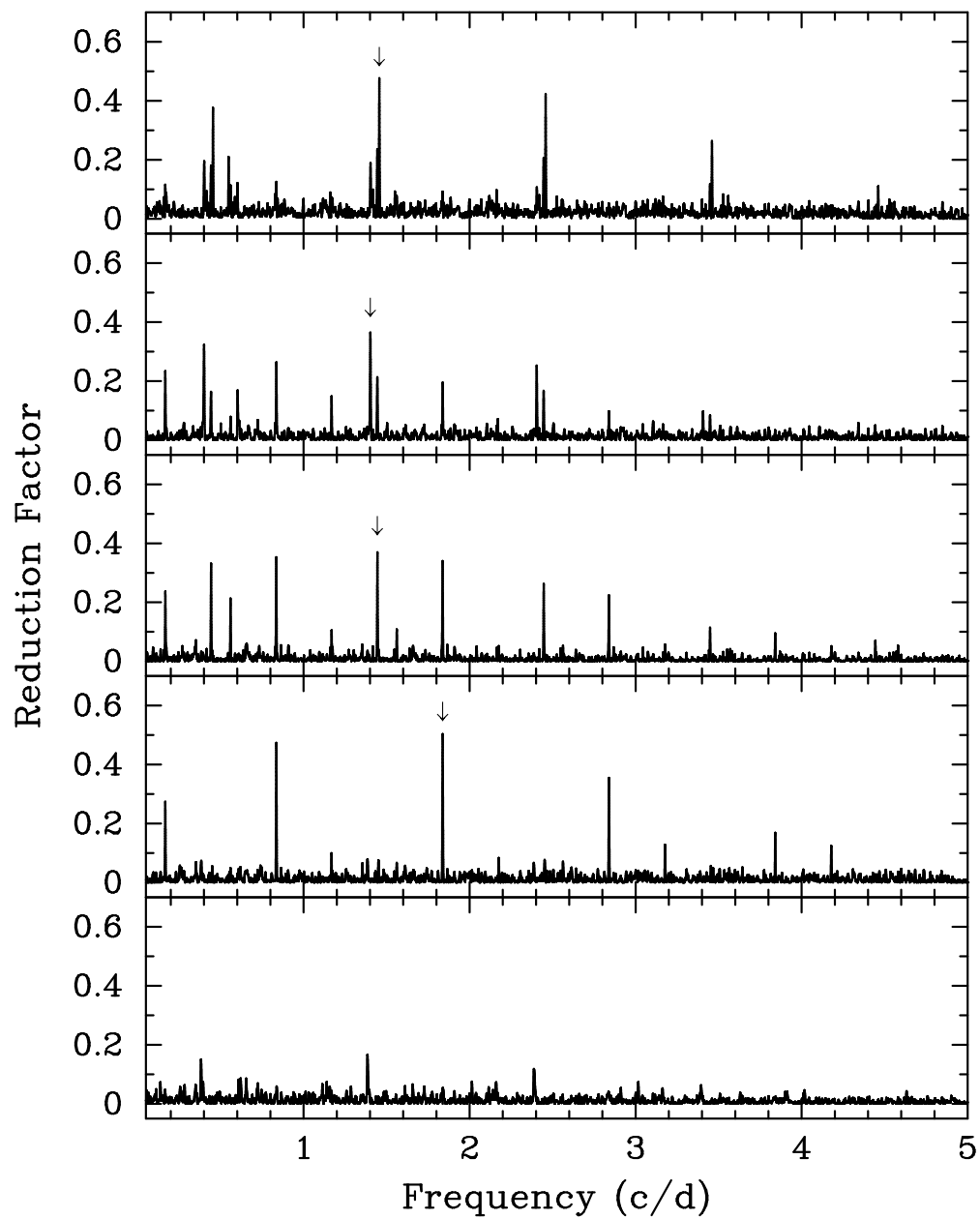


Fig. 20.— Least-squares frequency spectra of the HD 63436 Johnson *B* data set, showing the results of progressively fixing the four detected frequencies. The arrows indicate the four frequencies (*top to bottom*) 1.4557, 1.4020, 1.4443, and 1.8372  $\text{day}^{-1}$ . All four frequencies were confirmed in the Johnson *V* data set.

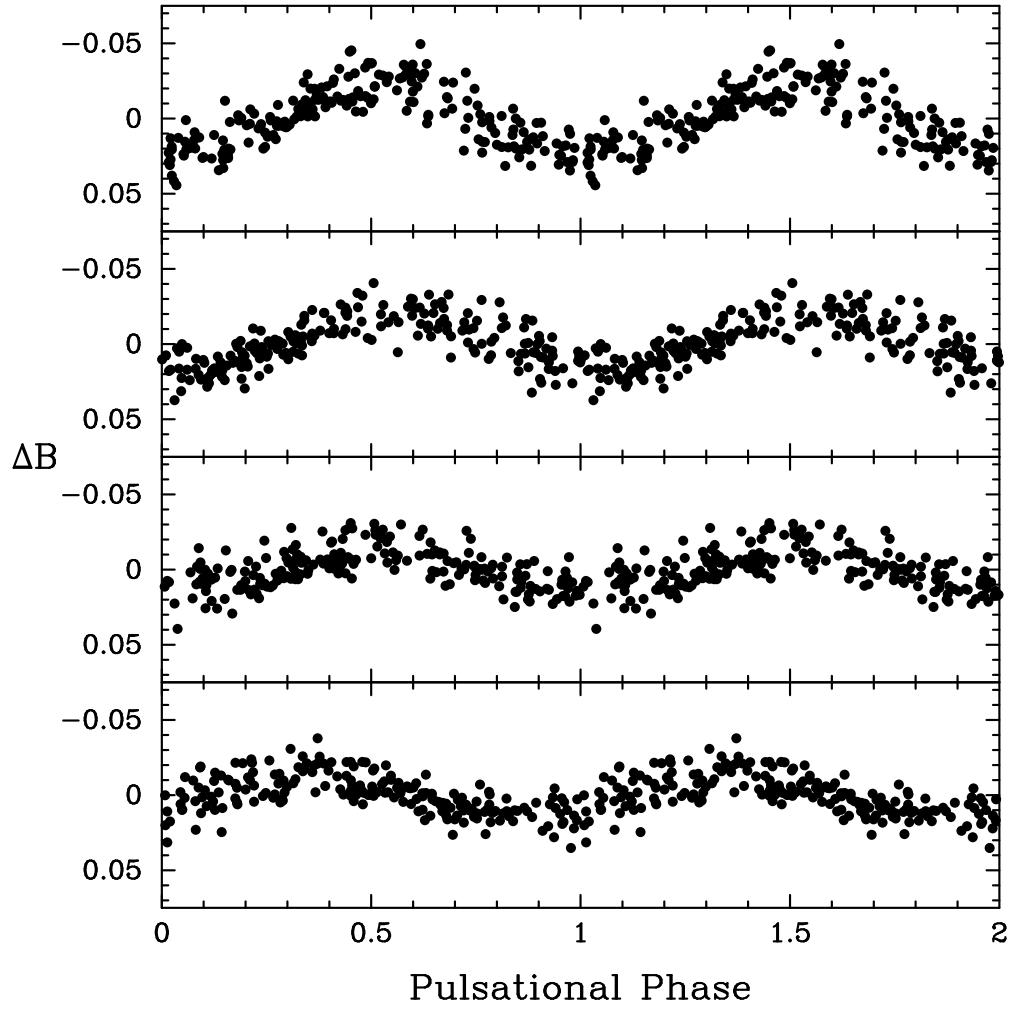


Fig. 21.— The Johnson  $B$  photometric data for HD 63436, phased with the four frequencies and times of minimum from Table 5. The four frequencies are (*top to bottom*) 1.4557, 1.4020, 1.4443, and 1.8372 day<sup>-1</sup>. For each panel, the data set has been prewhitened to remove the other known frequencies.

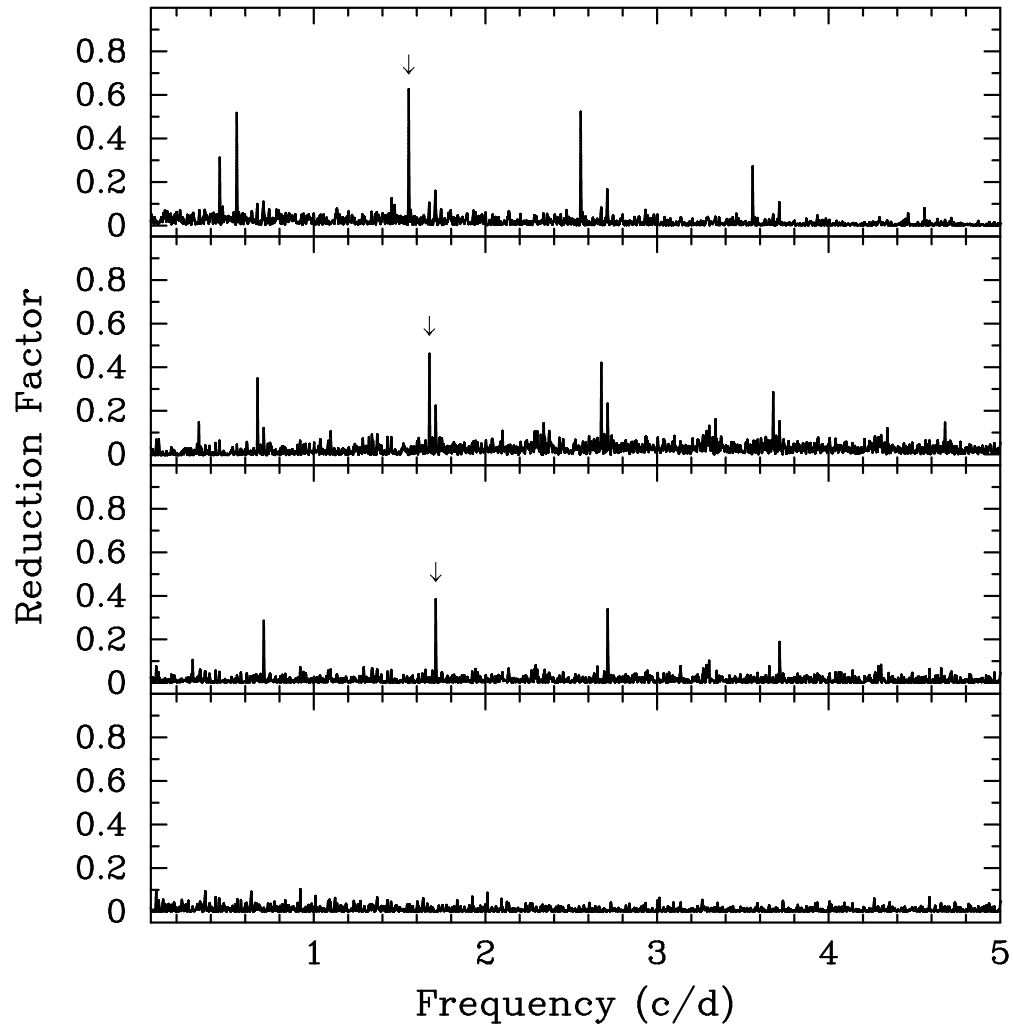


Fig. 22.— Least-squares frequency spectra of the HD 65526 Johnson *B* data set, showing the results of progressively fixing the three detected frequencies. The arrows indicate the three frequencies (*top to bottom*) 1.5527, 1.6735, and 1.7101  $\text{day}^{-1}$ . All three frequencies were confirmed in the Johnson *V* data set.

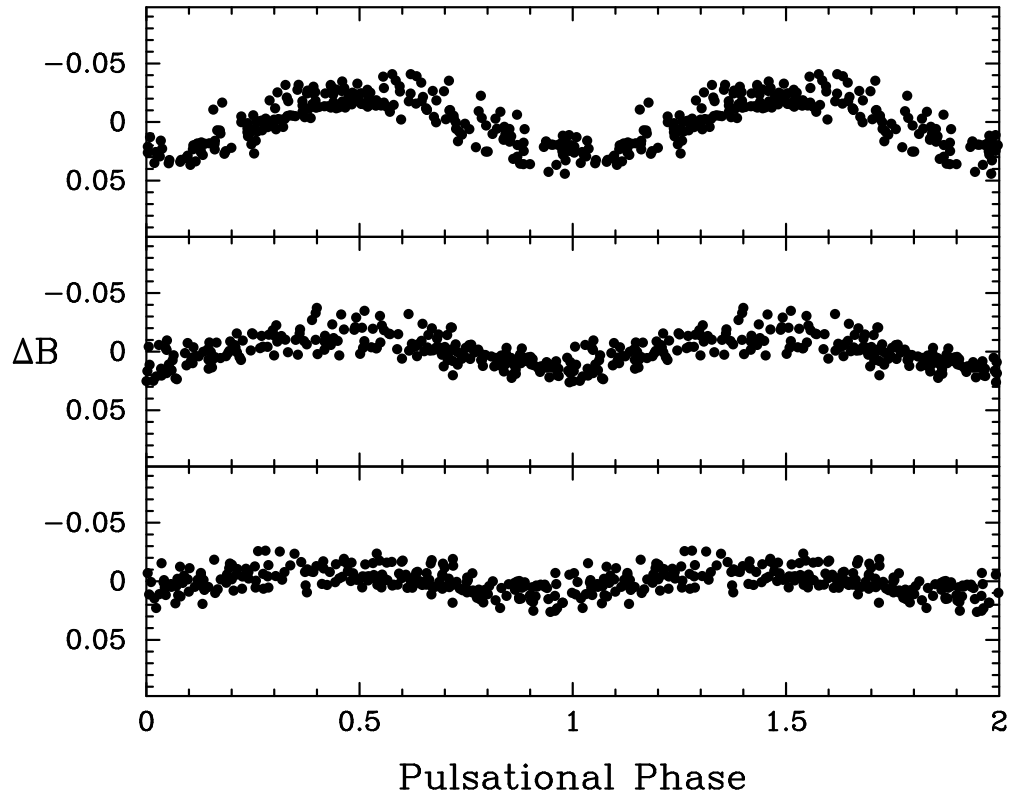


Fig. 23.— The Johnson  $B$  photometric data for HD 65526, phased with the three frequencies and times of minimum from Table 5. The three frequencies are (*top to bottom*) 1.5527, 1.6735, and 1.7101 day<sup>-1</sup>. For each panel, the data set has been prewhitened to remove the other two known frequencies.



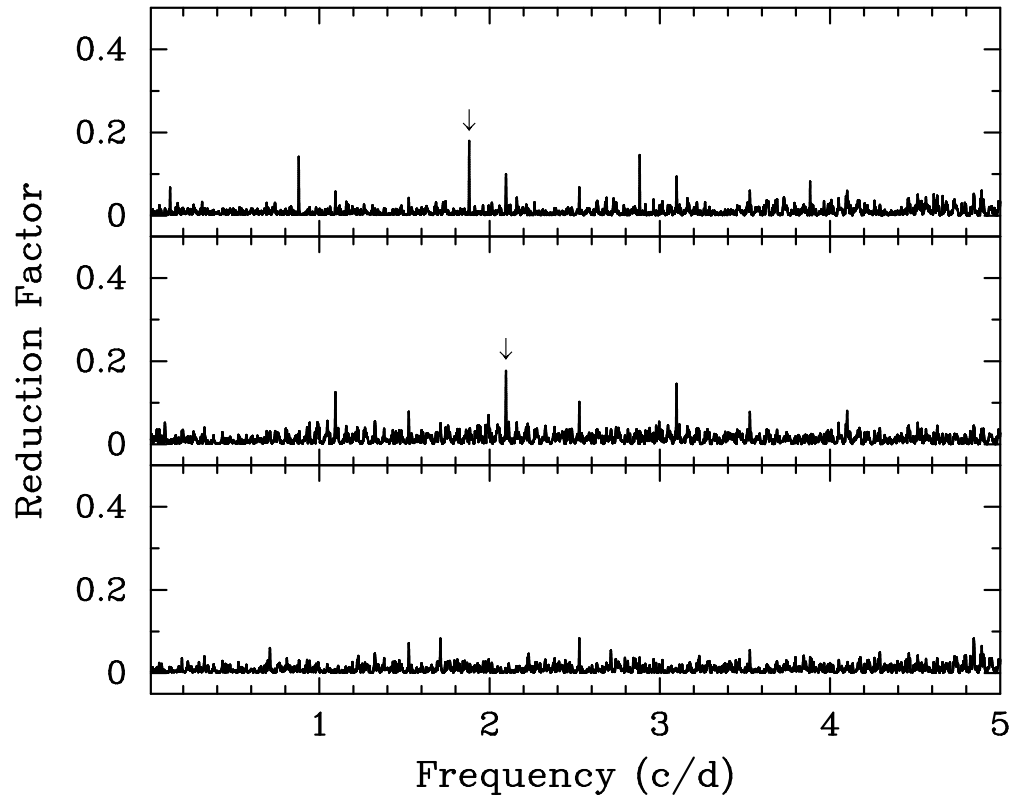


Fig. 24.— Least-squares frequency spectra of the HD 69682 Johnson *B* data set, showing the results of progressively fixing the two detected frequencies. The arrows indicate the two frequencies at  $1.8801 \text{ day}^{-1}$  (*top*) and  $2.0963 \text{ day}^{-1}$  (*middle*). Both frequencies were confirmed in the Johnson *V* data set.

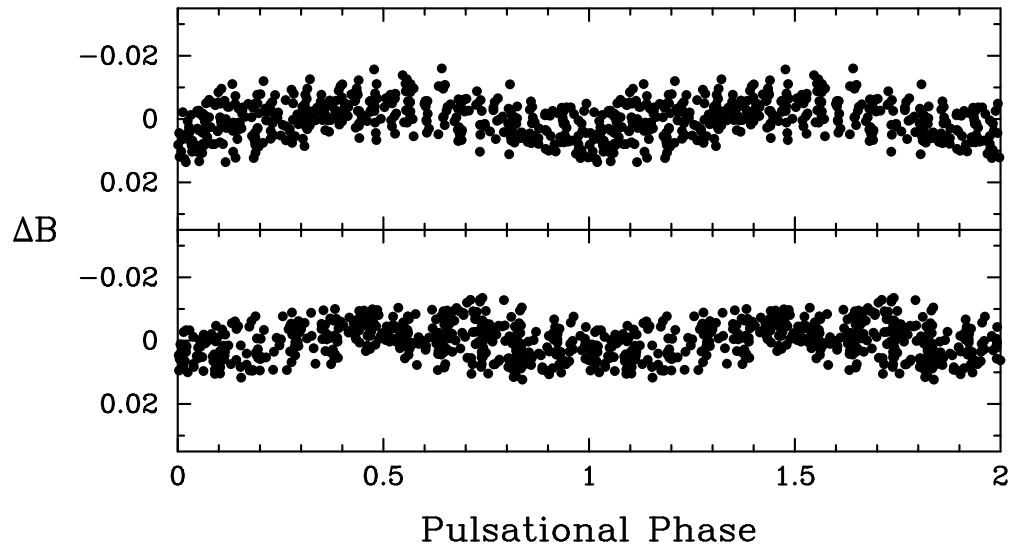


Fig. 25.— The Johnson  $B$  photometric data for HD 69682, phased with the two frequencies and times of minimum from Table 5. The two frequencies are  $1.8801 \text{ day}^{-1}$  (*top*) and  $2.0963 \text{ day}^{-1}$  (*bottom*). For each panel, the data set has been prewhitened to remove the other frequency.

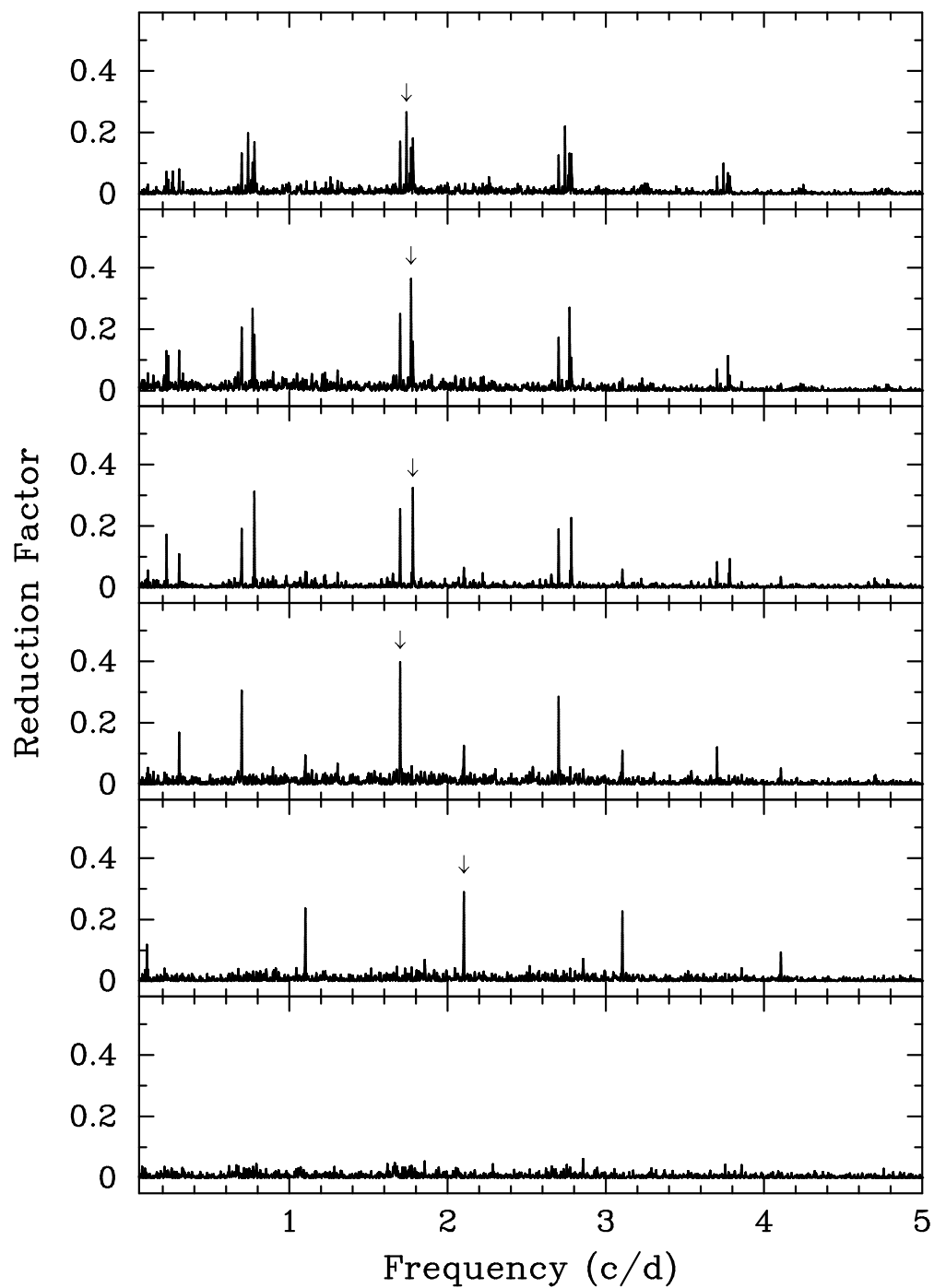


Fig. 26.— Least-squares frequency spectra of the HD 99267 Johnson *B* data set, showing the results of progressively fixing the five frequencies. The arrows indicate the five frequencies at (*top to bottom*) 1.7402, 1.7690, 1.7802, 1.7001, and 2.1029 day<sup>-1</sup>. All five frequencies were confirmed in the *V* data set.

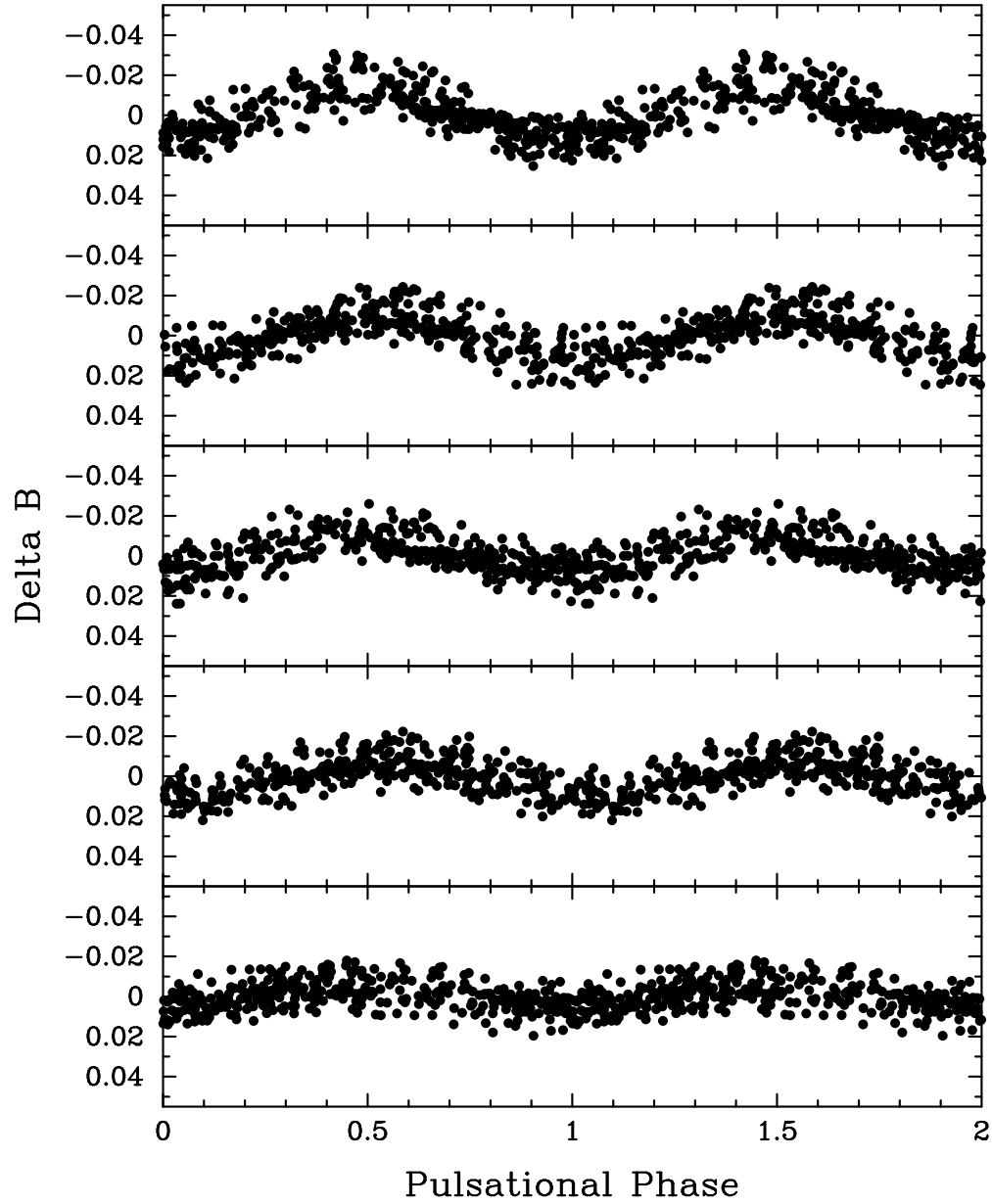


Fig. 27.— The Johnson  $B$  photometric data for HD 99267, phased with the five frequencies and times of minimum from Table 5. The five frequencies are (*top to bottom*) 1.7402, 1.7690, 1.7802, 1.7001, and 2.1029 day<sup>-1</sup>. For each panel, the data set has been prewhitened to remove the other four frequencies.

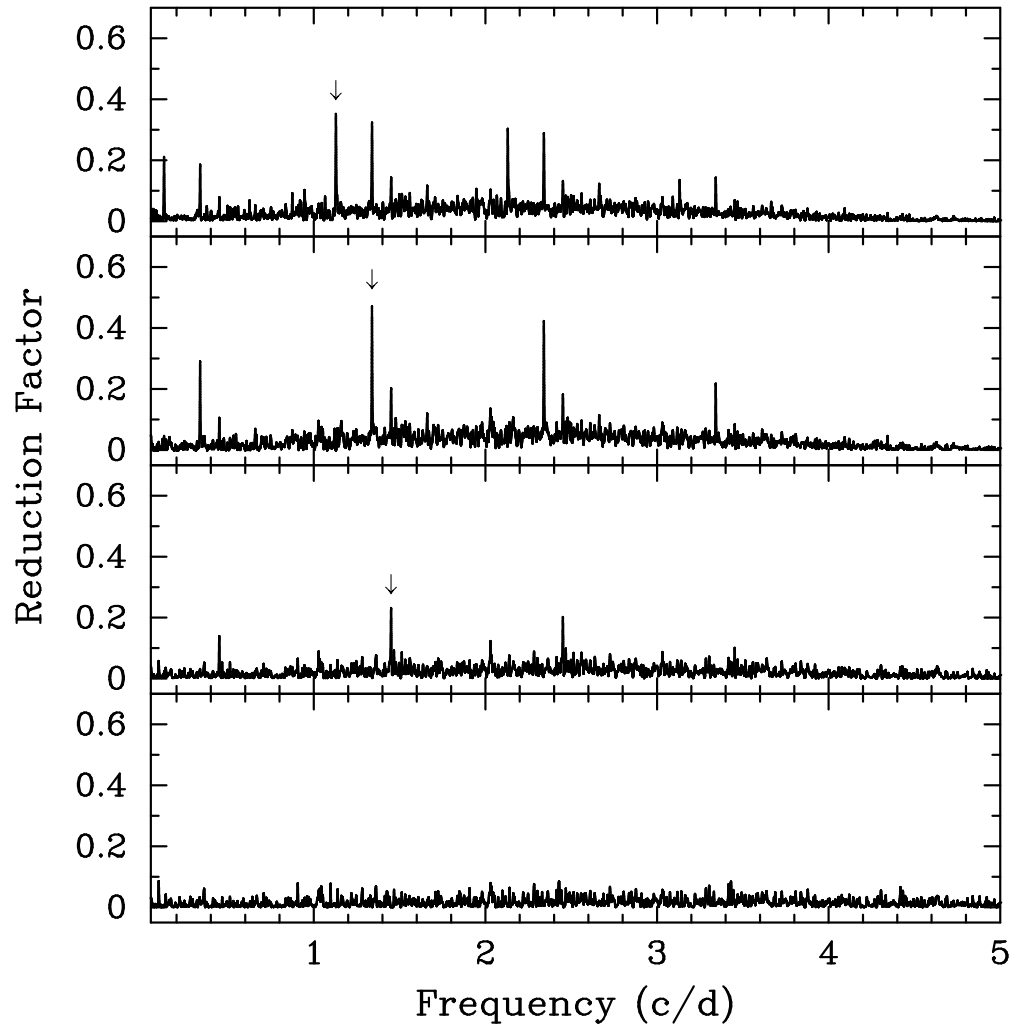


Fig. 28.— Least-squares frequency spectra of the HD 114447 Johnson *B* data set, showing the results of progressively fixing the three detected frequencies. The arrows indicate the three frequencies (*top to bottom*) 1.1284, 1.3386, and 1.4499  $\text{day}^{-1}$ . All three frequencies were confirmed in the Johnson *V* data set.

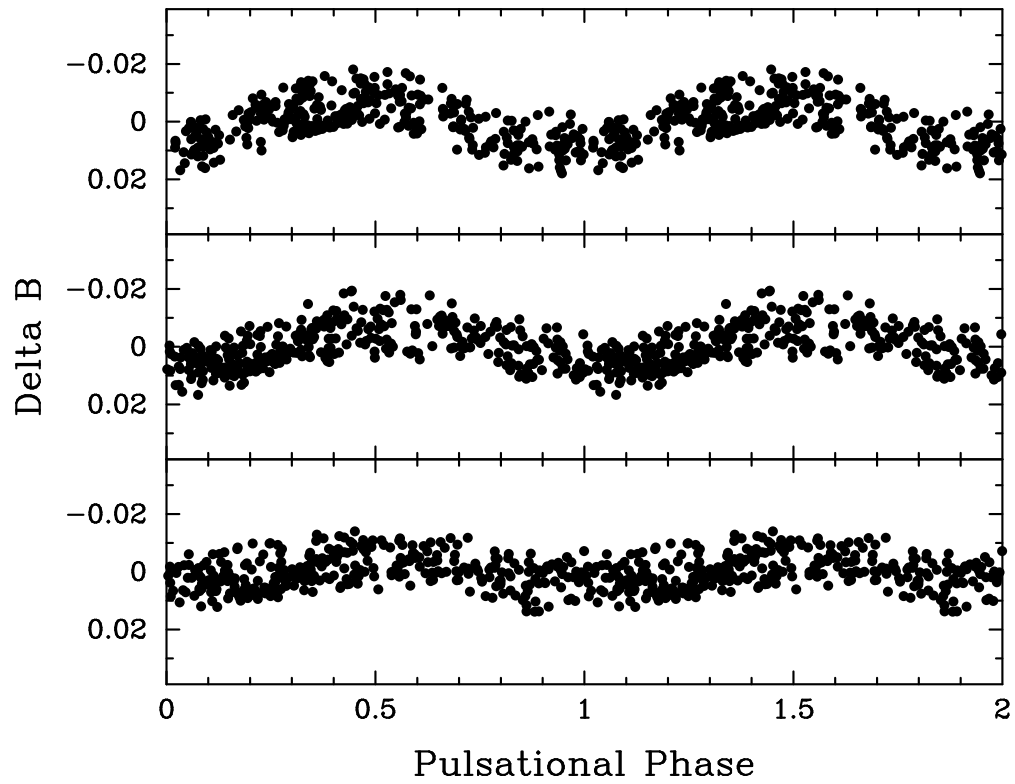


Fig. 29.— The Johnson  $B$  photometric data for HD 114447, phased with the three frequencies and times of minimum from Table 5. The three frequencies are (*top to bottom*) 1.1284, 1.3386, and 1.4499  $\text{day}^{-1}$ . For each panel, the data set has been prewhitened to remove the other two known frequencies.

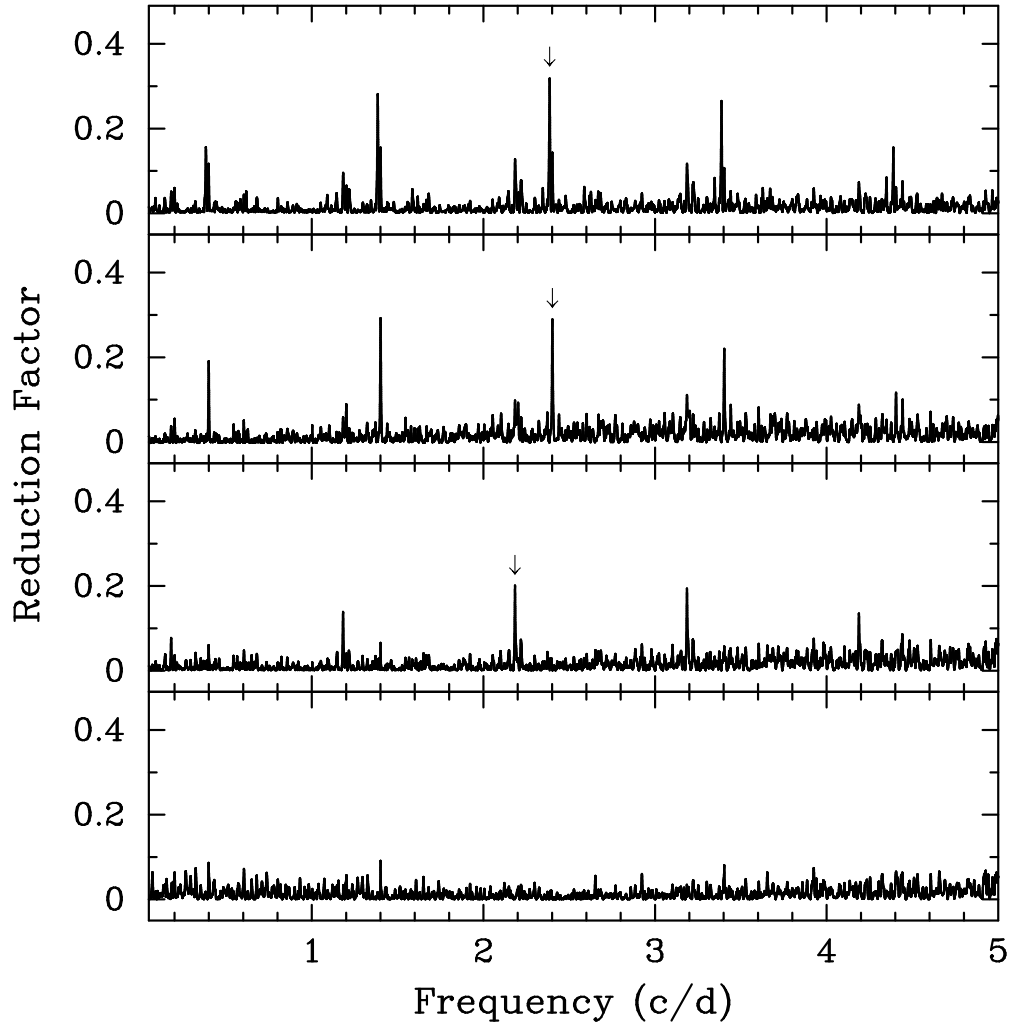


Fig. 30.— Least-squares frequency spectra of the HD 138936 Johnson *B* data set, showing the results of progressively fixing the three detected frequencies. The arrows indicate the three frequencies (*top to bottom*) 2.3855, 2.4018, and 2.1839  $\text{day}^{-1}$ . All three frequencies were confirmed in the Johnson *V* data set.

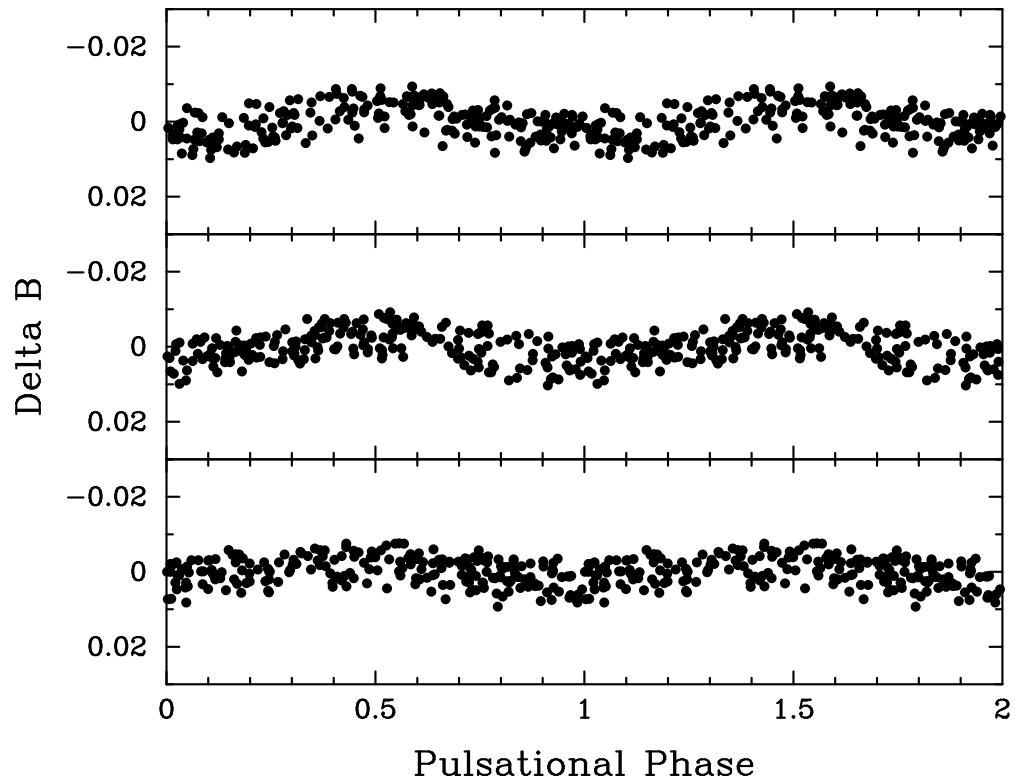


Fig. 31.— The Johnson  $B$  photometric data for HD 138936, phased with the three frequencies and times of minimum from Table 5. The three frequencies are (*top to bottom*) 2.3855, 2.4018, and 2.1839  $\text{day}^{-1}$ . For each panel, the data set has been prewhitened to remove the other two known frequencies.



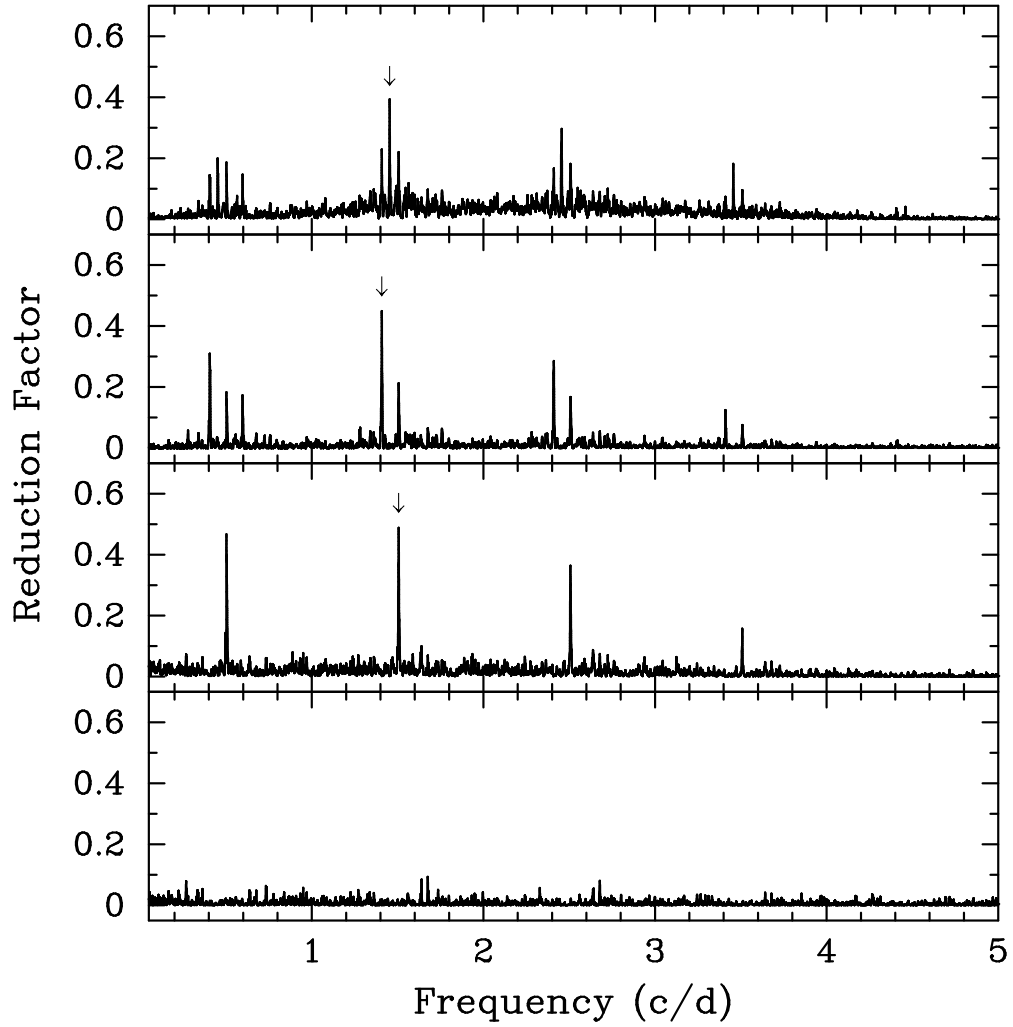


Fig. 32.— Least-squares frequency spectra of the HD 139478 Johnson *B* data set, showing the results of progressively fixing the three detected frequencies. The arrows indicate the three frequencies (*top to bottom*) 1.4531, 1.4073, and 1.5056  $\text{day}^{-1}$ . All three frequencies were confirmed in the Johnson *V* data set.

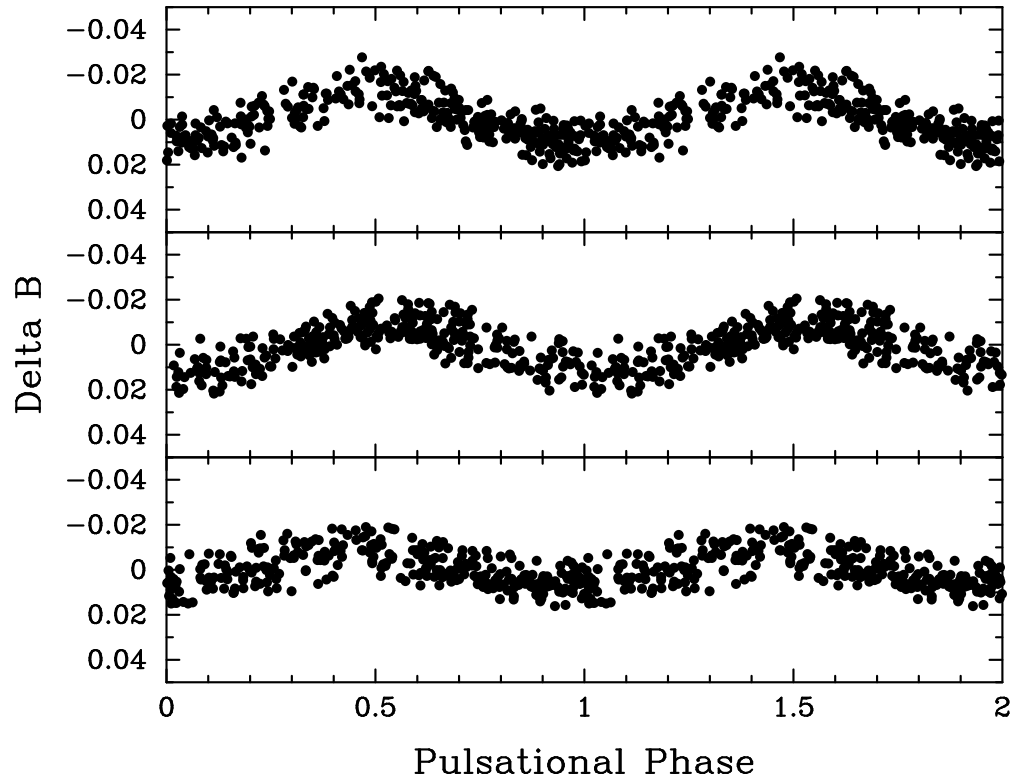


Fig. 33.— The Johnson  $B$  photometric data for HD 139478, phased with the three frequencies and times of minimum from Table 5. The three frequencies are (*top to bottom*) 1.4531, 1.4073, and 1.5056  $\text{day}^{-1}$ . For each panel, the data set has been prewhitened to remove the other two known frequencies.

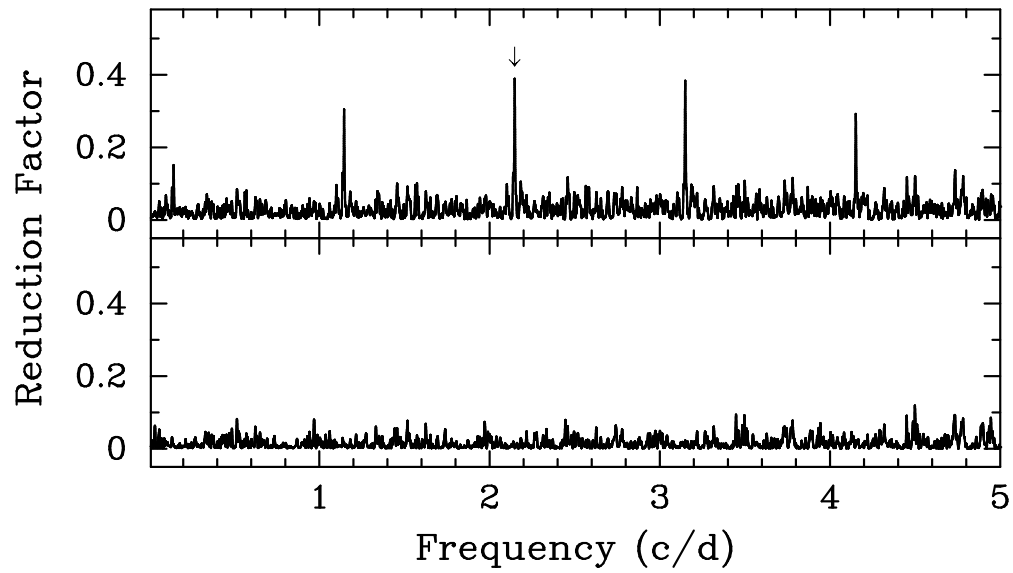


Fig. 34.— Least-squares frequency spectra of the HD 145005 Johnson *B* data set. The arrow in the top panel indicates the single detected frequency of  $2.1473 \text{ day}^{-1}$ . The bottom panel is the frequency spectrum resulting when the  $2.1473 \text{ day}^{-1}$  frequency is fixed. The same frequency was found in the Johnson *V* data set.

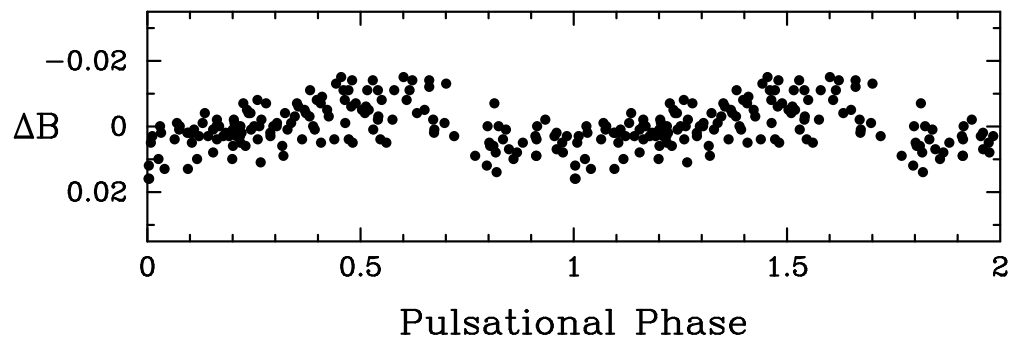


Fig. 35.— The Johnson  $B$  photometric data for HD 145005, phased with the  $2.1473 \text{ day}^{-1}$  frequency and time of minimum from Table 5.

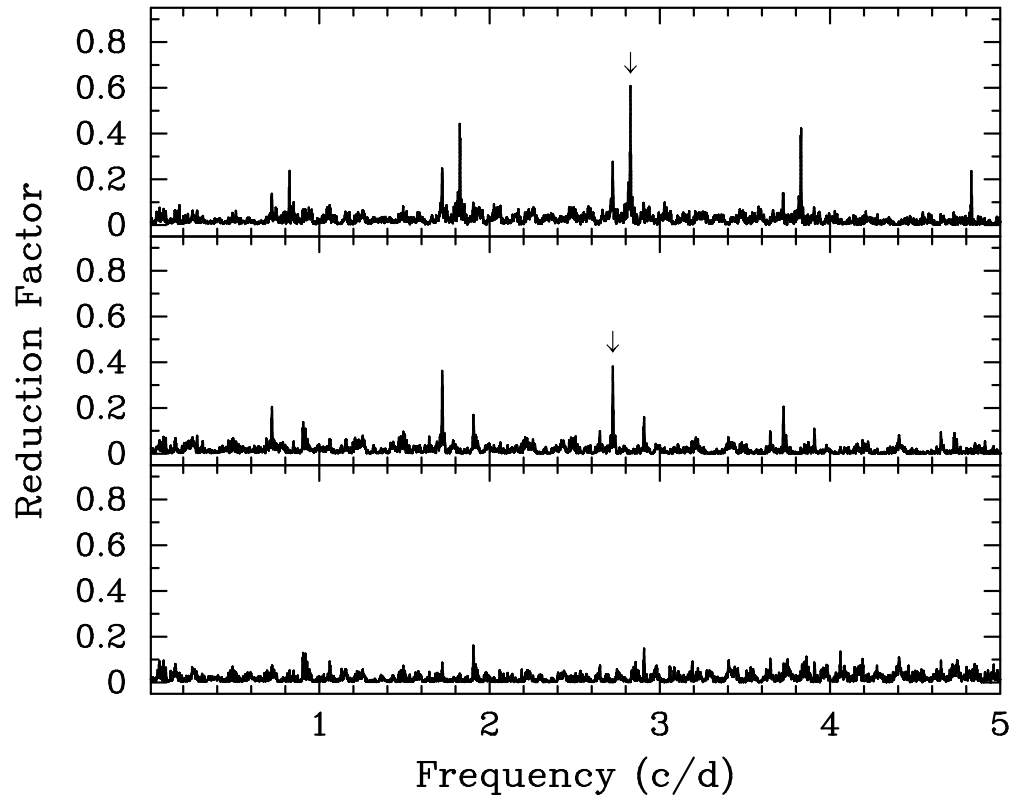


Fig. 36.— Least-squares frequency spectra of the HD 220091 Johnson *B* data set, showing the results of progressively fixing the two detected frequencies. The arrows indicate the two frequencies at  $2.8277 \text{ day}^{-1}$  (*top*) and  $2.7241 \text{ day}^{-1}$  (*middle*). Both frequencies were confirmed in the Johnson *V* data set.

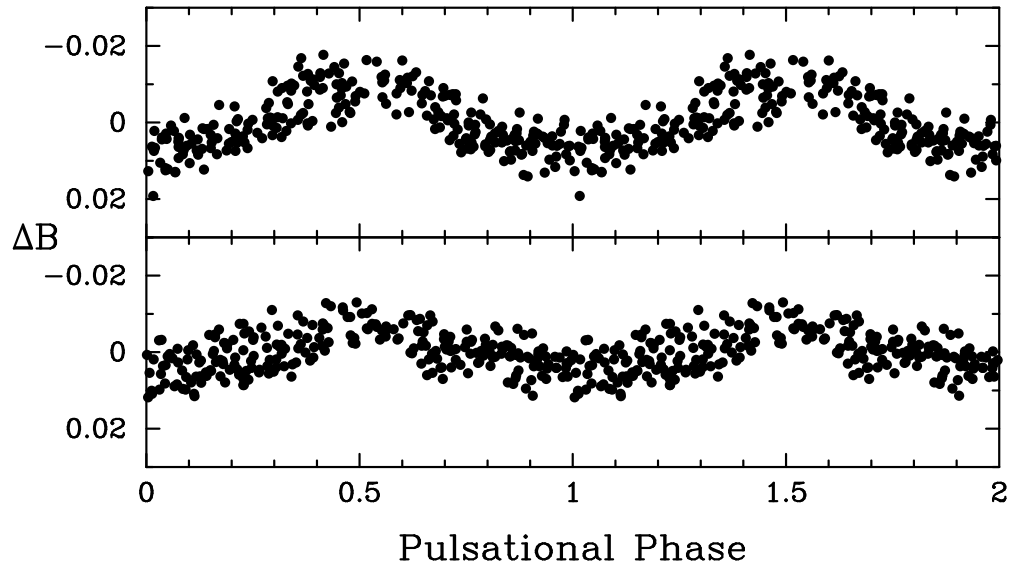


Fig. 37.— The Johnson  $B$  photometric data for HD 220091, phased with the two frequencies and times of minimum from Table 5. The two frequencies are  $2.8277 \text{ day}^{-1}$  (*top*) and  $2.7241 \text{ day}^{-1}$  (*bottom*). For each panel, the data set has been prewhitened to remove the other known frequency.

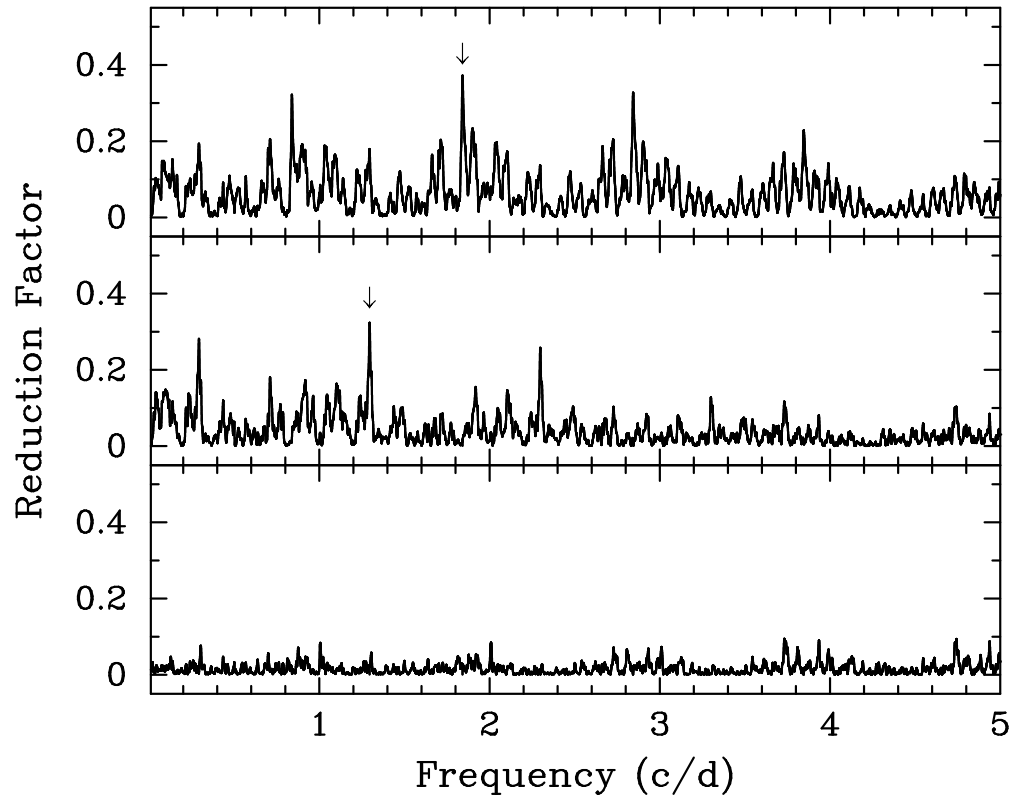


Fig. 38.— Least-squares frequency spectra of the HD 224945 Johnson *B* data set, showing the results of progressively fixing the two detected frequencies. The arrows indicate the two frequencies at  $1.8410 \text{ day}^{-1}$  (*top*) and  $1.2951 \text{ day}^{-1}$  (*middle*). Both frequencies were confirmed in the Johnson *V* data set.

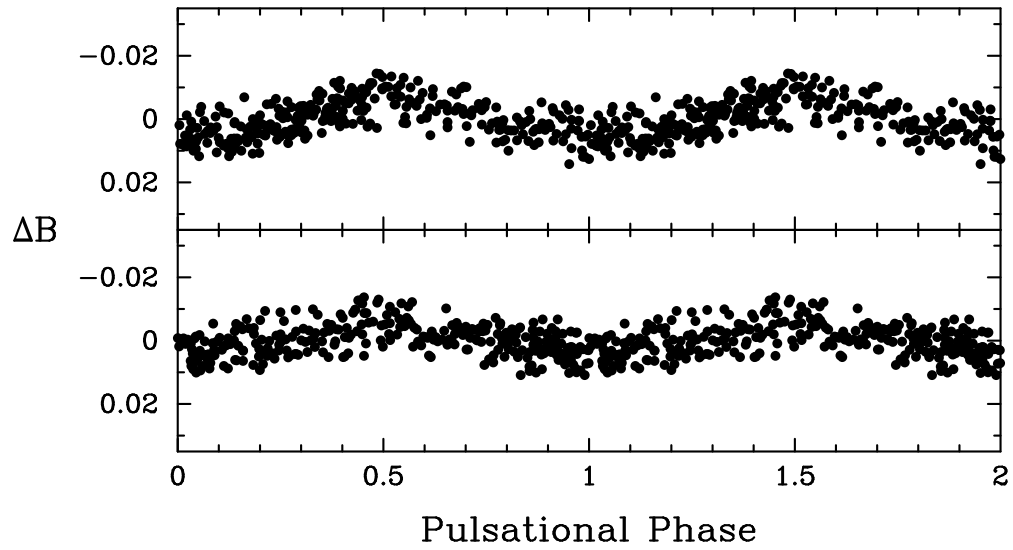


Fig. 39.— The Johnson  $B$  photometric data for HD 224945, phased with the two frequencies and times of minimum from Table 5. The two frequencies are  $1.8410 \text{ day}^{-1}$  (*top*) and  $1.2951 \text{ day}^{-1}$  (*bottom*). For each panel, the data set has been prewhitened to remove the other known frequency.



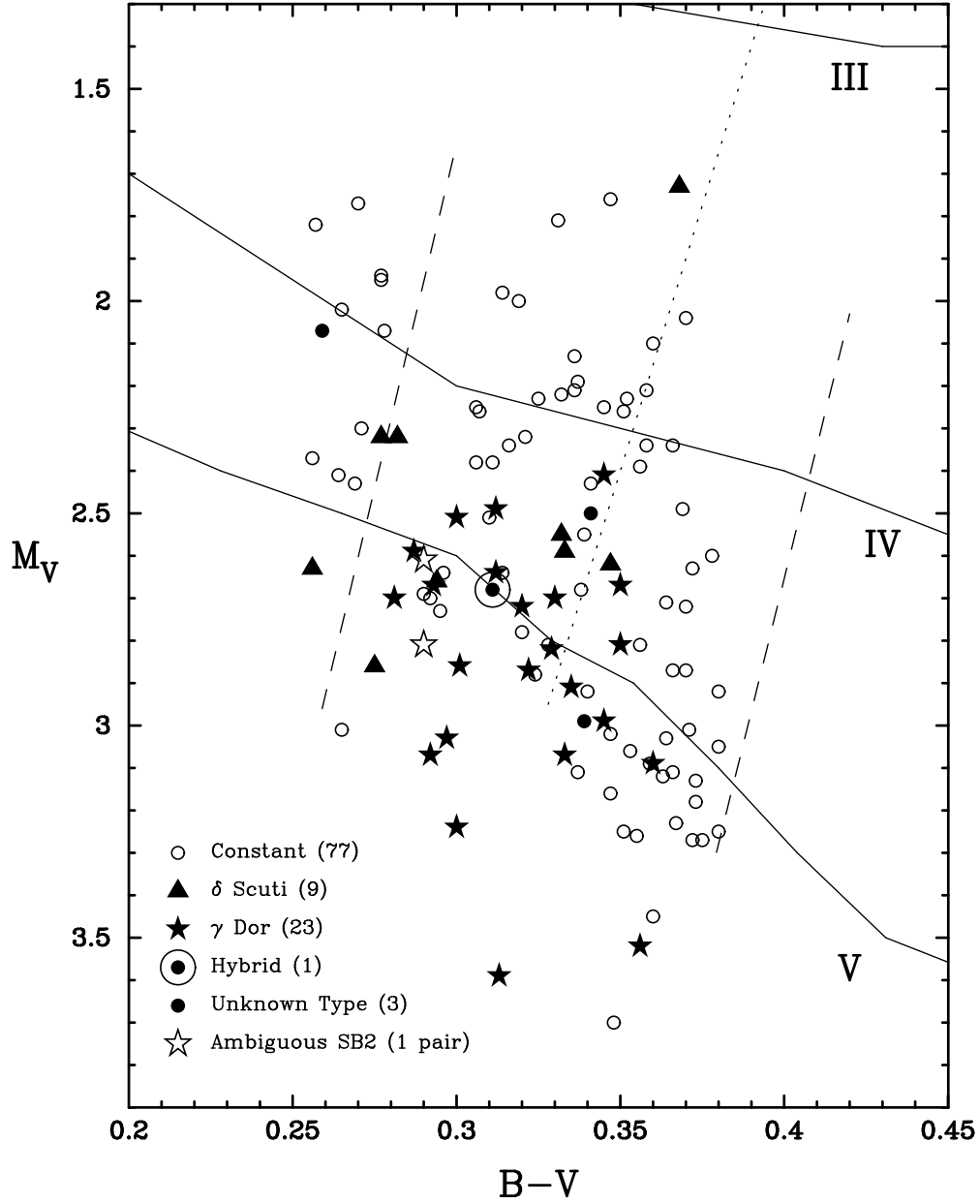


Fig. 40.— Results of our follow-up photometric and spectroscopic observations of the 37 variable stars found in the T12 survey. The luminosity classes and the  $\gamma$  Doradus and  $\delta$  Scuti instability strips are as described in Figure 1, except here we see only the cool edge of the  $\delta$  Scuti instability strip (dotted line). The 77 constant stars are again plotted as open circles. Among the 37 variable stars, we find 15 new and nine previously discovered  $\gamma$  Doradus stars (filled stars), eight new and one previously discovered  $\delta$  Scuti stars (filled triangles), three new variables of unknown type (filled circles), and HD 8801, previously discovered to exhibit both  $\gamma$  Doradus and  $\delta$  Scuti pulsations (circled point).

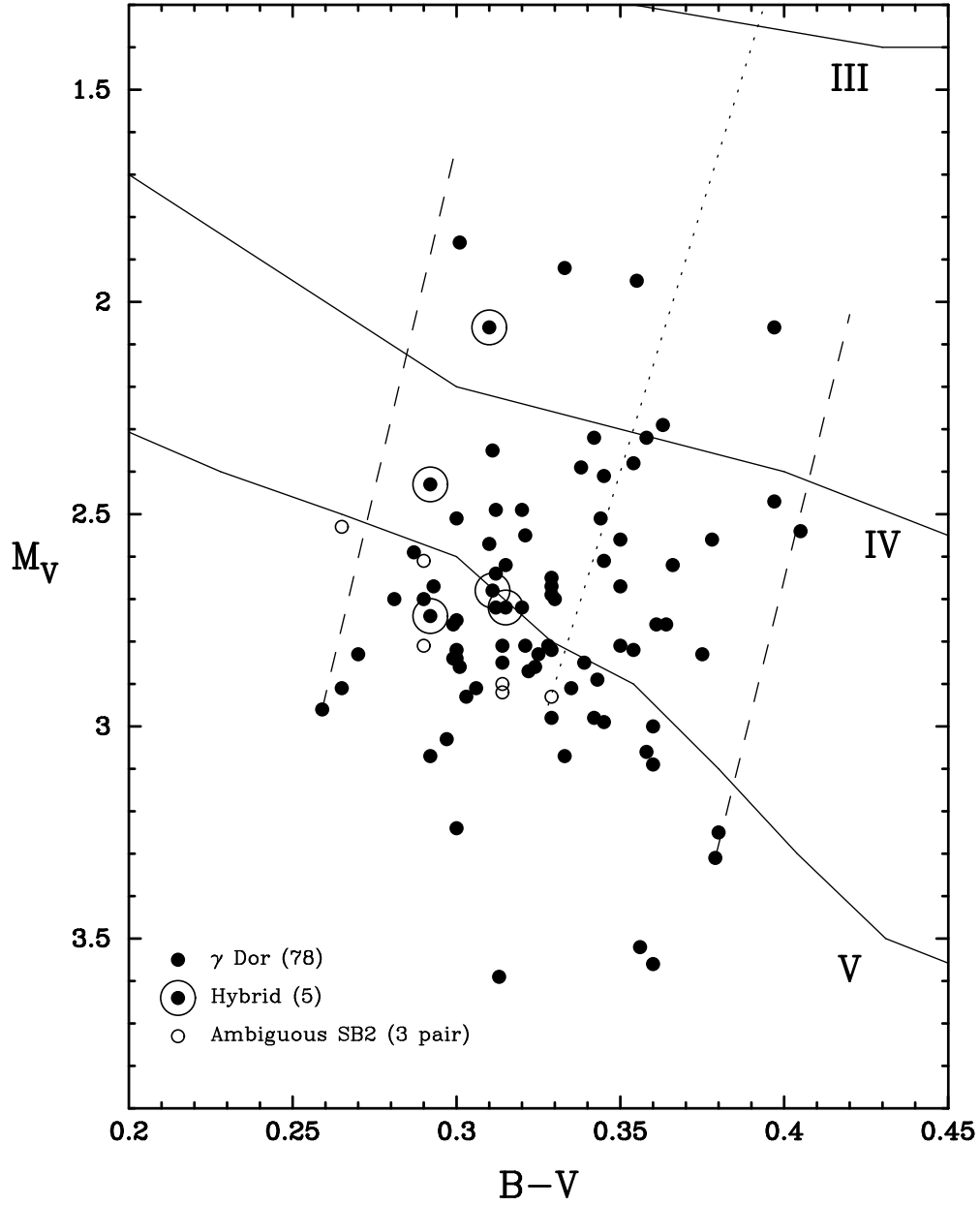


Fig. 41.— Location in the H-R diagram of all 86 confirmed  $\gamma$  Doradus field stars from Table 8. The 86 stars include 78  $\gamma$  Doradus pulsators, five self-excited hybrid stars HD 8801, HD 44195, HD 49434, HD 114839, and BD +18 4914 (circled points) and the six components of three SB2 binaries for which either (or both) components could be the pulsator (open circles). All 86 stars lie within the observed  $\gamma$  Doradus instability strip defined in Fekel, Warner, & Kaye (2003). All five hybrid pulsators lie within the overlap region of the  $\gamma$  Doradus and  $\delta$  Scuti instability strips. The star furthest below the main sequence is the metal-poor star HD 62196, with  $[\text{Fe}/\text{H}] \sim -0.5$ .